DESIGN, SYNTHESIS, AND CHARACTERIZATION OF POTENTIAL SELF-SORTING COMPOUNDS THROUGH DIFFERENTIAL SOLVATION

A THESIS SUBMITTED TO
THE GRADUATE SCHOOL OF NATURAL AND APPLIED SCIENCES
OF
MIDDLE EAST TECHNICAL UNIVERSITY

BY

GİZEM TEKİN

IN PARTIAL FULFILLMENT OF THE REQUIREMENTS
FOR
THE DEGREE OF MASTER OF SCIENCE
IN
CHEMISTRY

AUGUST 2016

Approval of the thesis:

DESIGN, SYNTHESIS, AND CHARACTERIZATION OF POTENTIAL SELF-SORTING COMPOUNDS THROUGH DIFFERENTIAL SOLVATION

submitted by **GİZEM TEKİN** in partial fulfillment of the requirements for the degree of **Master of Science in Chemistry Department**, **Middle East Technical University** by,

Prof. Dr. Gülbin Dural Ünver _____
Dean, Graduate School of **Natural and Applied Sciences**

Prof. Dr. Cihangir Tanyeli _____
Head of Department, **Chemistry**

Assoc. Prof. Dr. Akın Akdağ _____
Supervisor, **Chemistry Department, METU**

Prof. Dr. Ali Gökmen _____
Co-Supervisor, **Chemistry Department, METU**

Examining Committee Members

Prof. Dr. Metin Zora _____
Chemistry Department, METU

Assoc. Prof. Dr. Akın Akdağ _____
Chemistry Department, METU

Prof. Dr. Ali Gökmen _____
Chemistry Department, METU

Prof. Dr. Özdemir Doğan _____
Chemistry Department, METU

Assist. Prof. Dr. Bilge Baytekin _____
Chemistry Department, İhsan Doğramacı Bilkent University

DATE: 22/08/2016

I hereby declare that all information in this document has been obtained and presented in accordance with academic rules and ethical conduct. I also declare that, as required by these rules and conduct, I have fully cited and referenced all material and results that are not original to this work.

Name, Last name: Gizem Tekin

Signature:

ABSTRACT

DESIGN, SYNTHESIS, AND CHARACTERIZATION
OF POTENTIAL SELF-SORTING COMPOUNDS
THROUGH DIFFERENTIAL SOLVATION

Tekin, Gizem

M.S., Department of Chemistry

Supervisor: Assoc. Prof. Dr. Akın Akdağ
Co-supervisor: Prof. Dr. Ali Gökmen

August 2016, 129 pages

DNA achieved its double helix form with the help of hydrophilic and hydrophobic interactions. When the sequence of the DNA is examined, it is seen that the DNA bases are the most hydrophobic part, and therefore; they are located at the innermost part of the double helix to avoid interaction with water. This location also enables them to form hydrogen bonds with the complementary DNA base rather than forming them with water. The next part in the sequence is the sugars which have higher solubility in water compared to the DNA bases and lower solubility compared to the upcoming part, phosphate groups. The most hydrophilic part is the phosphate group which is located at the outermost part of the helix to increase its contact with water. Thus this is the thermodynamically most favorable form in water. With this in mind, DNA structure was taken as a model to examine molecular structures' formation and behavior in water. Meanwhile, a new concept, *differential solvation*, was introduced and developed. It was

suggested that with the help of differential solvation, molecular assemblies would be formed in water. Whether differential solvation is responsible for the formation of such molecular structures or not is the main question in this thesis. To address this, compounds having differential solvation in water were designed and synthesized. The final products' behaviors in water and in organic solvents were studied with NMR, UV-Vis, fluorescence, DLS and CD spectroscopy. Mainly, a compound which has differential solvation in water and a compound which has not differential solvation in water were compared and contrasted with the help of above mentioned methods.

In literature, molecular assemblies are widely characterized and investigated by circular dichroism (CD) spectroscopy. Since this instrument is very expensive and hard to reach, a homemade CD spectrometer was also built during this study. Necessary optical components were purchased and aligned to create circularly polarized light. The performance of the instrument was also compared with a commercial one.

Although both the conceptual and the instrumentation part need further studies, available data obtained during this thesis proves the formation molecular assemblies by differential solvation in water.

Keywords: differential solvation, molecular assembly, micelles, self-assembly, solvation derived assemblies, and chiral assemblies.

ÖZ

DİFERANSİYEL ÇÖZÜNÜRLÜKLE KENDİSİNİ SINIFLANDIRMA POTANSİYELİ OLAN MADDELERİN TASARIMI, SENTEZİ VE KARAKTERİZASYONU

Tekin, Gizem

Yüksek Lisans, Kimya Bölümü

Tez Yöneticisi: Doç. Dr. Akın Akdağ
Ortak Tez Yöneticisi: Prof. Dr. Ali Gökmen

Ağustos 2016, 129 sayfa

DNA çift sarmal yapısına hidrofobik ve hidrofilik etkileşimler sonucunda ulaşmıştır. Bir DNA sarmalındaki dizilim incelendiğinde, DNA bazlarının en hidrofobik kısım olduğu görülür ve bu yüzden de çift sarmalın en iç kısmında sudan en uzak olacak şekilde konumlanmışlardır. Bu konum aynı zamanda DNA bazlarının sudan ziyade karşı sarmaldaki DNA bazıyla hidrojen bağı kurmasını sağlar. Dizilimde sıradaki kısım ise şekerdir. Şeker kısmının sudaki çözünürlüğü DNA bazlarından fazla fakat bir sonraki kısım olan fosfat grubundansa azdır. En hirofilik kısım olan fosfat grupları ise çift sarmalın en dışında, su ile olan temasları artacak şekilde konumlanmıştır. Bu sebeple, su içerisinde termodinamik olarak en kararlı form budur. Bütün bu bilgiler ışığında DNA yapısı örnek alınmış ve moleküler yapıların sudaki oluşumu ve davranışları incelenmiştir. Aynı zamanda, yeni bir kavram olan *diferensiyel çözünürlük* taktim edilmiş ve geliştirilmiştir. Diferensiyel çözünürlük ile su içerisinde moleküler yapıların oluşacağı önerilmiştir. Diferansiyel çözünürlüğün suda moleküler yapıların oluşmasında

etkili olup olmadığı bu tezin odak noktası olmuştur. Bunu araştırmak için, su içerisinde diferansiyel çözünürlüğe sahip olan maddeler tasarlanmış ve sentezlenmiştir. Hedef ürünlerin sudaki ve organik çözücülerdeki davranışları NMR, UV-Vis, fluoresans, DLS ve CD analizleriyle çalışılmıştır. Genel olarak, suda diferansiyel çözünürlüğü olan ve olmayan iki madde yukarıda bahsedilen metodlar kullanılarak karşılaştırılmıştır.

Literatürde, moleküler toplanmalar büyük ölçüde dairesel dikroism (CD) spektroskopisi kullanılarak analiz edilmiştir. Bu cihaz oldukça pahalı ve ulaşılması zor olduğu için, tez sürecinde bir CD spectrometresi yapılmıştır. İhtiyaç duyulan optik ekipman satın alındıktan sonra, dairesel polarize olmuş ışık üretmek için gereken şekilde dizilmiştir. Tarafımızca yapılan bu spektrometrenin performansı ticari olarak satılan bir CD cihazıyla da karşılaştırılmıştır.

Hem kavramsal hem de instrumental kısımlarda daha fazla araştırmaya ve çalışmaya gerek vardır. Fakat, bu tez boyunca hali hazırda elde edilen veriler, su içerisindeki moleküler oluşumların diferansiyel çözünürlükten faydalanarak oluştuklarını göstermektedir.

Anahtar kelimeler: diferansiyel çözünürlük, moleküler toplanma, miseller, kendi kendine toplanma, çözünürlük bazlı toplanma, and kiral toplanma.

ACKNOWLEDGEMENTS

I would like to express my deepest appreciation to my advisor and also my guide for the last four years, Dr. Akın Akdağ. Without his belief in me, I would never be the person that I am today. I will always be grateful for his patience and encouragement, and I will always feel the pride of being his student for the rest of my life. I also would like to thank my co-advisor Prof. Ali Gökmen. He has always been very kind and understanding during this study. I respect his wise advices and deep knowledge. I would like to thank Prof. S. D. Worley for accepting me as a short-term scholar into his laboratory at Auburn University for my summer practice. It has been an honor to be one of his students. I would like to express special thanks to him for encouraging me to pursue my academic career.

I would like to thank my examining committee members; Prof. Dr. Metin Zora, Prof. Dr. Özdemir Doğan, and Assist. Prof. Dr. Bilge Baytekin. I appreciate the time they spent on my thesis, and their precious comments.

I would like to give my deepest thanks to my family, my dad, my mom, my sister and my dog, for always being there for me. Your endless love and support helped me so much for overcoming any obstacle.

I feel very privileged to be a member of the *four leaf clover*. My dear Cansu, Ezgi, and Gökçe, I want to thank you for your friendship and support, no matter how far we are.

I would like to thank all Akın Akdağ Research Group members. I would like to especially thank Perihan Öztürk, Gizem Çalışgan, and Duygu Tan for their friendship and support. I also want to express my sincere appreciation to Sevtap Güven, Sahra Altay, Ege Hoşgör, and Beril Özdemir for assisting me during my experiments, your

helps meant a lot. I also want to thank to our ex-group members Kıvanç Akkaş, Halil İpek, Sibel Ataol, Esra Nur Şimşek and Milad Fathi. I feel very lucky being a part of such a cheerful group. I wish all of you the very best.

I would like to thank Dr. İrem Erel for letting me perform DLS measurements in her laboratory. I would like to thank İrem Erel Research Group members for helping me in that process.

Finally, I would like to express my gratitude to all METU Chemistry Department members for everything they have done during my last seven years.

To my family and my dear Üvi

TABLE OF CONTENT

LIST OF FIGURES

FIGURES

LIST OF SCHEMES

SCHEMES

LIST OF TABLES

TABLES

LIST OF ABBREVIATIONS

CD	Circular Dichroism
CMC	Critical Micelle Concentration
DBU	1,8-Diazabicyclo[5.4.0]undec-7-ene
DCC	N,N'-Dicyclohexylcarbodiimide
DCM	Dichloromethane
DLS	Dynamic Light Scattering
DNA	Deoxyribonucleic Acid
DMAP	4-Dimethylaminopyridine
DMF	Dimethyl Formamide
DMSO	Dimethyl Sulfoxide
DMSO-d_6	Deuterated Dimethyl Sulfoxide
IR	Infrared
NMR	Nuclear Magnetic Reasonance
PDI	Polydispersity Index
PEM	Photo- Elastic Modulator
SEM	Scanning Electron Microscopy
TEG	Triethylene Glycol
THF	Tetrahydrofuran
UV-Vis	Ultaviolet-Visible Spectroscopy

CHAPTER 1

INTRODUCTION

1.1. Complexity

The idea that the life on earth emerged from non-living materials through a growing molecular complexity is a widely accepted assumption by the scientists after Oparin's proposal in 1924.[1] 'Complexity' investigates the systems exhibiting complex global behavior (too many interactions to account for) as a result of local interactions. Another decent definition is made by Parrish and Edelstein-Keshet stating that 'Complexity theory indicates that large populations of units can self-organize into aggregations that generate pattern, store information, and engage in collective decision-making'.[2]

The notion that the life originated from inanimate matter brings the question that whether it is possible to reproduce it in the laboratory. Eschenmoser and Kisakürek addressed this question by indicating that how the experiments towards chemical aetiology can be rewarding examining the organization of organic matter giving rise to the 'artificial chemical life'.[3] Reproducibility of life in the laboratory still remains as a challenge but it is certain that the life began with molecules and their interactions (complexity) and such areas deserve to be investigated thoroughly to suggest new ideas about the origin of life.[4]

1.2. Self-Organization

It would be better to start by defining the term '*self*'. In this thesis and in the life science terminology, the prefix '*self*' labels processes which are dictated by the 'internal rules' of a system.[4] Self-organization processes may proceed via thermodynamic or kinetic control. In thermodynamic control, the resulting complex is energetically more stable than the competing assemblies, on the other hand; the kinetically favored protocols establish the organized state based on its faster formation than the competing ones.[5] Generally biological processes are occurring via locally thermodynamic control, for example; protein folding to secondary, tertiary, and quaternary structures.[6] This important biological process occurs spontaneously exoergic, with a negative free-energy change.

1.2.1. Self-Sorting

Although self-assembly and self-sorting are widely used synonymously, these two concepts are different. In self-assembly, a complex mixture of precursors is turned into a single species with high fidelity, however; in the case of self-sorting a system with several components are produced with high fidelity. Thus, it is possible to define self-sorting as a spontaneous process in which a low-order multicomponent system is transformed into a high-order system with more than one component as seen in the Figure 1.[5] Also Isaacs defined the term as 'high-fidelity recognition of self, from nonself'.[7]

Formation of self-sorted systems could take place via different routes. Studies, to the date, widely have taken advantages of hydrogen bonding,[8] metal ligand interactions,[9] solvophobic effects[10], and reversible covalent bonds.[11]

Self-sorting is an environmentally-labile process. Main factors affecting the process are temperature, concentration, equilibrium constants and solvents.[7] Self-sorting may also be kinetically or thermodynamically driven.

Micelle formation is a good example of self-sorting driven thermodynamically. When soap molecules at higher concentration than the CMC (critical micelle concentration) are added to water, they form micelles spontaneously. The hydrophobic edges of soap molecules exclude the water molecules so that the hydrophilic parts are at the water interface. This process has a negative free energy change accompanied with an increase in the entropy. The increase in the entropy is resulting from the water molecules which are set free upon aggregation resulting from the unfavorable contact of hydrophobic regions with water. On the other hand, the organized system (micelle formation) is acting like a by-product which is not enough to decrease the disorder.[4]

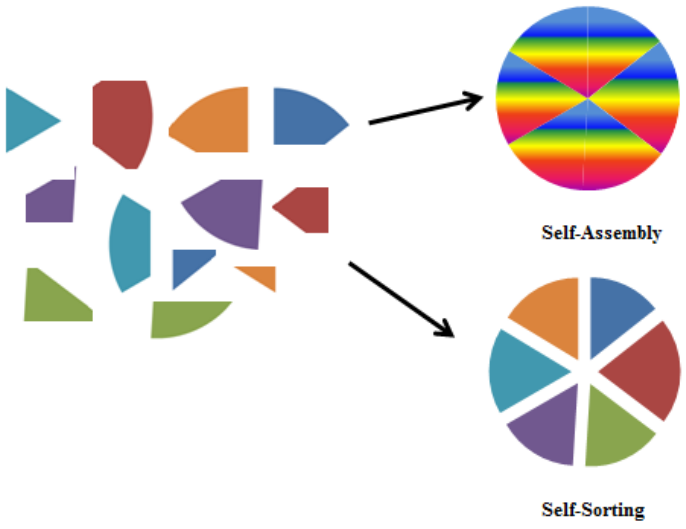

Figure 1. A schematic representation of self-assembly and self-sorting processes.

In the micelle case, there are only hydrophobic and hydrophilic regions that govern the self-sorting process. But what if there would be a part which is in between the hydrophobic and the hydrophilic? How would that middle soluble part affect the self-organization process? These questions are strived to be answered throughout this thesis in which a new concept is introduced to elaborate the approach to the problem; *differential solvation*.

1.3. Differential Solvation

Differential solvation is the differential (gradual) change of solubility along a molecular chain. That is, as one side of a molecule has high solubility in a given solvent, the other side has very limited solubility, and the linker (connecting molecular part) has in between solubility. Such molecules are expected to form more ordered self-assembled systems. This solubility comparison is made in water in this study.

Different from the micelles, the solubility in water along the molecules is not changing suddenly from hydrophilic to hydrophobic. A molecule having differential solvation must have three major parts, two of which are hydrophobic (probe) and hydrophilic (head) part and there is an additional *linker* part that connects these two and has middle solubility in water (Figure 2).

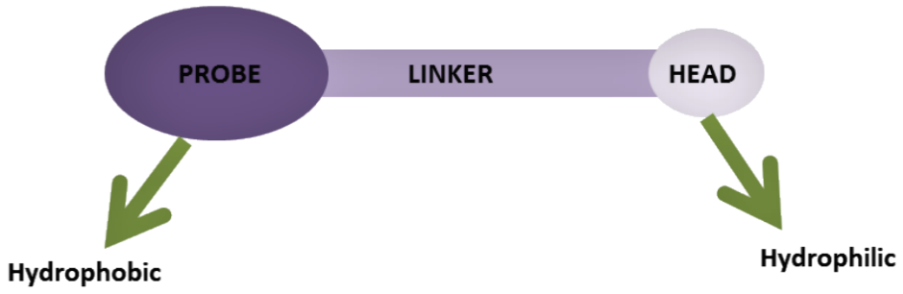

Figure 2. Structural pattern of a compound having differential solvation.

Since the solubility along the molecule is gradually changing, the resulting organized molecular structure must be different from a closed shell like micelles. It is presumed that this solvation pattern will result in a helical organization like in the case of DNA. To understand this presumption, it would be better to take a closer look at the DNA structure.

1.4. The Structure of DNA

DNA, deoxyribonucleic acid, is a molecule that carries genetic information in all living organisms and many viruses. DNA consists of two strands that are held together by hydrogen bonds. Each strand is composed of *nucleotide*s that could be further cleaved into *nucleoside*s and phosphate groups. The major components of a nucleoside are 2'-deoxyribose sugar and one of the four nitrogen-containing heterocyclic bases (adenine, guanine, cytosine, and thymine). Hence, each repeating unit in a nucleic acid polymer contains these three parts linked together, namely; a phosphate group, deoxyribose sugar and one of the four DNA bases.[12]

These four bases are planar heterocyclic molecules which are divided into two categories; *purine* bases and *pyrimidine* bases. Purine bases are *adenine* and *guanine* and pyrimidine bases are *thymine* and *cytosine*. Thymine is replaced with *uracil* in ribonucleic acids (RNA). The most stable tautomers of the bases are given in Figure 3.

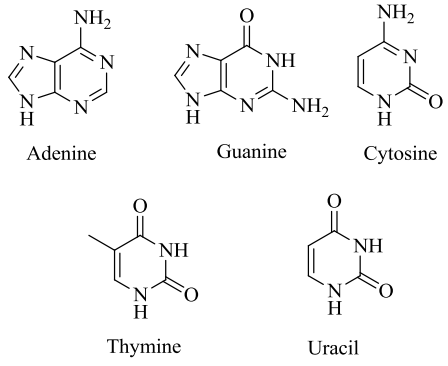

Figure 3. The bases in DNA and RNA.

Each nucleoside are linked through phosphate groups which are attached to the 3' and 5' positions of the sugar, therefore; full repeating unit in a nucleic acid is 3',5'-nucleotide (Figure 4).[12]

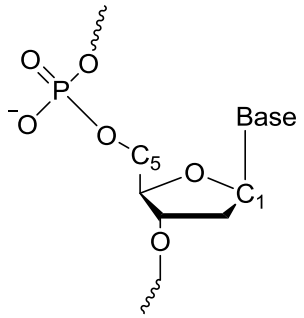

Figure 4. The repeating unit in a polynucleotide chain.

The bond connecting the sugar and the base is known as *glycosidic bond* and its stereochemistry in all natural nucleic acids is β in which the base is above the plane of the sugar when viewed onto the plane. Thus, the base is on the same plane as the 5' hydroxyl substituent.

1.4.1. Base-Pairing and Hydrogen Bonding

The important experimental results stated by Chargaff showed that the molar ratios of adenine:thymine (A:T) and guanine:cytosine (G:C) in DNA equal to unity.[13] After this important proposal, Watson and Crick in 1953 stated that these purine and pyrimidine bases are held together with specific hydrogen bonds which lead to the formation of planar base pairs. Thus DNA double helix consists of two strands that are held together with intermolecular hydrogen bonds. [14]

Since A:T and G:C ratios are one , it is concluded that adenine recognizes thymine and guanine recognizes cytosine via forming hydrogen bonds. The A:T base pair has two hydrogen bonds whereas G:C pair has three (Figure 5).

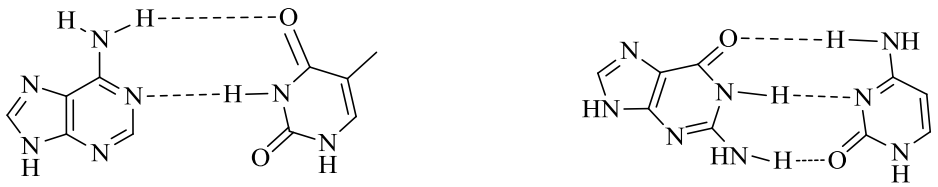

Adenine:Thymine Guanine : Cytosine

Figure 5. Base pairing between adenine-thymine and guanine-cytosine.

The additional hydrogen bond in the guanine:cytosine pair is calculated to cause additional stability compared to adenine:thymine. Also, theoretical studies revealed that the free energies of A:T and G:C pairs in aqueous solution are -4.3 and -5.8 kcal/mol.[15]

1.4.2. Base-Stacking

Pi-stacking (π-π stacking) refers to the noncovalent interactions experienced between aromatic rings. Aromatic rings tend to adopt a face-to-face geometry to increase the interactions of pi-systems because this geometry is favored energetically.[16] Aromatic stacking is a very important stabilizing interaction in DNA and also in RNA structure. In general, the distance between two base planes in stacked structure is 3.4Å which is also equal to the rise of DNA helix per base pair.[16]

There are several factors that affect the stability of π-π stacking of bases. These are electrostatic (dipole-dipole and dipole-induced dipole) interactions, dispersion (momentary dipole-induced dipole) effects, and solvation effects.[17]

The electrostatic effects result from the localized charges on the specific parts of the molecule. Dispersion effects depend on the polarizability and contact surface area of stacked species. Finally, solvent-driven effects are resulting from the relative energies of

stacked and unstacked bases along with the amount of surface solvated upon stacking. It was found that hydrophobic surface contact is the most stabilizing factor in binding [18] and later, it was stated that purines tend to stack more effectively than pyrimidines since they have larger surface area and greater polarizability.[16]

However, there are some restrictions in the case of base stacking. At the first glance, fully stacked geometry is highly favored since it excludes water, but on the other hand, this geometry causes a negative-to-negative repulsion between base-pairs. Thus, to minimize this repulsion, base pairs in DNA slide over one another with different slides as seen in the Figure 6. The charge repulsion is deceased while the negative-positive charge attraction increased with either negative or positive slide.[19]

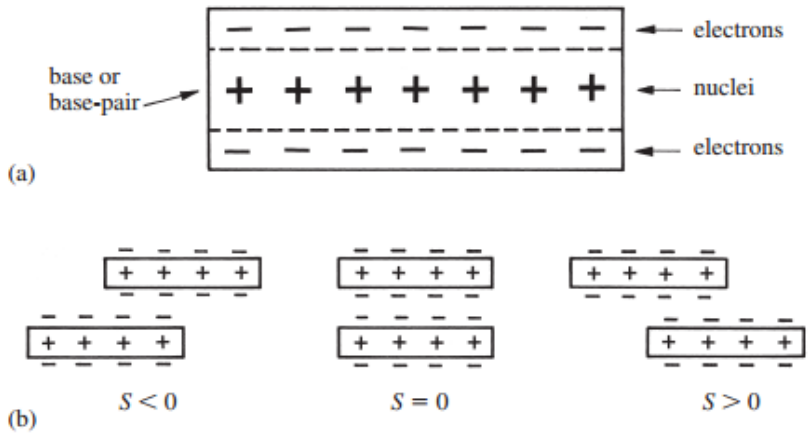

Figure 6. a) Distribution of electric charge in a base or base-pair. b) positive and negative slide at a base pair step (Figure is taken from Ref. 19).

1.4.3. Steric Effects

The steric effects on DNA stability could be understood by considering matched and mismatched pairs in the double strand. The DNA double helix has a more rigid structure

than its corresponding single stranded form. This rigidity and stability is provided by the above mentioned hydrogen bonding (*vide supra*), base stacking and electrostatic interactions. Thus, a matched double strand is a product of thermodynamically (enthalpically) favored process. However, conformations of matched bases are also important since they cause steric costs on the stability. Singly mismatched pairs generally cost the helix *ca.* 4 kcal/mol of free energy.[20] Although this stability loss can be related to a differential stacking, the majority of the energy cost is resulting from the distortion in the geometry after formation of a nonstandard geometry. This distortion eventually effects the neighboring pairs and causes unfavored conformational interactions.[16] The effect of hydrogen bonding in such a situation is not very dominant because mismatched pairs can also form hydrogen bonds with each other.[21] With these in mind, the question 'why DNA has a helix structure?' arises.

1.5. Why a Helix?

As mentioned above, a DNA nucleotide consists of phosphate, sugar and one of the four bases. The solubility of these individual parts in water is; the phosphate has the highest solubility among the parts, then the sugar comes, and the bases are almost insoluble.

The DNA bases are nitrogen containing heterocyclic organic molecules. When the fundamental rule of solubility '*like dissolves like'* is considered, these organic molecules will not dissolve in water. As mentioned above, these bases have a great tendency to form hydrogen bonds, because they have hydrogen atoms bonded to relatively more electronegative atoms. So, they can basically form hydrogen bonds with water and be solubilized. However, it is important to consider the *water in human body*. The water in our cells is at physiological pH, which is approximately 7.4, close to the neutral pH. When the solubility of these bases is investigated, it is found that adenine is soluble in acidic solution and uracil is soluble in more basic solutions. Thus, in neutral pH, bases will be insoluble in water. Still, solubility is a relative term.

The insolubility of the bases in water does not pose a serious problem since in nucleotide form they become soluble. Once they are attached to the water-soluble phosphate-sugar backbone, they can function in the cells. However, this solubility pattern is significant when the whole DNA structure is considered. The bases try to avoid water to maintain their orientation where they form hydrogen bonds with the complementary bases. Therefore, hydrophobic packages are formed so that the water-insoluble bases will be away from water and water-soluble sugar-phosphate part is in direct contact with water. This was actually what Rosalind Franklin and Raymond Gosling deduced after they were able to obtain the X-Ray crystallography pattern of DNA in 1952 (Figure 7).[22]

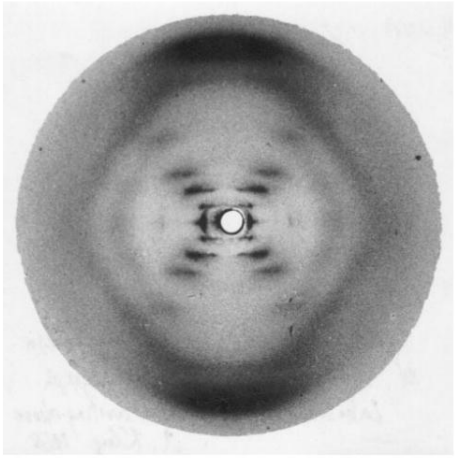

Figure 7. X-Ray image of DNA taken by Rosalind Franklin. (Figure is taken from Ref. 22)

Along with this '*differentially*' changing solubility in water, the factors mentioned above; base stacking, steric effects, electronic effects, are also taking roles in the formation of a helical structure of DNA. What if nature preferred to have phosphate, hydrophobic unit, and the bases respectively?

The strands of DNA should adopt such a conformation so that the bases will be away from water, the bases will stack effectively and there will be minimum drawbacks resulting from steric and electrostatic reasons. Calladine, Drew, Luisi and Travers explain basically how DNA forms a helix in their book *Understanding DNA*.[19] To fulfill all the needs, the strand could form a skewed ladder as seen in the Figure 8.

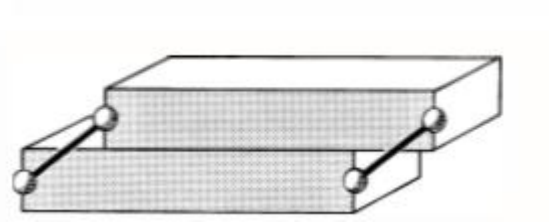

Figure 8. The skewed ladder model for DNA (Figure is taken from Ref. 19).

At the first glance, the skewed ladder model seems acceptable, however; when the individual atoms are considered, this model causes too much close contact and thus become a sterically unacceptable model. Moreover, this kind of stacking provides only a limited avoidance of water.

The skewed ladder model is a good approximation, but it will be ideal if a helical twist is introduced. With the help of this helical twist, the steric constrictions will be minimized and also it will provide a more effective hydrophobic area for the bases to recognize each other (Figure 9).[19]

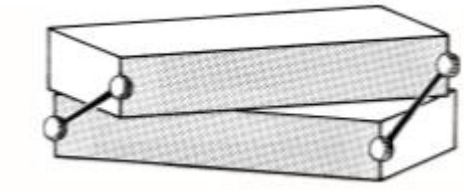

Figure 9. Helically twisted skewed ladder model (Figure is taken from Ref. 19).

This helically twisted skewed ladder model is much closer to the structure of B-DNA (naturally hydrated form of DNA) double helix which was published as Watson-Crick Model in 1953 after they utilized the data obtained by Franklin. They stated that chains followed right handed helices with 3',5' linkages having the bases inside of the helix and the phosphates on the outside. They further explained that the sugars were nearly perpendicular to the bases leaving 3.4Å between base planes; the double strand had a helical twist of 36°, the complete helical turn was completed over 10 nucleotide units causing each turn to take 34Å (Figure 10).[14] Considering all these, the '*differential solvation*' is facilitated by nature.

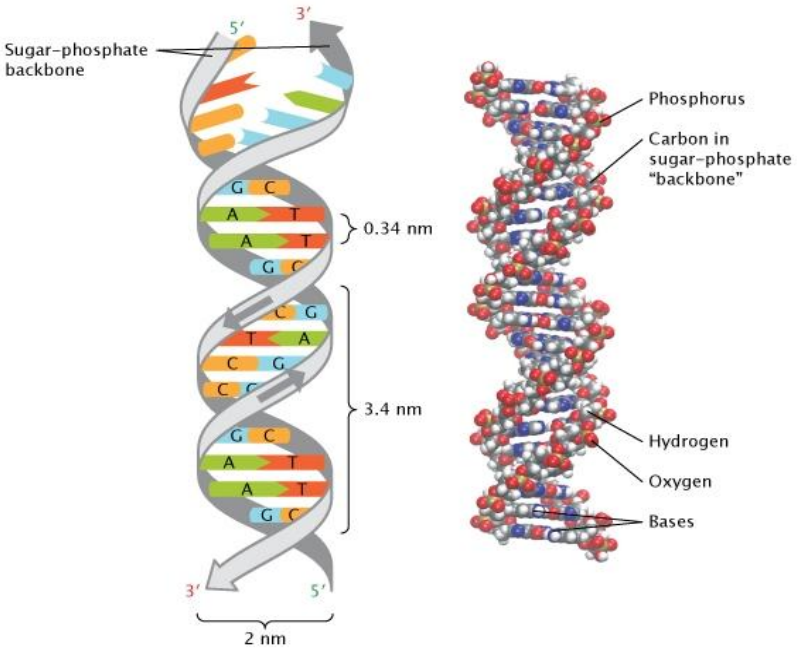

Figure 10. The structure of DNA (Figure is taken from Pray, L. (2008) Discovery of DNA structure and function: Watson and Crick. *Nature Education* 1(1):100).

In summary, the insolubility of bases and the solubility of phosphate groups act as the driving force in the formation of double helix in water. Also, very small noncovalent intermolecular interactions, partial charges and the geometry help the core of the DNA where the recognition takes place to be formed. That is, with changing the solubility, a hydrophobic core was created for bases.

1.6. Covalent versus Non-covalent Interactions

Covalent interactions describe the formation of a bond between two species upon sharing an electron pair. The first theoretical studies towards understanding the nature of covalent interactions were done by G. N. Lewis.[23] Over the years, the nature of the covalent interactions, their formation and cleavage, have been studied widely both experimentally and theoretically.

When it comes to the non-covalent interactions, they are separated from covalent interactions in the sense that they do not involve sharing of electrons. They rather form molecular structures through electromagnetic interactions. J. D. van der Waals was first one to discover the non-covalent interactions and this discovery led him to formulate the state of real gases.[24] Non-covalent interactions generally lead to the formation of molecular clusters or aggregates, whereas the covalent interactions lead to the formation of classical molecules. Non-covalent interactions are widely investigated under following categories which are hydrogen bonding, stacking interactions, electrostatic interactions, hydrophobic effects, charge transfer interactions, and metal-ligand interactions.

The properties of the molecular aggregates resulting from the non-covalent interactions are different from the individual molecules interacting. The properties of the subsystem tend to differ more with the larger interactions. Generally the non-covalent interactions are weaker than the covalent interactions. Nevertheless, they can be detected by the

change in the stretching frequencies and this can reach hundreds of inverse centimeters, especially in hydrogen bonded systems.[25]

Although non-covalent interactions are still a relatively newly-discovered area, their role in nature is essential. Also these interactions govern all biological materials. For instance, the structure of DNA and proteins and molecular recognition are only a few examples which are investigated under the name of non-covalent interactions.[25]

Non-covalent interactions are the key concept of *supramolecular chemistry* which was defined as 'chemistry beyond the molecule' by Lehn.[26] In his study, he described supramolecular chemistry as an active research topic on molecular recognition, catalysis, transport, molecular surfaces, and the polymolecular assemblies. Supramolecular assemblies formed via intermolecular interactions were referred as formation of *systems* (molecular collectives formed via intermolecular interactions having more than one type of component) with high selectivity of recognition, transformation, regulation and also molecular communication. All of which could be linked to artificial intelligence and more.

Covalent and non-covalent interactions also differ in stability. A covalent bond could reach to a maximum length of about 2 Å due to orbital overlap. However, in non-covalent systems, complete orbital overlaps are not observed and thus, intermolecular distances could reach to tens of angstroms. Entropy is also a very important term in the formation of non-covalent systems. In such aggregates, $T\Delta S°$ is usually, at room temperature, comparable to the enthalpy term $\Delta H°$ and the entropy change is always negative. Therefore, the change in the Gibbs' free energy (ΔG) during the formation of aggregates is close to zero. However, in the covalently bonded molecules, enthalpy term is greater than the entropy term and accordingly the ΔG is mainly determined by the enthalpy. The total stabilization energy in the formation of aggregates is about 1 to 20 kcal/mol, whereas in the covalent system it is about 100 kcal/mol and higher.[25] Still,

both the covalent and non-covalent interactions are favored by the enthalpy term and disfavored by the entropy.

1.7. Other Studies

Self-assembled or self-sorted systems are challenging to study in water due to competing molecular interactions. With the solvation adversity in mind, the molecules will compete over intermolecular interactions with themselves and the solvent molecules. For example; unless any precautions are taken, an organic molecule capable of forming hydrogen bonds will make hydrogen bonds with water rather than its organic complementary molecule since water is a very powerful hydrogen donor and acceptor. To overcome this problem, DNA adopts the helical structure and forms hydrophobic packages in which water is excluded and thus complementary bases are able to form hydrogen bonds with each other. Over the years, scientist developed 'precautions' to study organic molecular systems in water.

In Nature, many naturally occurring small molecules are chiral such as amino acids and sugars which lead to chiral supramolecular assemblies. While the origin of chirality still remains obscure, the homochirality in biomolecules is a huge research area.[27] Self-assembly has, for a few decades, been one of the key points in the formation of chiral molecules. How chiral molecules behave in supramolecular level and how achiral molecules turn into chiral assemblies are hot topics in several fields. To understand the working principles of Nature, it is important to study such systems in water. However, several studies were not able to be investigated in water or some were preferred to be studied in organic solvents to understand the key points of such systems. Also assemblies containing chiral centers attract attention since chiral molecules can create *chiral spaces* within the molecular assembly and thus, their chiral selectivity is worth examining.

Lyle Isaacs *et al* studied enantiomeric self-recognition driven by hydrophobicity by using a metal complex **Y** shown in the Figure 11.[28] They reported that upon addition of a palladium based metal complex, [{Pd(ONO_2)(en)}$_2$], to a racemic mixture of facial amphiphile **X** results in the formation of a single molecular aggregate in water. Heterochiral aggregate remains hypothetical since the carboxylate group in the organic compound could only interact with palladium effectively in a specific geometry and this causes the enantiomeric recognition of **b**. Their model offers a new way to study enantiomeric self-recognition in water.

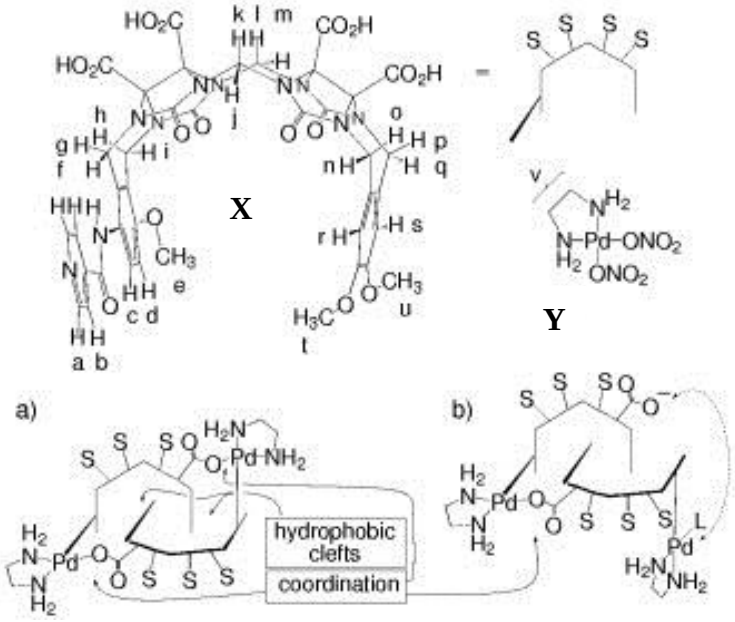

Figure 11. The complexes studied in the above mentioned work of Lyle Isaacs (Figure is taken from Ref. 28)

In another study, Percec's group studied homochiral columns formed via self-sorting during a helical organization of hat-shaped molecules, cyclotriveratrylene crowns (CTV), having chiral, achiral, and racemic alkyl side chains.[29] This side chains contained *R* and *S* chiral groups, achiral groups, racemic by mixing and racemic by

synthesis chains. In organic solvents, such compounds were proved to form helical structure by CD and UV analysis. Their further analysis in solution phase and in bulk revealed how self-assembly, racemization and deracemization took place. Enantiopure CTVs assemblied into single handed columns and racemic ones generated equal amounts of right and left handed columns. In neither case intercolumnar racemization was detected which can be interpreted as single handed columns are single handed helices in each situation. Even CTVs containing achiral side chains ended up in handed columns. Their study offers an insight how nature preferred homochiral structure and more stable assemblies during its evolution but still it proposes limited information because those systems were not examined in aqueous environment. This is also a proof for the Nature's way of self-sorting.

The effect of chiral centers on the supramolecular structures, how they induce chirality to the supramolecular system, is a widely examined subject. A distinct study by Roche *et al* presented a supramolecular helix which *disregards* chirality.[30] They reported that perylene bisimide (PBI) based compounds having chiral side chains turn into supramolecular helices irrespective of the enantiomeric purity of the alkyl chains attached. They attached six different alkyl chains with different stereochemical combination; racemic by synthesis, racemic by mixing, and homochiral ones. Their study revealed that all combinations ended up forming identical single-handed structures regardless of the chiral purity. They further proposed that the high crystalline order of the helices occurred via a *cogwheel mechanism*, which was explained in detail in the publication, ignoring the chirality of the building materials of the system. However, all the physical analysis were done in organic solvents, thus it is possible to make only predictions about the system's behavior in water.

To our knowledge, a general approach is widely accepted in which chiral selectivity was induced by simple chiral molecules' themselves. However, the exact opposite of this approach has not really been investigated.

This hypothesis suggests that chiral selectivity, the homochirality in Nature could also be considered, might be induced by chiral spaces formed in the supramolecular level. Basically, enantiomeric purity could have been supplied by molecular systems which provide *chiral privilege* for the molecules that are coherent with the chiral space within the assembly. Such a system would be capable of self-sorting. In other words, molecules having the same stereochemical configuration would be accepted by the assembly, however; the ones having the opposite configuration would be excluded. To study this hypothesis in water, it would be a wise choice to utilize the concept of *differential solvation*.

In this thesis, a molecular system which forms a helical assembly in water with the help of π-π stacking is investigated by using the differential solvation principles. After proving such molecules could really turn into a helical system, its selectivity towards chiral impurities is examined. To create a chiral space within the system, chiral centers having the same stereochemical configuration were introduced into the molecular chains. Also with the help of these chiral centers, the target compounds will be CD (circular dichroism) active and thus the helical assemblies can be examined. The expected molecular structure is given in the Figure 12.

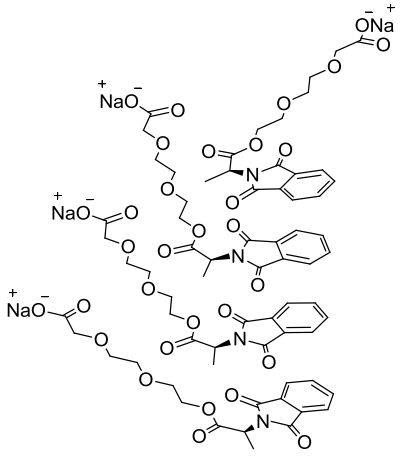

Figure 12. An example of the target helical assemblies in water.

1.8. Circular Dichorism

Circular dichroism spectrometry (CD) is a special type of optical spectroscopy that measures the difference between the absorbance of left circularly polarized light and the right circularly polarized light as a function of wavelength.[31] CD spectrum acts as fingerprints for most of the chiral biological compounds like proteins and nucleic acids. Therefore, this method is widely preferred for the analysis of chiral molecules, secondary protein structures or any other chiral supramolecular type assemblies.

If a compound contains a chiral center, it will absorb one type of the circularly polarized light to a greater extent than the other one and thus it will give signals at the corresponding wavelengths. CD signals can either be positive or negative depending on the stereochemical configuration. Compounds that are mirror images of each other will have spectra that are symmetric with respect to x-axis, that is; they will have signals at the same wavelength with same magnitude but with opposite signs.

The main components of a commercial CD spectrometer are a light source, a monochromator, a polarizer, a photo-elastic modulator (PEM), a sample holder, and a detector. Block diagram of the instrument is given in the Figure 13. The light becomes linearly polarized after it goes out of the Rochon polarizer. PEM is a special equipment that helps modulating the linearly polarized light and split it into right circularly polarized light and left circularly polarized light. If the compound is not CD active, than it will absorb left and right circularly polarized light equally, resulting in no signal output. On the other hand, a CD active compound will give unequal intensities of each circularly polarized light to the detector and CD signals will be observed in the output.

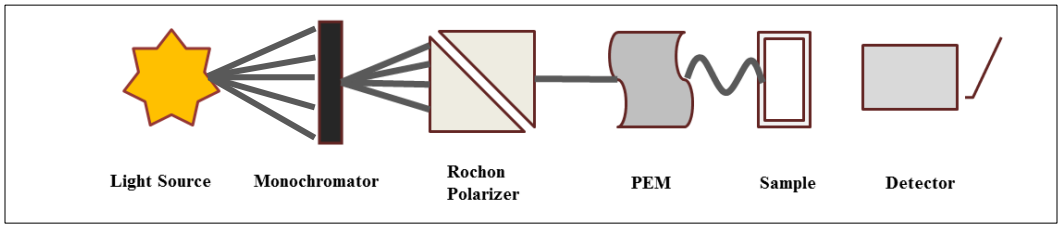

Figure 13. The block diagram of a CD instrument.

Plane-polarized light is composed of two components in equal amounts; right circularly polarized light and a left circularly polarized light. Plane-polarized light acts like a *racemic mixture* of lights. A CD spectrometer separates this racemic light into its constituents and provides *chiral light*.[31]

In CD spectroscopy, difference in the absorbance of each component of plane-polarized light is measured, $\Delta A = A_l - A_r$. Thus, a positive signal implies that the compound absorbs left circularly polarized light more than right circularly polarized one. When the Beer's Law is applied to the formula, it becomes $\Delta A = \Delta \varepsilon Cl$, where $\Delta \varepsilon$, $(\varepsilon_l - \varepsilon_r)$, stands for the differential molar absorptivity of the circularly polarized lights in the unit of $M^{-1}cm^{-1}$. C stands for the concentration (M), and *l* is the length of the cell (cm).

$\Delta \varepsilon$ is generally denoted as *molar circular dichroism* which is a wavelength-dependent property and specific for each compound under given temperature, pH and etc. A CD spectrum generally is given as molar ellipticity $[\Theta]$ versus wavelength, where $[\Theta] = 3298.2\ \Delta \varepsilon$.

When the light passes through a circular dichroic material, light becomes elliptically polarized. This light is not totally circular but elliptical in shape. After that transition, the magnitudes of the circular components of the light will not be the same due to the difference in the absorbance, which is also a definition for circular dichroism.[32]

To visualize the above mentioned principles, it would be better to give examples about the studies in which scientist took advantage of CD spectroscopy. In an article, which was published for educational purposes, (+) and (–)-menthol was oxidized to (+) and (–)-menthone with a green process and the resulting products were analyzed by CD spectroscopy.[33] The oxidation procedures for the specific reaction were given in the literature; however, they all utilized very expensive and toxic chemicals. In this study, calcium hypochlorite, $Ca(ClO_2)$, which is an environmentally friendly, cheap and strong enough oxidant was used for the oxidation reaction (Figure 14).

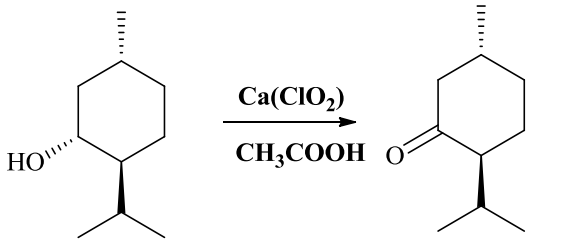

(–)-Menthol (–)–Menthone

Figure 14. The green oxidation of (–)–Menthol to (–)–Menthone.

The oxidation product was verified by IR spectroscopy and CD analysis was done as well. The reactants were not CD active due to the lack of chromophores. However, when they are oxidized to the corresponding carbonyl compound, they become CD active. The stereochemical difference between (+) and (–) - menthone were observed clearly on the CD spectrum given in Figure 15.

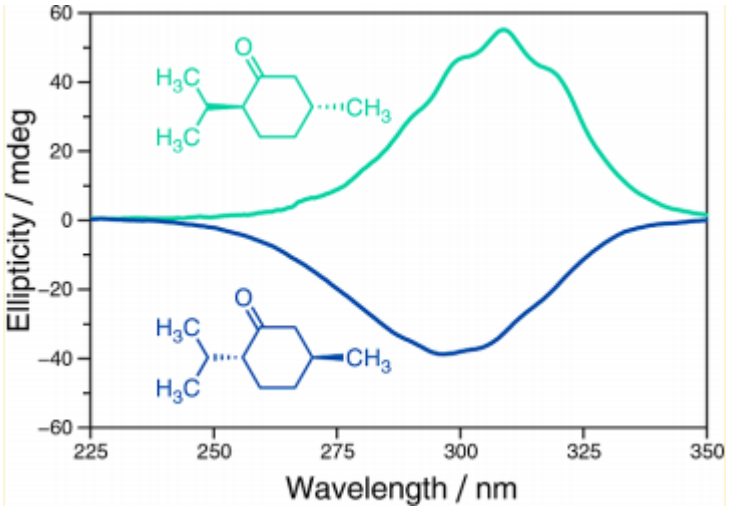

Figure 15. The CD spectra of (+) and (–)–menthone (Figure is taken from Ref. 32).

As seen in the spectrum, enantiomers absorbed the circularly polarized light differently and they resulted in signals with opposite signs. (–) - Menthone showed positive Cotton Effect, on the other hand, (+) – menthone showed negative Cotton effect with the almost same magnitude in hexane solution.

CD spectroscopy is also employed widely in supramolecular systems. Fenniri *et al* represented a compound which self-assembles into helical rosette nanotubes with tunable chiroptical properties.[34] They examined the process of formation of rosette type both right and left handed helical assemblies of compound **1** at high (≥ 1 mM) and low (≤ 0.04 mM) concentrations in methanol. After the formation of the rosette, addition of a chiral amino acid (promoter) triggers the transformation from racemic to chiral nanotubes by binding electrostatically to the crown ether moiety. Depending on the concentration, the transition process may take place faster or slower. When the solution of assembly was treated with a chiral amino acid (*D*-alanine or *L*-alanine), an induced circular dichroism (ICD) was observed resulting from the binding of zwitterionic chiral

amino acid to the prochiral compound **A**. CD spectra of solutions in methanol with either chiral amino acid were given in Figure 16.

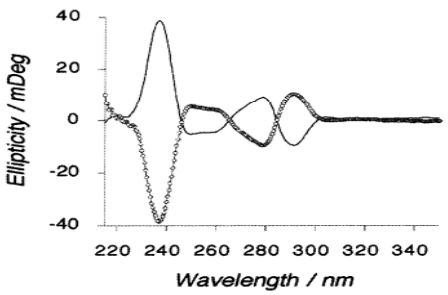

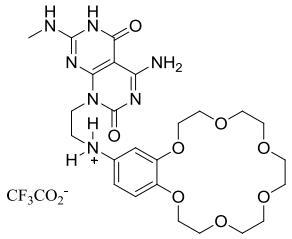

A

Figure 16. CD spectra of A (0.04 mM) + *L*-Ala (0.4 mM) (O) and 1 (0.04 mM) + *D*-Ala (0.4 mM) (-) recorded continuously until the induced circular dichroism (ICD) stabilized (< 24 h after mixing) (Spectra taken from Ref. 33).

When a control experiment was conducted, *D*-alanine and *L*-alanine were CD silent in the given wavelength range. The induced CD effect was analyzed further with different amino acids. Although signal intensities differed, amino acids with the same stereochemical configuration gave rise to the same helicity. They further stated that the chirotopical outcome of the complex drastically depend on the minor structural differences. To specify; small, aromatic, and relatively more hydrophobic amino acids are preferred more by this specific system. Also achiral promoter showed no inductive effect on the assembly.

CHAPTER 2

AIM OF STUDY

In this thesis, molecules having differential solvation in water are to be designed and synthesized. These compounds are expected to form helical assemblies in water. To examine the behavioral changes in water, the ^{1}H NMR spectra of the compounds both in $CDCl_3$ and D_2O were compared. Also solutions of the compounds having differential solvation and the compounds which do not have differential solvation were prepared and their UV-Vis, fluorescence, and DLS analyses were conducted and compared. Gathering the proofs about the formation of more ordered assemblies by the compounds having differential solvation in water, compounds having chiral centers were synthesized (Figure 17).

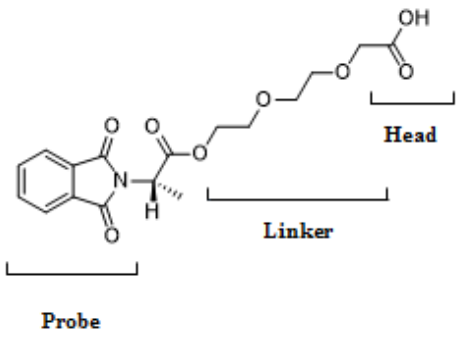

Figure 17. One of the target compounds containing a chiral center and having differential solubility in water.

The effect of the chiral center on the formation the assemblies were aimed to be examined with the same physical analysis methods and also CD spectroscopy. After the formation of the assemblies, chiral impurities with the opposite stereochemical configuration are planned to be introduced to the chiral assembly. The selectivity of the assembly towards these chiral impurities is planned to be investigated. In this step, self-sorting of the molecules with the same stereochemical configuration is expected. However, the self-sorting investigations remained as future studies.

All experiments on the assemblies are conducted in water with no additional inorganic metal complex. Moreover, a home-made CD spectrometer is built during this study and the efficiency of the spectrometer is compared with a commercial one.

CHAPTER 3

RESULTS AND DISCUSSION

This thesis is divided into three categories; design, synthesis, and characterization. The results and discussions will be given in these sub-sections explicitly.

3.1. Design

To form helical assemblies in water, molecules with gradually changing solubility are designed. While doing this, DNA structure is taken as a model. While designing the compounds, we preferred to start with simple molecules and started with monotosylated triethylene glycol (**1**). The tosylate part acts as the most hydrophobic part and the triethylene glycol part has the middle solubility in water.

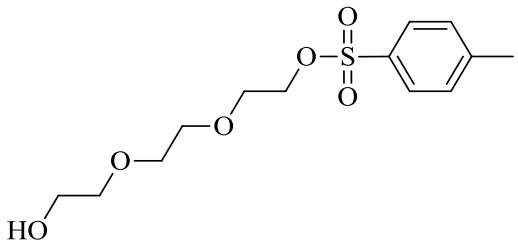

1

To increase the hydrophilicity of the head part, alcohol functionality is oxidized to the corresponding carboxylic acid (**2**).

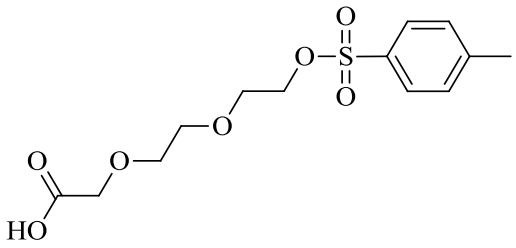

2

To see if there is any difference between two kinds of compounds, one of which with differentially changing solubility and the other with sudden change in the solubility, the middle soluble part is replaced with a hydrophobic alkyl chain, namely octane chain (**3**). Again, the alcohol group is oxidized to the carboxylic acid (**4**).

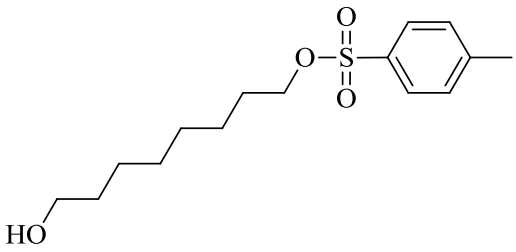

3

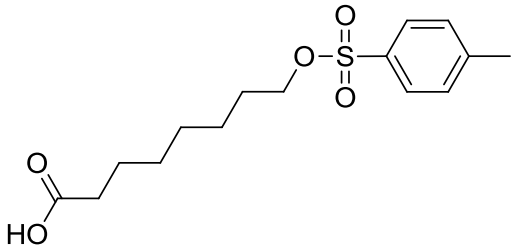

4

It was expected that these two types of compounds would behave differently in water. Because of the triethylene glycol part, the molecule would have a gradually changing solubility and thus would thermodynamically form more regular structures in water, a helix assumingly. On the other hand, the ones with the octane side chain have a sudden change of solubility from hydrophobic to hydrophilic and thus would not have much chance to form regular assemblies but rather collapse into micelles or other low-order assemblies to avoid water.

These assemblies are supposed to be formed via π-π stacking by using the π electrons of the benzene ring in the *p*-toluenesulfonyl group. However, the sulphur center of the *p*-toluenesulfonyl substituent is tetrahedral and therefore the benzene ring is not on the plane. This may lead to an ineffective stacking of the rings and thus may affect the formation of the helical assemblies. Because of these concerns, substituents having planar structure are preferred as a next step, and the *p*-toluenesulfonyl tosyl group is replaced with the phthalic anhydride along with the same linker and head parts (**5**, **6**, **7**, and **8**).

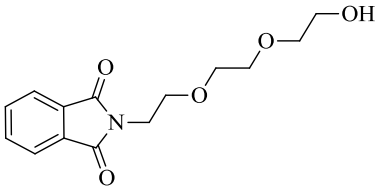

5

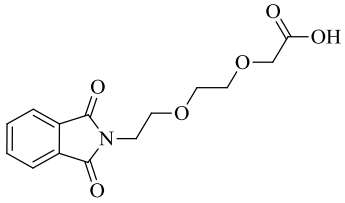

6

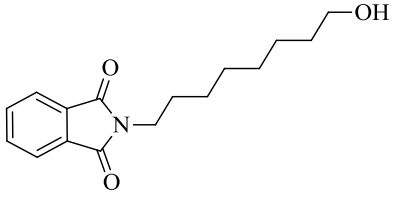

7

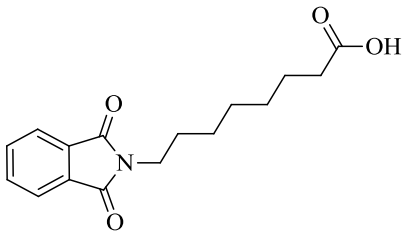

8

After examining these compounds, a chiral center is introduced into these molecules to further investigate the behavior of the resulting molecular structures. To achieve this goal, *L*- alanine is used and it is directly attached between the probe and the linker part, forming compounds **9**, **10**, **11**, and **12**.

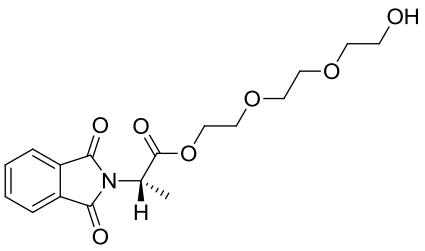

9

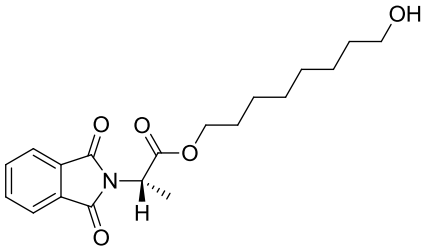

10

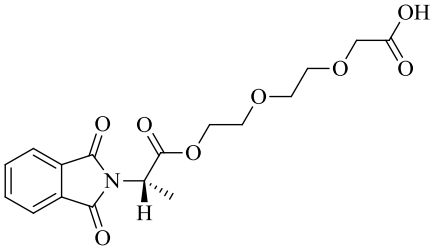

11

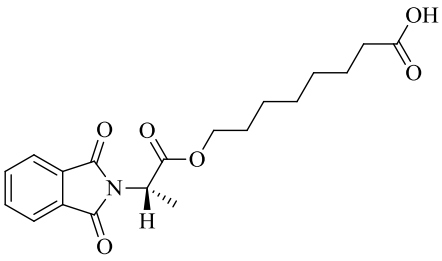

12

The helices' selectivity towards the chiral impurities is desired to be examined. To do this, the same molecules with the opposite stereochemical configuration are synthesized by using *D*- alanine (**13**, **14**, **15**, and **16**).

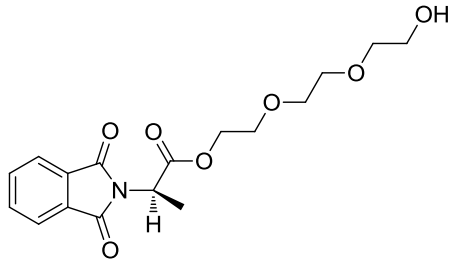

13

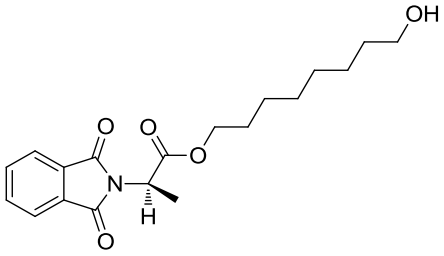

14

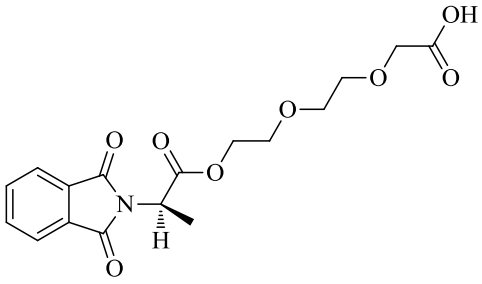

15

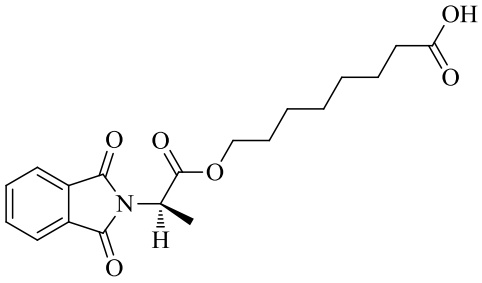

16

So far, the synthesized compounds were not completely solid yet not completely liquid; they were highly viscous greasy materials. To get solid compounds, we decided to change the phathalic anhydride group with naphthalic anhydride unit. When the compounds become solid, it would be easier to study their SEM images. SEM images could help to investigate closely the structures of the assemblies that are formed. Accordingly, the following compounds (**17**, **18**, **19**, and **20)** were aimed to be synthesized. However, these compounds' physical analyses remained as a future study.

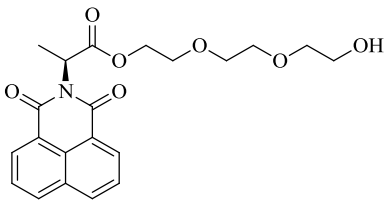

17

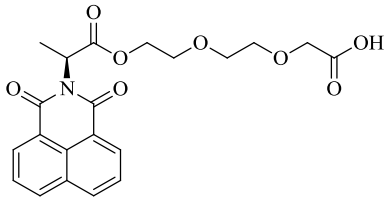

18

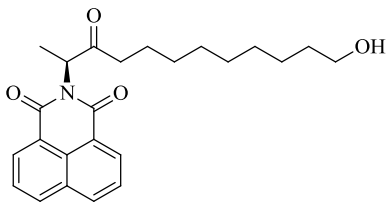

19

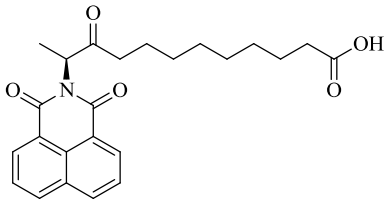

20

3.2. Synthesis

The first target compounds; monotosylated triethylene glycol (**1**) and monotosylated 1,8-octanediol (**3**) were synthesized using the same procedure. It is not easy to control the tosylation reaction and stop them at the monotosylated step. Therefore, the resulting mixture is purified with column chromatography to separate the ditosylated and monotosylated diols. After the separation of the desired product, the alcohol functionality is oxidized to the corresponding carboxylic acid with the Jones Reagent with the yields of 40% for the triethylene glycol and 82% for the 1,8-octanediol substituted ones.

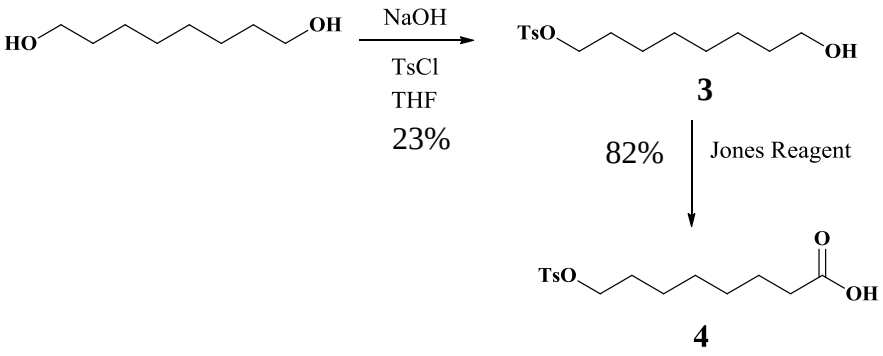

Scheme 1. Synthesis of compound **4**.

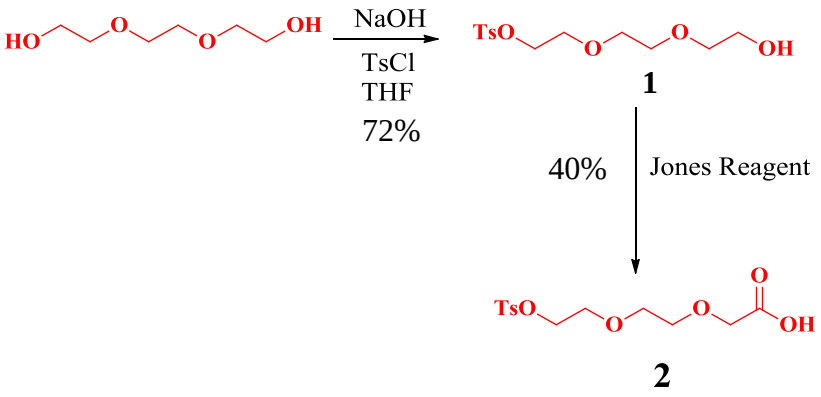

Scheme 2. Synthesis of compound **2**.

To enhance the stacking, a planar probe part was needed. Phthalic anhydride was preferred for this purpose. To synthesize the target compounds, potassium phthalimide salt and the monotosylated or monobrominated diols were reacted. The tosylated and brominated compounds were preferred because of their good leaving group abilities. Also catalytic amount of KI was used in these reactions since it is both a good nucleophile and a good leaving group and eventually the usage of KI accelerates the reaction. The resulting alcohols were purified with column chromatography and obtained with the yields of 56% for compound **5** and 55% for compound **7** and again they were oxidized to the corresponding carboxylic acids.

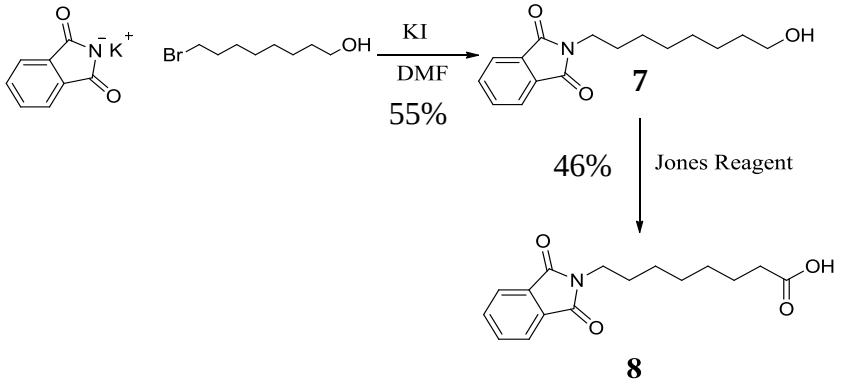

Scheme 3. Synthesis of compound **8**.

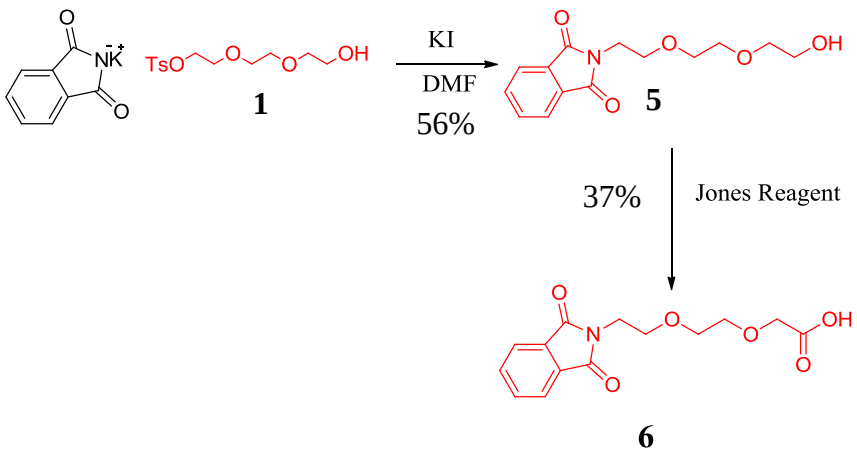

Scheme 4. Synthesis of compound **6**.

After the above mentioned compounds were synthesized, the chiral centers were introduced within the same compounds. To achieve this goal, *L*-alanine and *D*-alanine were attached between the probe and the linker part. After the addition of the alanine groups, a chiral center was produced by which we assumed to have a significant role in the formation of the assemblies. To reach the desired compounds, first of all, an addition reaction of phthalic anhydride and alanine was conducted.

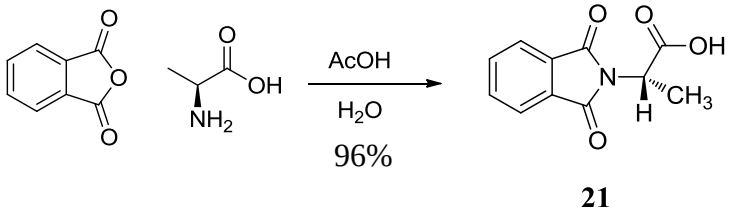

Scheme 5. Synthesis of compound **21**.

However, there was no example of the following target compounds in the literature, the synthetic pathway was designed by us and related procedures were applied to our case and optimized. To achieve this goal, Stehlich Esterification reaction, which directly

combines the above carboxylic acid and the diol, was conducted. Yet, this reaction did not work in our case. The resulting compound separated via column chromatography did not turn out to be the desired compound.

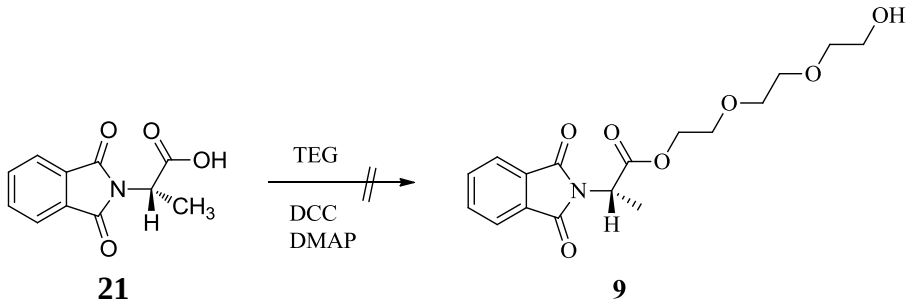

Scheme 6. Steglich Esterification trial for the synthesis of compound **9**.

The same problems were encountered in the case of 1,8-octanediol. Again the desired product could not be separated from the reaction mixture.

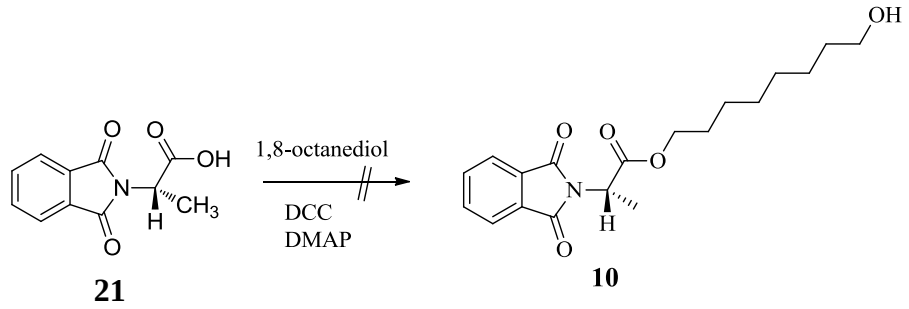

Scheme 7. Steglich Esterification trial for the synthesis of compound **10**.

Then, the synthesis route was altered; compound **21** was first chlorinated by using thionyl chloride. This product was not characterized and used directly for the next step reaction in which the acyl chloride and the diol were reacted with a different procedure using triethylamine in DCM. This time, the alcohols could be separated by column

chromatography. Still, the chromatography process was hard to complete because of the several other side products and thus the yields of these reactions were relatively low, 31% for compound **9** and 22% for compound **10**. The purified alcohols were again oxidized to the acids. Both the alcohols and the carboxylic acids were not known in the literature and they are characterized during this study.

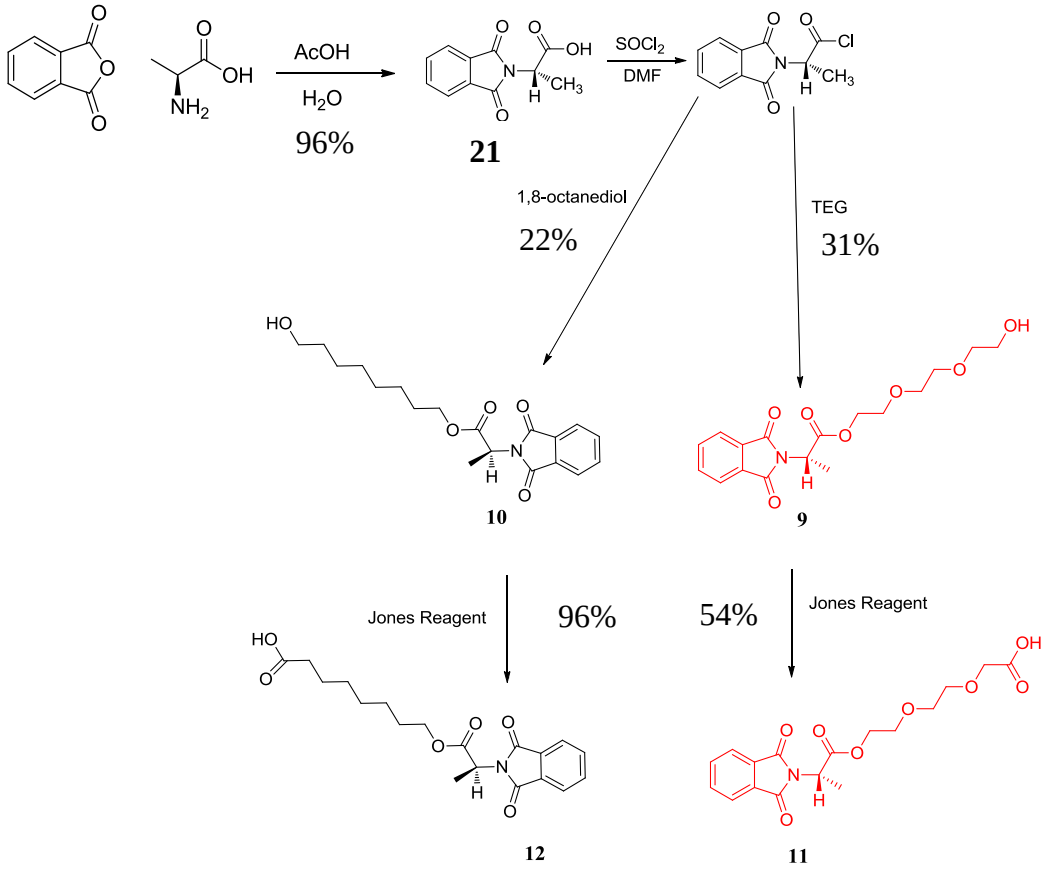

Scheme 8. Synthesis of compounds **11** and **12**.

When the reactions with *L*-alanine were completed, the same reactions were done by using *D*-alanine. The compounds with *D*-alanine were synthesized to compare their behavior with the compounds having *L*-alanine units. Also their chiral selectivity will be

studied. For the synthesis of these compounds, the same procedures were employed; however, due to the limited abundance of *D*-alanine and also its higher cost, smaller amounts were used in these reactions. Again, the alcohols and the carboxylic acids have not been synthesized in the literature until this study (Scheme 9).

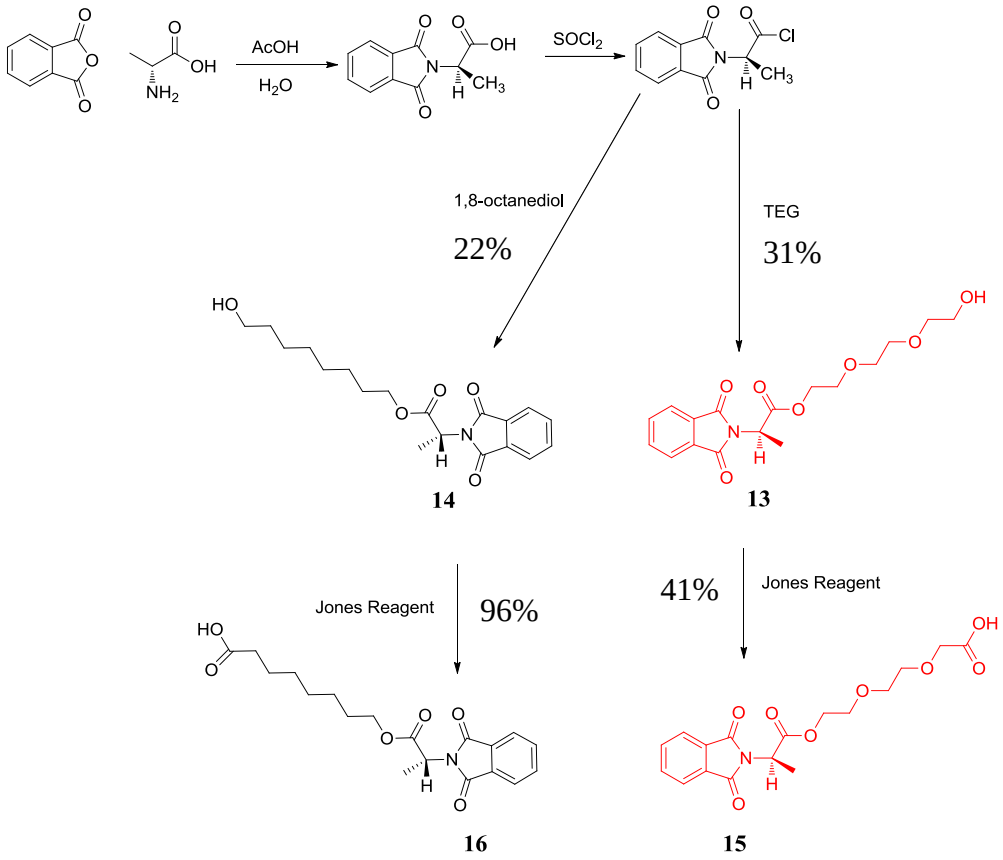

Scheme 9. Synthesis of compounds **15** and **16**.

Additionally, compounds with different chain lengths were wanted to be examined. Ethylene glycol and diethylene glycol were subjected to double addition of the compound **21**. The reason for the synthesis of such compounds was to study the gauche effect. By doing this, it would be possible to predict the conformation of the molecule and accordingly have an idea about the resulting molecular assembly. These two

compounds were synthesized in the same way mentioned above but with double equivalent of the phthalic group. However, the studies on this point are not concluded and will not be mentioned in this thesis. Synthesis of the compounds **24** and **25** are given below.

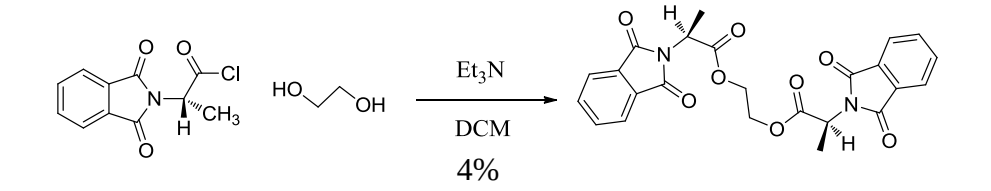

24

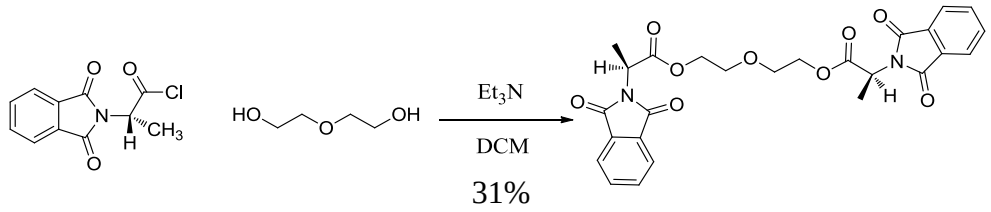

25

Scheme 10. Synthesis of compounds **24** and **25**.

To solidify the compounds, we decided to increase the molecular weights and replaced the phthalic anhydride group with the 1,8-napthalic anhydride. 1,8-Naphthalic anhydride was not purchased but synthesized in the laboratory. The addition reaction between 1,8-naphthalic anhydride and *L*-alanine did not work with the same procedure as that of phthalic anhydride. Most probably, due to the difference in the reactivity of 1,8-naphthalic anhydride and phthalic anhydride (Scheme 11).

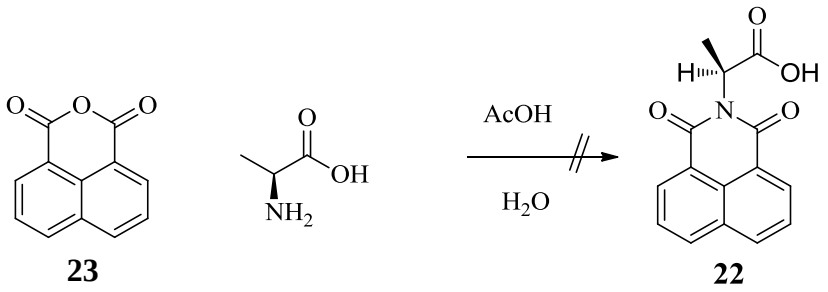

23 **22**

Scheme 11. Synthesis trial of compound **22** with acetic acid.

Therefore, an alternative procedure was found and conducted. The desired compound **22** was obtained successfully as shown in Scheme 12.

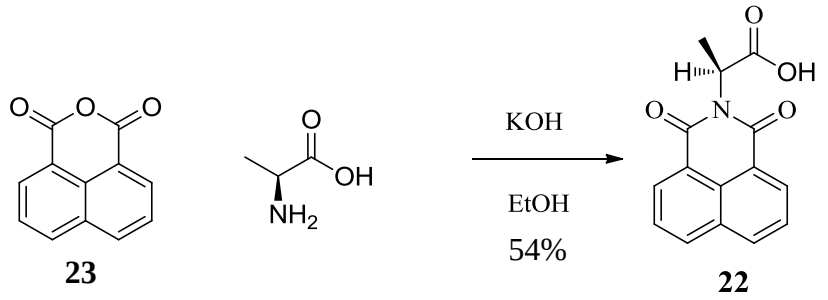

23 **22**

Scheme 12. Synthesis of compound **22**.

After the synthesis of this compound, it was chlorinated and the same procedure was applied as in the case of phthalic anhydride. However, this step did not work with 1,8-naphthalic anhydride group. Moreover, the only product obtained was double addition of acyl chloride to the diol (Scheme 13).

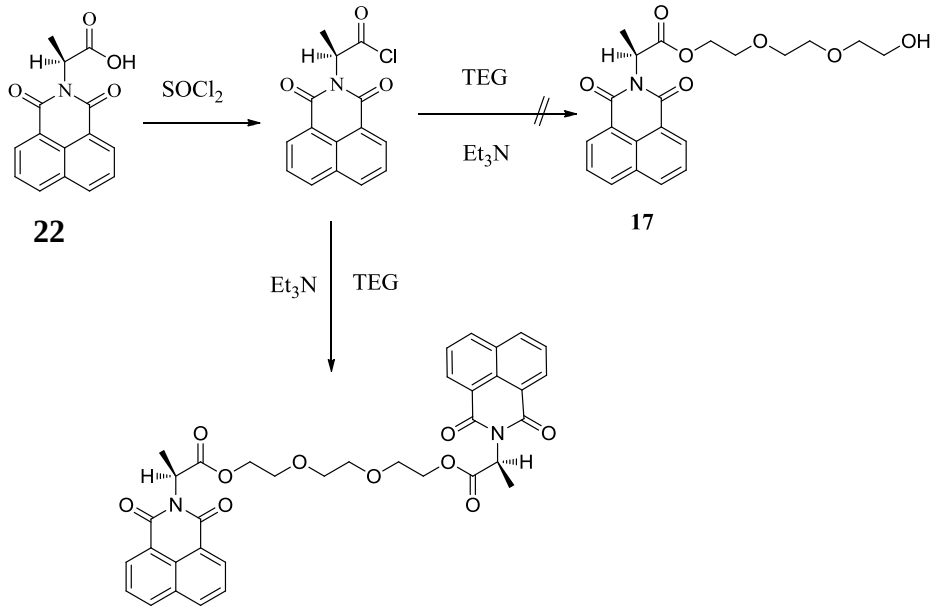

Scheme 13. Synthesis attempt of compound **17** with trimethylamine.

After the failure of this procedure, Steglich esterification reaction was applied. Again the desired compound could not be separated (Scheme 14).

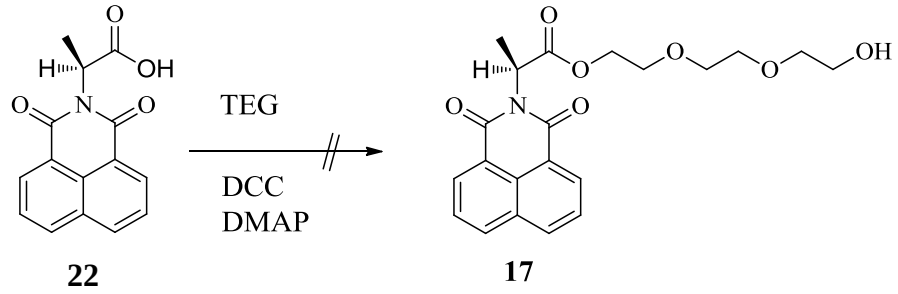

Scheme 14. Steglich Esterification trial for the synthesis of compound **17**.

As an alternative, Mitsunobu Reaction procedure was tested. However, compound **17** could not be separated from this reaction mixture either (Scheme 15).

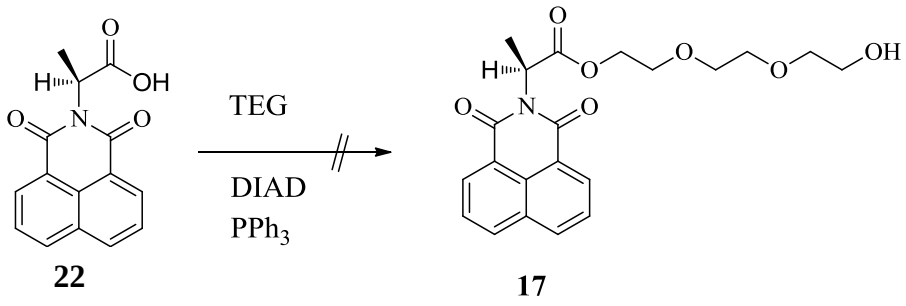

Scheme 15. Mitsunobu Reaction trial for the synthesis of compound **17**.

After all these trials, the chlorination step was excluded and compound **22** reacted with monochlorinated or monotosylated diols in the presence of DBU. This was the most promising procedure and used for the synthesis of the desired compounds (Scheme 16 and 17).

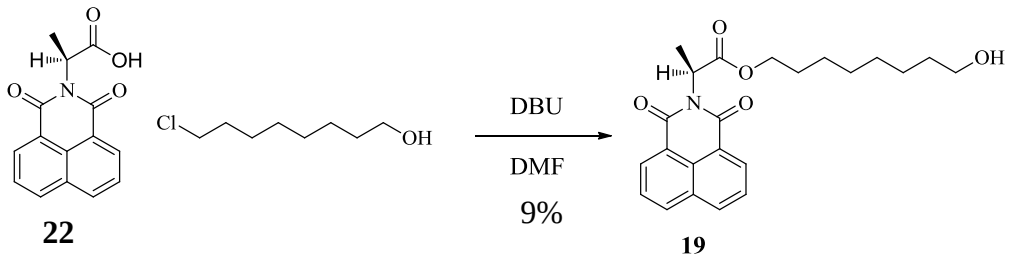

Scheme 16. Synthesis of compound **19**.

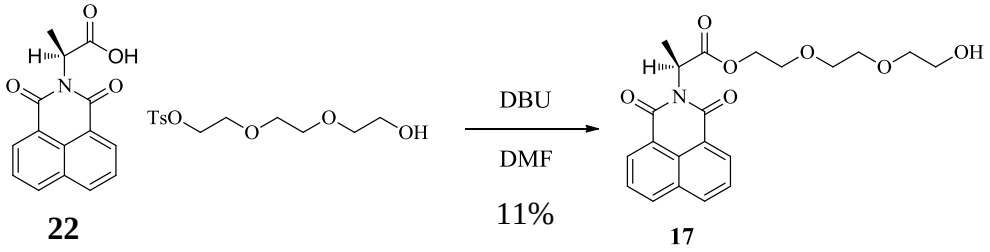

Scheme 17. Synthesis of compound **17**.

The column chromatography of these compounds were even more complicated which resulted in much lower yields, 11% for compound **17** and 9% for compound **19**. As the purification processes were finished, the products were directly oxidized to their carboxylic acid derivatives. Also, compounds **17** and **19**, and their carboxylic acid derivatives are not known in the literature. However, compound **18** could not be isolated. The overall synthesis scheme of these compounds is given below.

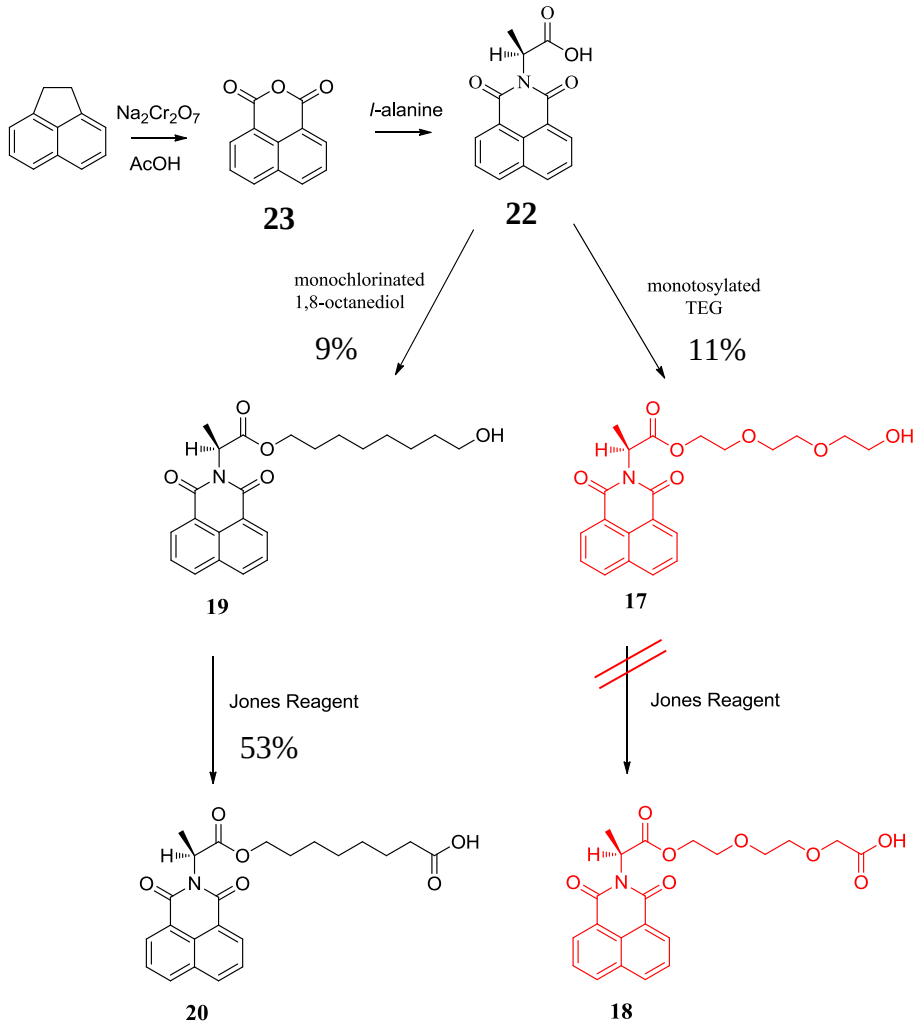

Scheme 18. Synthesis of Compounds **17**, **18**, **19**, and **20**.

3.3. Characterization

The above mentioned compounds were synthesized successfully. The characterization of the molecular structures resulting from these compounds was studied by NMR, UV-VIS, fluorescence, DLS and CD analysis. In the characterization period, the solubility of the compounds played an important role. To give an idea; formic acid, acetic acid, propanoic acid and butyric acid are infinitely soluble in water, on the other hand, from valeric acid ($CH_3(CH_2)_3COOH$) to benzoic acid, the solubility is decreasing from 50g to 3.4g in 1L of water.[35] A similar decreasing trend is also seen in the alcohols. The important point here is that, the solubility in water is decreasing as the number of the carbons in the compound is increasing. With these in mind, the characterization data of the assemblies will be investigated.

3.3.1. NMR Interpretations

First of all, monotosylated triethylene glycol **1** and monotosylated octanol **3** were studied. Their NMR spectra both in $CDCl_3$ and D_2O were compared. When both compounds were in water, their spectra altered significantly. The clear spectra in chloroform-D turned out to be a very complex one showing lots of additional side peaks in D_2O. We interpreted that such a spectrum is a sign of the formation of different aggregates in water. Both **1** and **3** showed such characteristics. When their spectra in D_2O were compared, it was seen that, compound **1** gave a clearer spectrum which is a result of more ordered aggregates due to having differential solvation in water. On the other hand, compound **3** showed more complex peaks in the alkyl region of the spectrum as can be seen in the Figure 18. Still, the clear NMR of monotosylated TEG **3** could either be resulting from more ordered structures or having higher solubility in water. To investigate this further, the carboxylic acid derivatives of these compounds were studied.

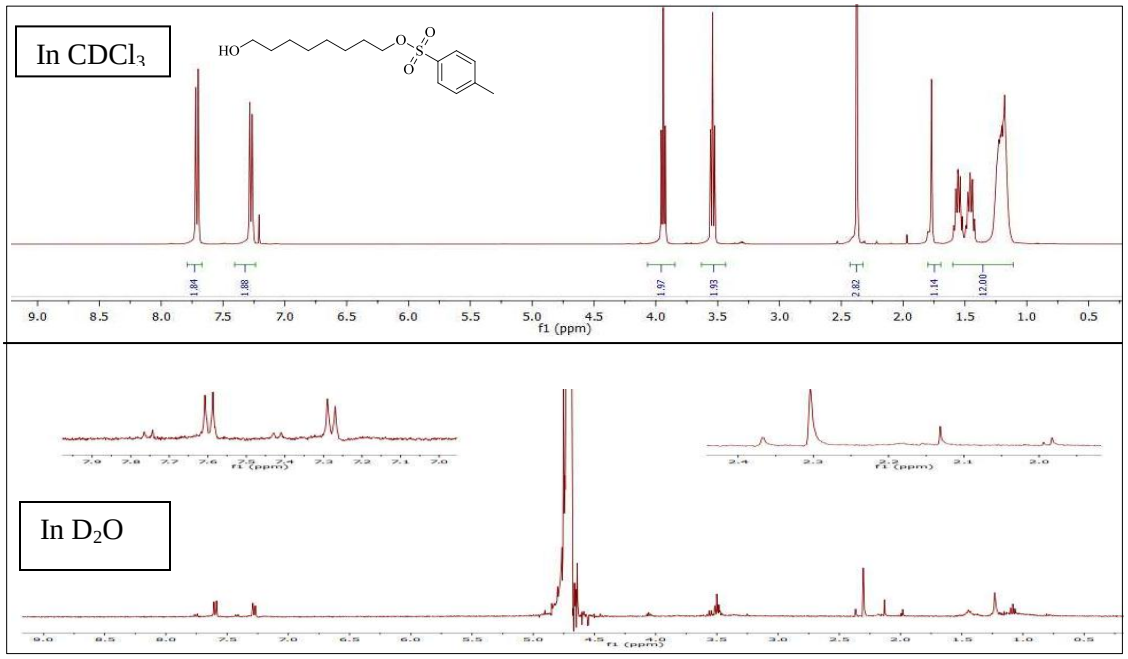

Figure 18. ^{1}H NMR spectra of monotosylated octanol **3** in $CDCl_3$ and D_2O.

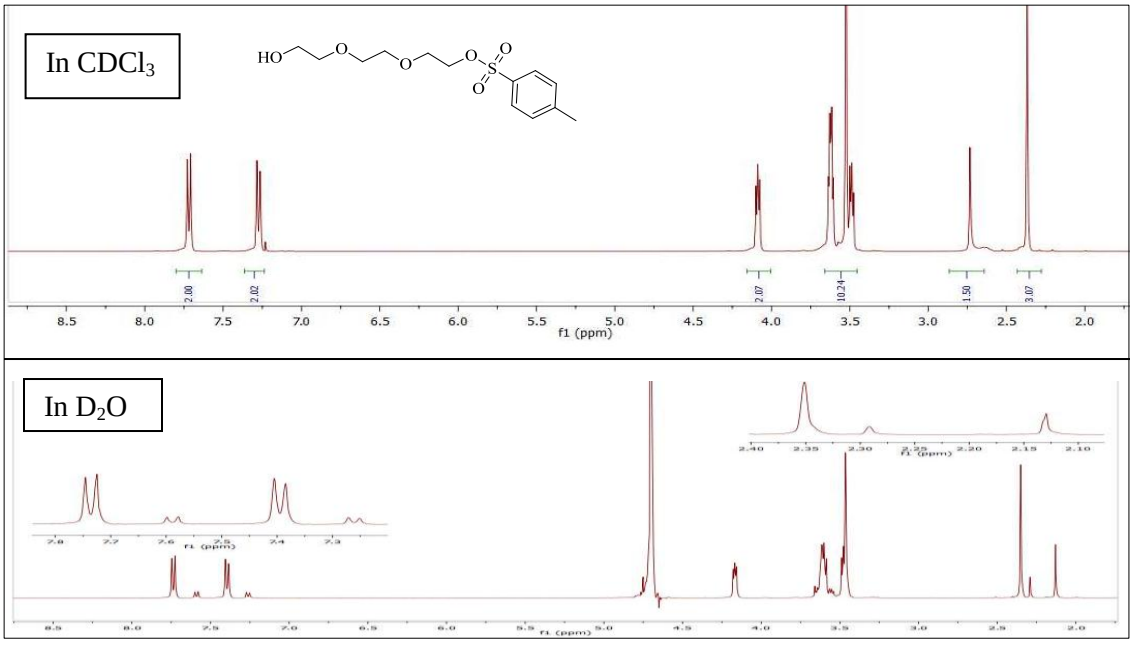

Figure 19. ^{1}H NMR spectra of monotosylated TEG **1** in $CDCl_3$ and D_2O.

The sodium salt of the carboxylic acid derivative of monotosylated octanol **4** showed additional signals in the aromatic region which indicates the presence of different assemblies in water rather than having uniform assemblies. When the sodium salt of the carboxylic acid derivative of monotosylated TEG **2** was examined, the side signals in the aromatic region were diminished significantly. This might mean that compound **2** is able to form more united and ordered molecular structures in water. Also when the relative integrals of the side peaks were compared, compound **2** had much lower values than compound **4**.

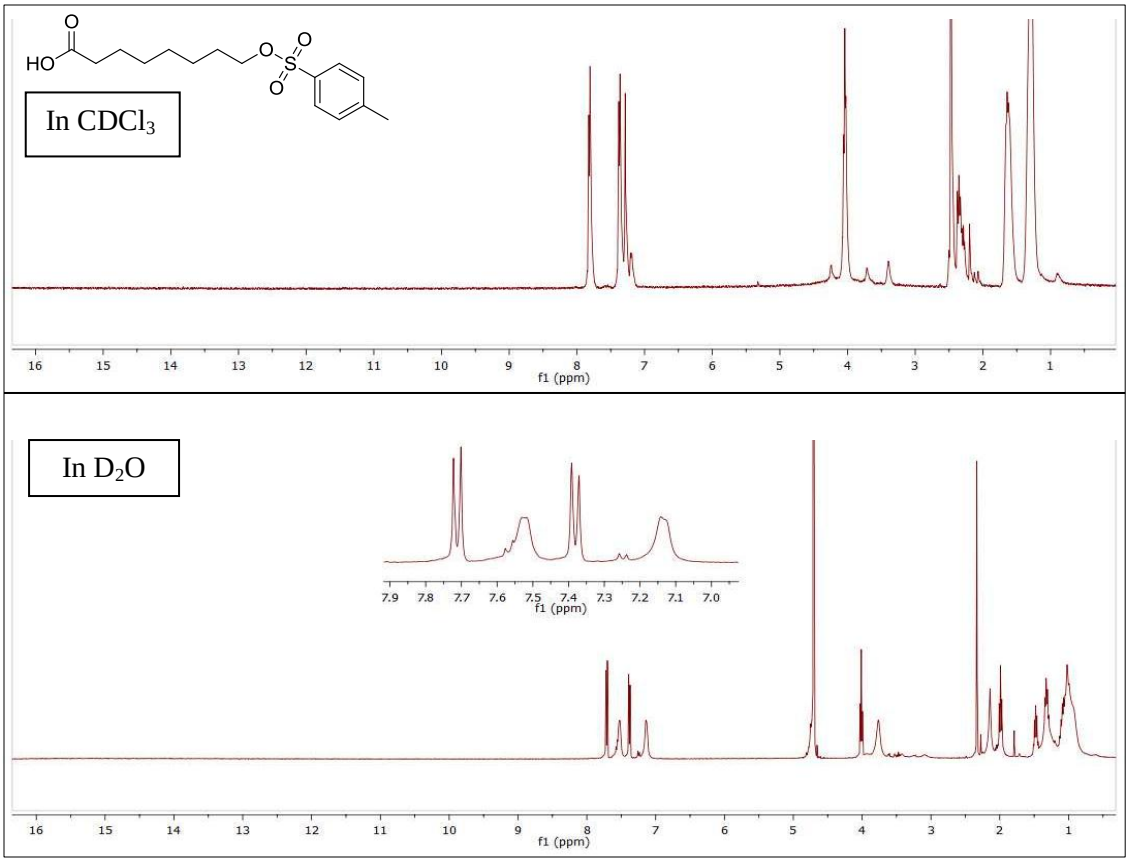

Figure 20. ^{1}H NMR spectra of the sodium salt of compound **4** in $CDCl_3$ and D_2O.

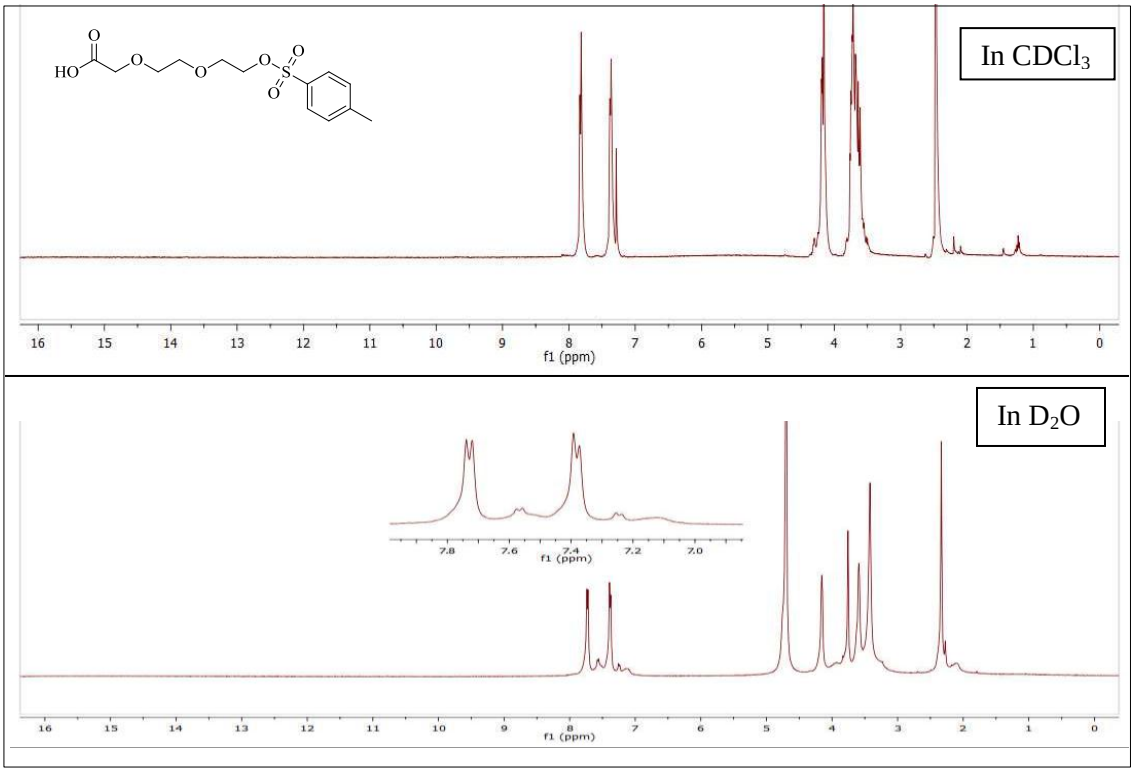

Figure 21. ^{1}H NMR spectra of the sodium salt of compound **2** in $CDCl_3$ and D_2O.

After the study of tosylated compounds, the probe part was switched to phthalic anhydride. In the case of the sodium salt of the carboxylic acid of octanol side chained phthalic anhydride **8**, numerous peaks appeared around 3.6 ppm which is considered as the indications of formation of aggregates. When this was compared with its TEG derivative **6**, protons that belong to TEG chain gave multiplet together with very small side peaks. Also, in the aromatic region, aromatic protons gave a peak more like a singlet unlike the multiplet seen in the octanol case. This is highly due to the formation of a more ordered assembly when the side chain is TEG, and accordingly, molecules stack more efficiently. Therefore, all the aromatic protons were undistinguishable, showed up a singlet-like broad peak. Moreover, when the smaller peaks near the

aromatic signals were integrated, the integrals of compound **6** turned out to be smaller. This indicated that compound **6** formed ordered assemblies to a greater extent. Nevertheless, this could also be due the higher solubility of the TEG side chain over octanol. Even though such points are open to discussion, the data reveal the formation of more ordered aggregates. We expected that due to differential solvation, compound **6** could form an ordered assembly like a helix. These observations support our expectations to some extent.

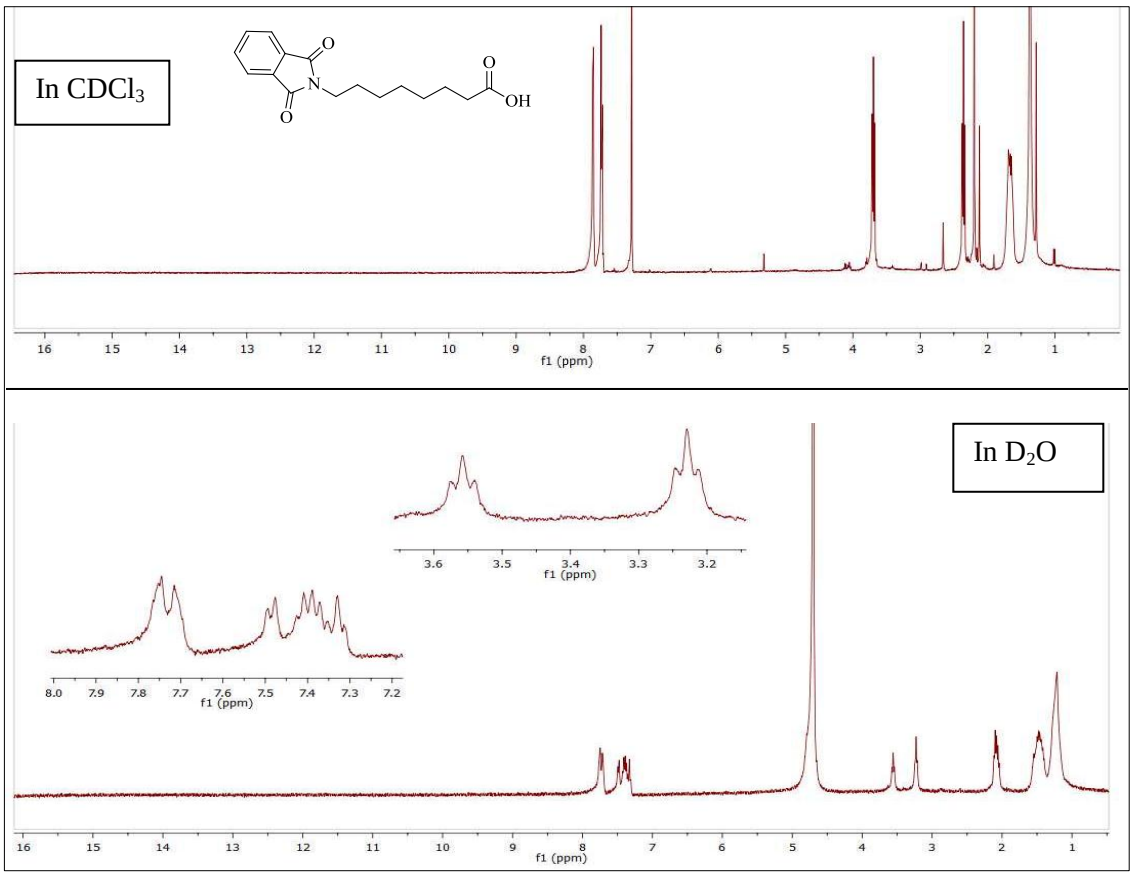

Figure 22. ^{1}H NMR spectra NMR Spectra of the sodium salt of compound **8** in $CDCl_3$ and D_2O.

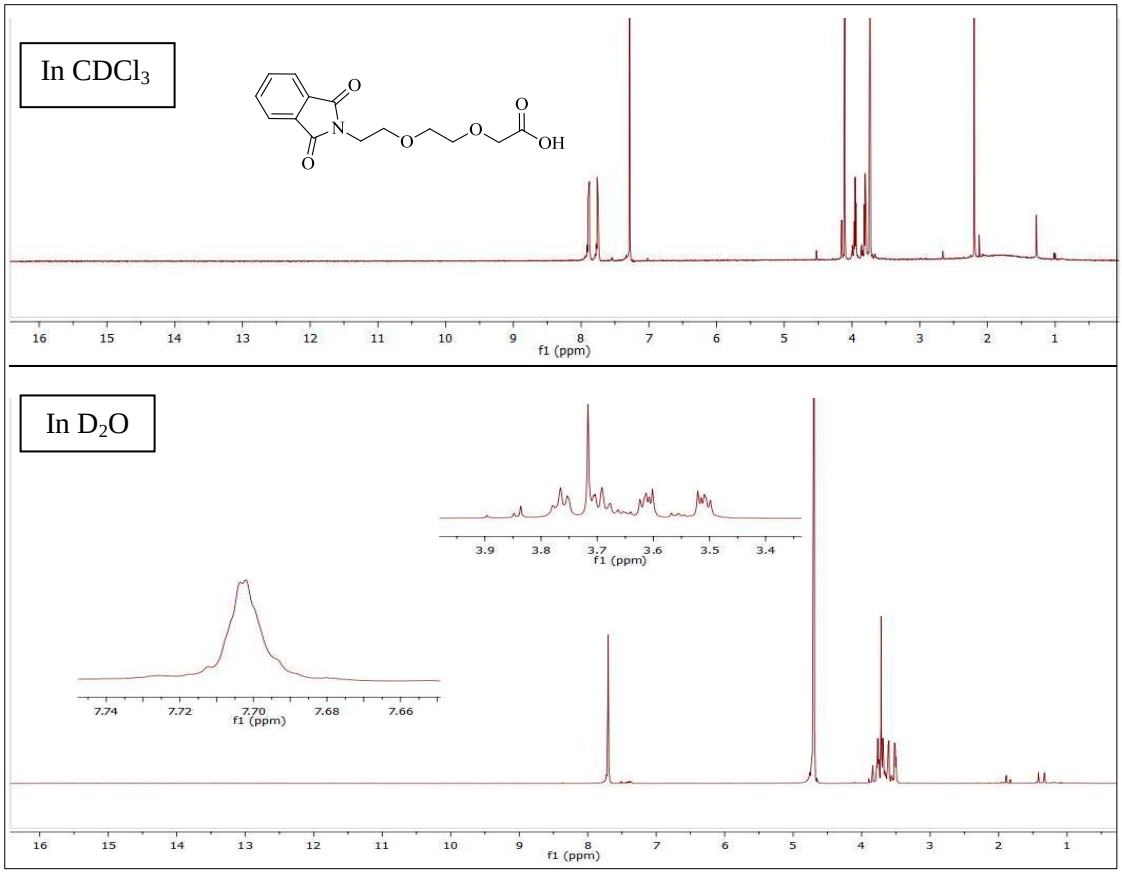

Figure 23. ^{1}H NMR spectra NMR Spectra of the sodium salt of compound **6** in $CDCl_3$ and D_2O.

As to compounds having chiral centers (*L*-alanine and *D*-alanine), the first observation would be that the solubility was decreased in both cases. The alanine unit provided additional carbon atoms and accordingly the solubility in water became less since as the number of carbon atoms increase the water soluble part (alcohol or carboxylic acid unit) become even smaller part of the molecule.[35, 36] The more complex and complicated spectra are signs of this. For the ones having octanol side chain with *L*-alanine (**12**), and *D*-alanine (**16**), we observed line broadening in the alkyl region. Also, in the aromatic region, there are lots of peaks without an order. This is a clear indication of the

formation of aggregates. On the other hand, the ones with the TEG side chains with *L*-alanine (**11**), and *D*-alanine (**15**) again gave more ordered and clear spectra.

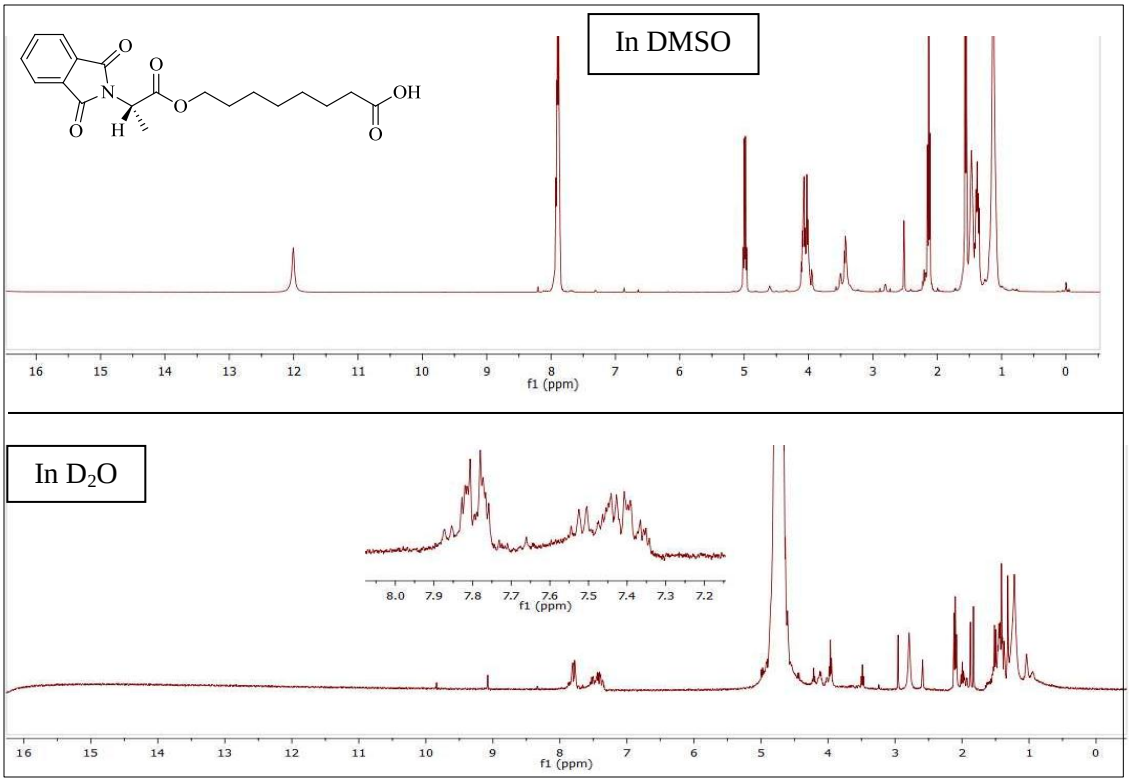

Figure 24. ^{1}H NMR spectra of the sodium salt of the compound **12** in DMSO-d_6 and D_2O.

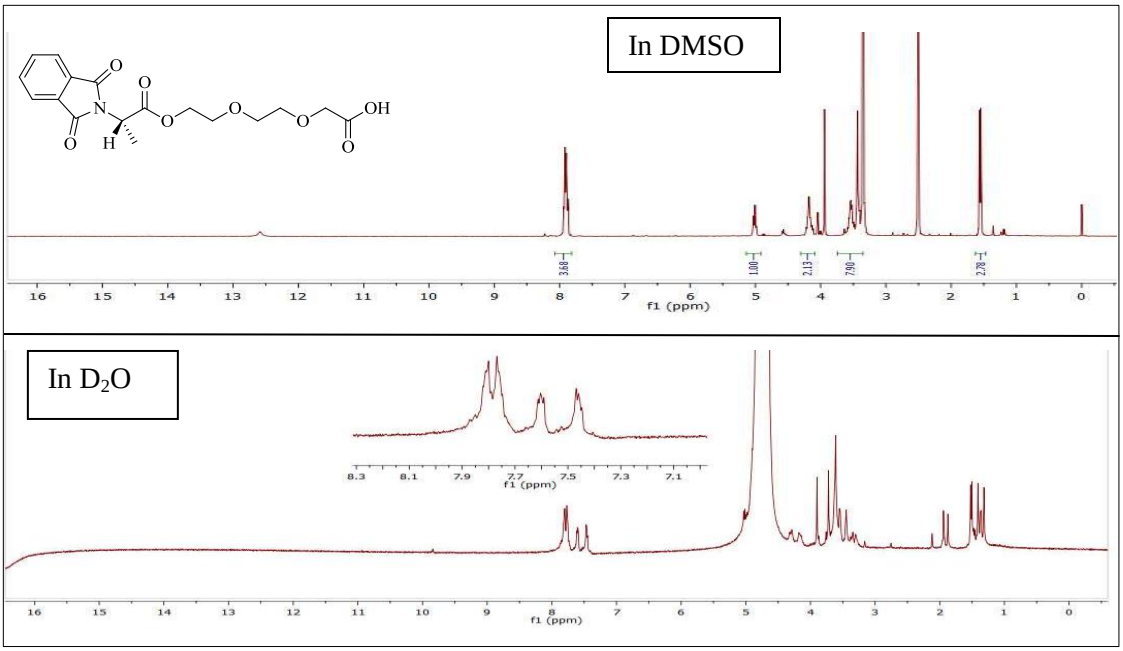

Figure 25. ^{1}H NMR spectra of the sodium salt of the compound **11** in DMSO-d_6 and D_2O.

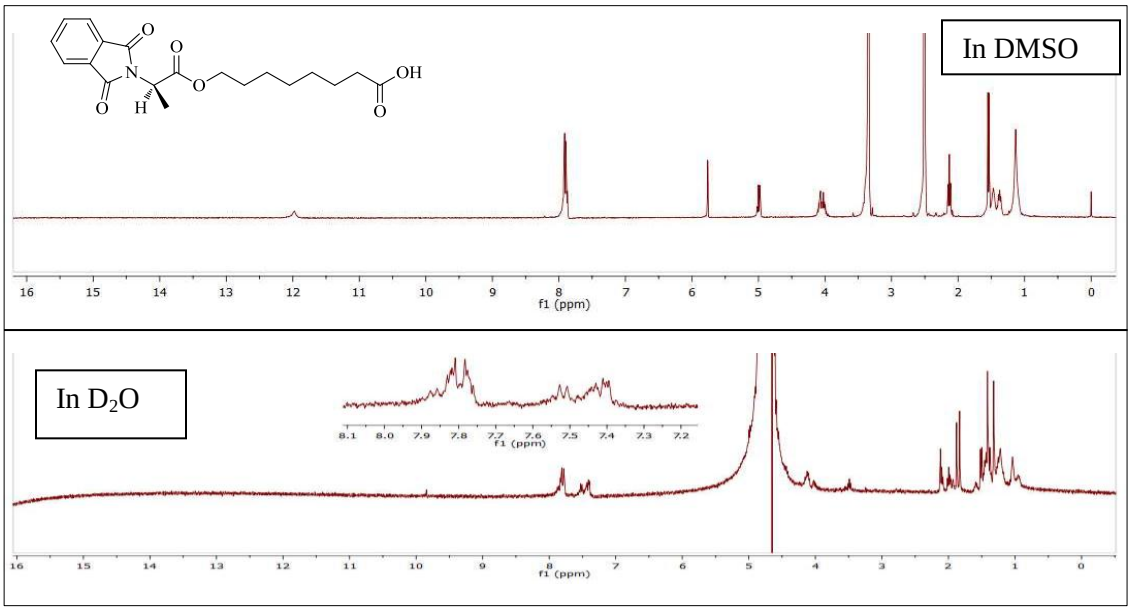

Figure 26. ^{1}H NMR spectra of the sodium salt of the compound **16** in DMSO-d_6 and D_2O.

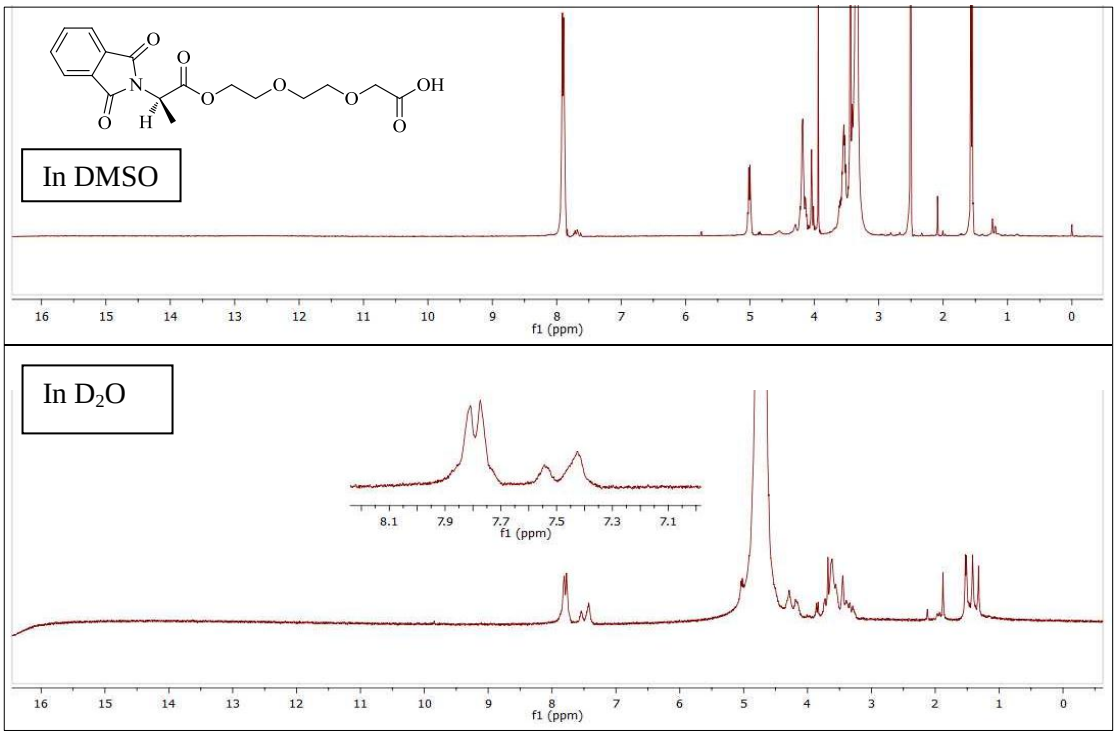

Figure 27. ^{1}H NMR spectra of the sodium salt of the compound **15** in DMSO-d_6 and D_2O.

3.3.2. UV-Vis Interpretations

Scheibe[37] and Jelly [38] observed spectral changes of pseudoiso-cyanine chloride (PIC chloride), shown in Figure 28, in aqueous solutions more than seventy years ago. In their independent studies, they discovered that the absorption maxima shifted to lower energies when the solutions were prepared in water. Such a trend had not been observed in other solvents. Followed by the several different experiments, they both concluded that such spectral changes were reversible upon heating and cooling which showed the self-assembly of PIC compounds. These studies revealed that, the monomeric forms and the self-assembled forms of a compound show spectral differences. Today, aggregates having an absorption maxima shifted to longer wavelengths (bathochromically shifted,

red shifted) with respect to its monomeric absorption maxima are named as Scheibe aggregates or *J-aggregates* (J denotes Jelley). On the other hand, if the shift is towards lower wavelengths (hypsochromic shifted, blue shifted), then the aggregates are called as *H-aggregates*.[39]

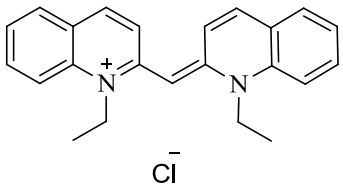

Figure 28. The structure of PIC chloride.

In our case, we expected that the molecules having TEG side chains would form more ordered assemblies in water. Accordingly, a shift in the absorption maxima should be observed in such compounds unlike the ones with the octanol side chain. The more ordered structures are also expected to give narrower spectra.

The UV-Vis analyses below were done with 0.01 M aqueous solutions of the monotosylated compounds, **1** and **3**, and 0.001 M aqueous solutions of the other compounds under study. However, due to the difference in solubility, the concentrations are different. Therefore, we only paid attention to the absorption maxima.

When **1** and **3** were examined, it was seen that the TEG side chained shifted to the longer wavelengths indicating that they formed bigger aggregate than the octanol side chained one.

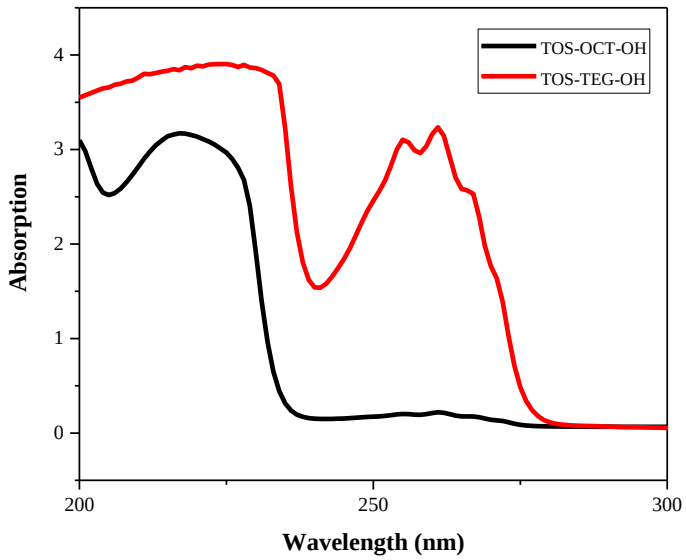

Figure 29. UV-Vis spectra of compounds **1** and **3** in water.

When it comes to the compounds with phthalic anhydride probe, as can be seen in Figure 30, the octane derived compound had two distinct absorption maxima around 300 nm. For the TEG derived one, these two maxima were not separated. This observation showed that aggregations with variety sizes were formed for octane derived compound. For the TEG one, more united aggregates were formed. This observation will be more elaborated in our light scattering experiments (*vide infra*).

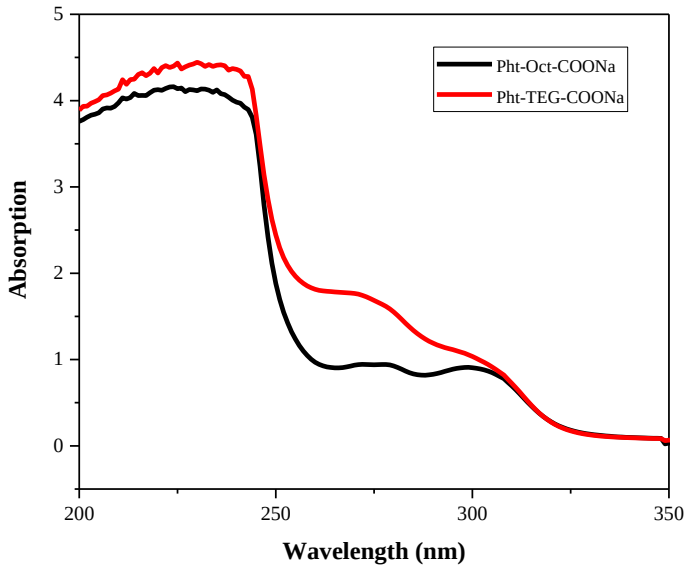

Figure 30. UV-Vis spectra of the sodium salts of compounds **6** and **8** in water.

For the molecules with chiral centers, for both D and L alanine integrated compounds, the ones with TEG side chains gave narrower peaks indicating uniformity of sizes with respect to octane ones. Also compound **11** gave an absorption maxima shifted to longer wavelengths showing that J-aggregates are formed. However, compound **15** did not show such a shift as in the case of **11**. Although they have the same molecular structure, except for the stereochemical configuration, their spectra did not exactly match. The causes of this difference are still not clear.

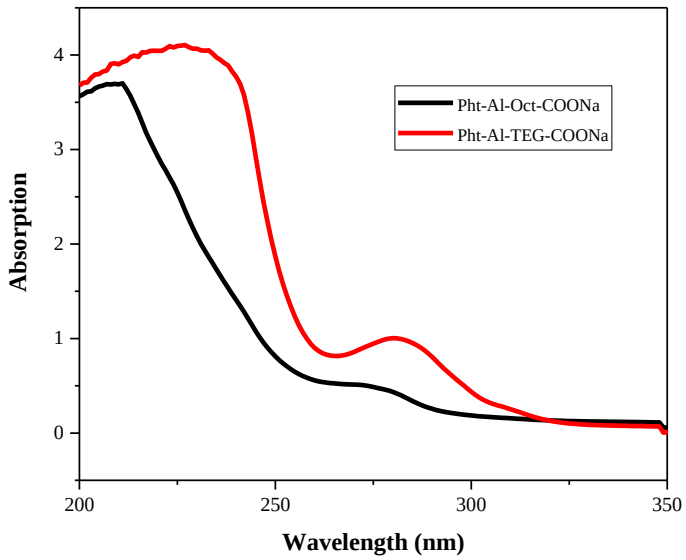

Figure 31. UV-Vis spectra of the sodium salts of compounds **11** and **12** in water.

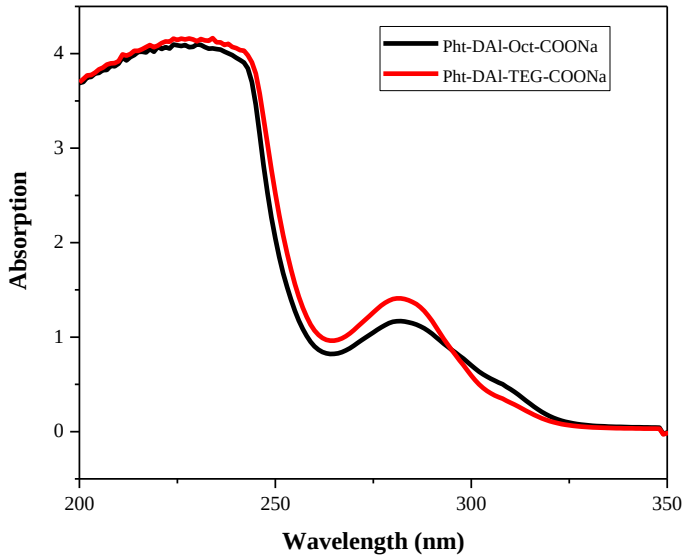

Figure 32. UV-Vis spectra of the sodium salts of compounds **15** and 1**6** in water.

The UV-Vis analyses of the same compounds were done after the solutions were heated to 70^{o}C and cooled back to the room temperature. However, no spectral changes were observed (see Appendix C).

3.3.3. Fluorescence Interpretations

Fluorescence spectra of the samples were studied and analyzed. Unlike the NMR and UV-Vis spectra, TEG side chained and octanol side chained compounds did not show significant differences. However, when the UV-Vis and the fluorescence spectra of the same compound were compared, a large Stock Shift was observed. To our opinion, these shifts indicate the presence of aggregates with variety of sizes. The spectra of the compounds, sodium salts for the acidic ones, in water are given below in the figure.

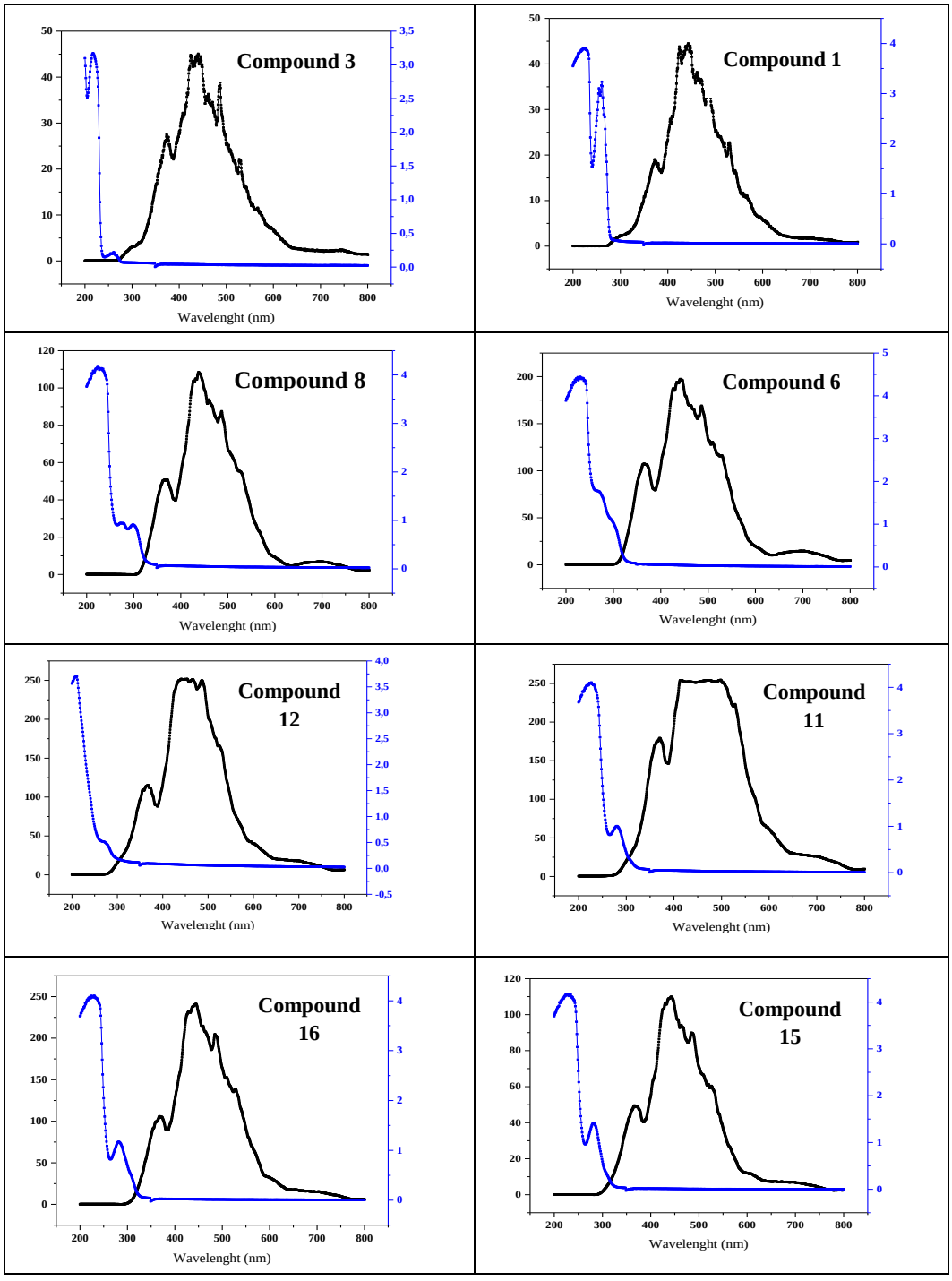

Figure 33. Fluorescence Spectra of the indicated compounds in water.

3.3.4. DLS Interpretations

To measure the size of the formed molecular structures in water, DLS measurements were conducted. The experiments were done in 10 separate runs for each sample, their aqueous solutions, at 25^{o}C. Also their polydispersity index, PDI, were measured and compared during these experiments.

Again, we started with monotosylated compounds **1** and **3**. For compound **3**, monotosylated octanol, we observed a wide variety of size peaks ranging between 257-623 nm. Along with this wide range, PDI values for this sample remained lower than those of compound **1**, monotosylated TEG. This means that, the distribution of the molecular weights of the formed structures is not homogeneous. In other words, compound **3** was only able form micelles with various molecular weights since it did not have the opportunity to form more regular structures due to lack of differential solvation in water. When the DLS analyses of compound **1** were examined, unlike compound **3**, it could form structures with a much smaller size range between 240-358 nm. Moreover, the PDI values are very close to unity and equal to exactly unity for some measurements. To conclude, compound **1** was able to form more regular and homogeneous structures unlike compound **3** due to having differential solvation superiority. The related data are tabulated below.

Table 1. DLS Measurements of compound **3** (on the left) and compound **1** (on the right) at 25 ^{O}C.

Run	PDI	Size Peak (nm)
1	0.865	346.1
2	0.987	257.4
3	0.830	292.0
4	0.617	282.6
5	0.605	453.2
6	0.580	450.9
7	0.452	623.6
8	0.584	477.1
9	0.578	568.5
10	0.441	612.5

Run	PDI	Size Peak (nm)
1	1.000	263.3
2	1.000	240.5
3	1.000	310.4
4	0.811	358.1
5	0.762	350.0
6	0.926	260.0
7	0.712	264.6
8	0.682	289.6
9	0.651	268.8
10	0.809	343.5

For the compounds **6** and **8**, the same trend was also observed. Compound **6** which had the TEG unit gave PDI values closer to unity. When the sizes are compared, it is seen that **6** formed structures with much greater diameters as can be seen in the table below. This may be interpreted as again a consequence of differential solvation. In other words, **6** had the opportunity to gather increased number of molecules resulting in more ordered molecular structures in water. On the other hand, compound **8**, containing octane chain, could not form such structures because it had to collapse immediately into smaller micelles or other similar molecular structures to avoid water.

Table 2. DLS Measurements of compound **8** (on the left) and compound **6** (on the right) at 25 ^{O}C.

Run	PDI	Size Peak (nm)
1	0.683	430.6
2	0.600	538.2
3	0.625	532.6
4	0.457	675.3
5	0.599	653.9
6	0.538	655.4
7	0.609	395.6
8	0.600	306.4
9	0.610	320.0
10	0.532	675.7

Run	PDI	Size Peak (nm)
1	0.818	1461
2	0.847	1122
3	0.992	1073
4	0.970	1403
5	0.908	1269
6	0.766	1379
7	0.754	1487
8	0.965	1234
9	0.643	1368
10	0.876	1347

As it can be seen in size distribution by intensity plots, **8** gave several different peaks for each run; however, compound **6** always gave two peaks in every measurement. Related plots are given in Figure 34.

Chiral molecules **11** and **12**, *L*-alanine introduced, were also examined. Although they did not show such explicit differences like the above mentioned ones, still, compound **11**, with the TEG side chain, yielded more precise data than the compound **12**, with the octane side chain. So, it is still possible to conclude that molecules having differential solvation are able to form more regular assemblies with similar sizes. Related data are given in Table 3.

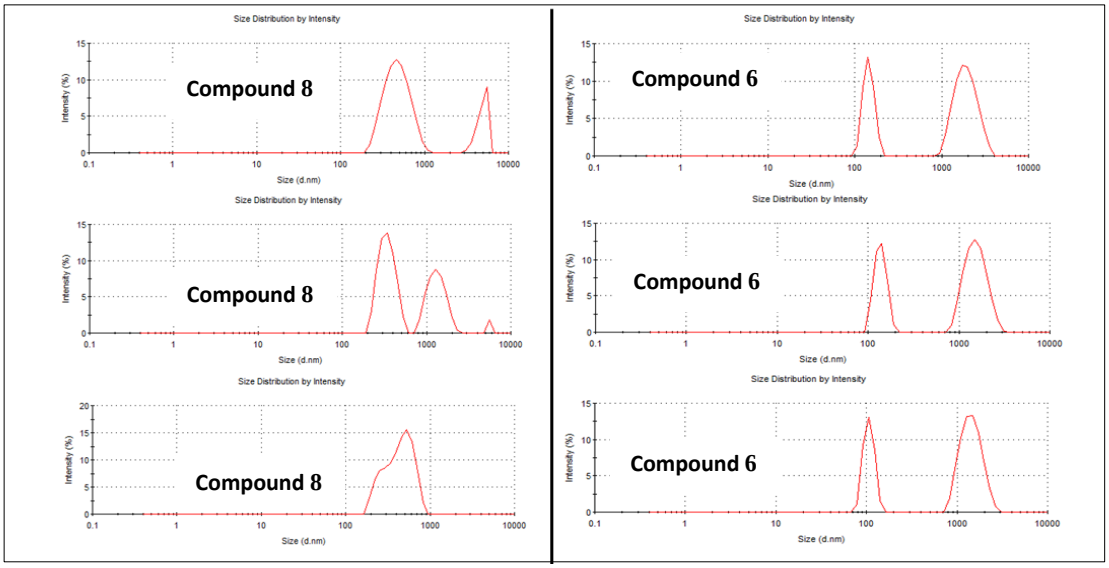

Figure 34. Size Distribution by Intensity plots of **8** and **6** for three different runs.

Table 3. DLS Measurements of compound **12** (on the left) and compound **11** (on the right) at 25 ^{O}C.

Run	PDI	Size Peak (nm)
1	0.636	395.5
2	0.613	295.4
3	0.528	253.2
4	0.730	271.5
5	0.553	478.3
6	0.821	221.9
7	0.494	416.0
8	0.639	344.9
9	0.667	241.9
10	0.723	260.2

Run	PDI	Size Peak (nm)
1	0.456	373.3
2	0.419	300.8
3	0.330	449.0
4	0.515	304.5
5	0.443	351.7
6	0.520	285.9
7	0.399	361.8
8	0.407	396.0
9	0.452	345.2
10	0.512	200.3

Other chiral molecules having *D*-alanine unit yielded unexpected results. Unlike *L*-alanine bearing molecules, compounds **15** and **16** showed opposite outcomes. In this case, compound **16**, the one with the octane chain, had PDI values closer to unity and compound **15** seemed not to show the similar characteristics of the other TEG bearing molecules. Also, when the sizes are compared, **16** has narrower size interval than that of **15**. So, this case remained as an anomaly and the reasons for this behavior need more investigation. The DLS data of these compounds are given in Table 4.

Table 4. DLS Measurements of compound **16** (on the left) and compound **15** (on the right) at 25 ^{O}C.

Run	PDI	Size Peak (nm)
1	0.672	243.6
2	0.727	143.9
3	0.868	134.9
4	0.753	169.1
5	0.492	211.2
6	0.769	136.7
7	0.517	189.4
8	0.597	213.2
9	0.737	164.8
10	0.743	153.4

Run	PDI	Size Peak (nm)
1	0.564	281.6
2	0.742	138.8
3	0.545	218.9
4	0.675	205.0
5	0.543	244.6
6	0.673	168.4
7	0.455	276.3
8	0.518	168.6
9	0.632	222.0
10	0.619	189.2

3.3.5. Circular Dichroism Interpretations

For this thesis, we also aimed to investigate the CD spectra of the compounds under study since such molecular assemblies are widely characterized by this method in the literature as mentioned before. A CD spectrometer measures the difference in the absorbance of right circularly polarized light versus left circularly polarized light. Therefore, the chiral centers in the molecule and accordingly the resulting chiral molecular structures in water play a vital role for this characterization method. We desired to see the spectral differences between the chiral molecules **11**, **12** and **15**, **16** by using a CD spectrometer. However, by the time, we could not afford a CD spectrometer. So, we decided to make our homemade spectrometer.

For this purpose, we used some special equipment like a Rochon polarizer and a λ/4 retarder. Other than these, a deuterium lamp as light source is used. The light coming out of the source reaches to the Rochon polarizer and the polarized light goes through the λ/4 retarder which turns the linearly polarized light into the circular polarized light. The resulting circularly polarized light goes to the sample and reaches to the detector. Each part is attached to one another with fiber optic cables. A basic block diagram of the homemade spectrometer is given in Figure 35.

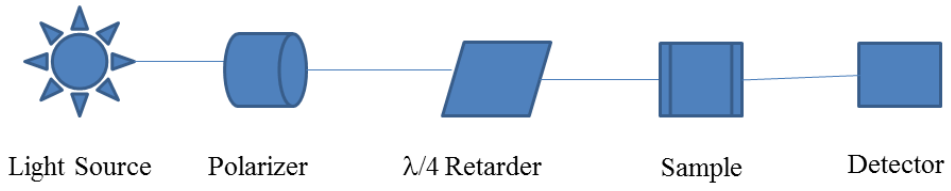

Figure 35. The block diagram of the homemade CD spectrometer.

It is very similar to conducting an absorbance measurement, however; we had to change the orientation of the light to take the difference in the absorbance of the right and left circularly polarized light. By doing this, it would be possible to send right circularly polarized light and left circularly polarized light each time. To achieve this, a special device was attached to the polarizer which helps to change the orientation of the polarizer by 90^{o}. If the light sent at 0^{o} is left then the one perpendicular to it is right circularly polarized. A photograph of our CD spectrometer is given in Figure 36.

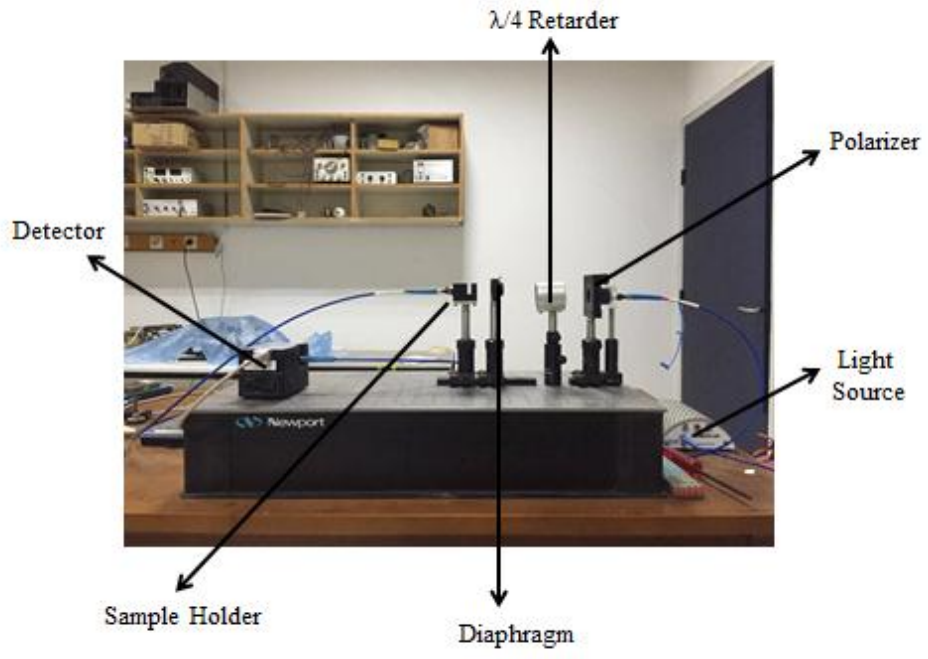

Figure 36. A photograph of the homemade CD spectrometer.

The measurements were done as follows; the absorbance data are taken as it is done with a UV-Vis instrument. When the first measurement is finished, the polarizer's position is altered by 90^{o} and another absorbance measurement is done. So, at the end we have the

absorbance data for the right circularly polarized light and one for the left circularly polarized light. In a CD measurement, the difference between these two is seen. To do this, we basically subtracted the two absorbance data from one another. As a result, we could draw a $\Delta\varepsilon$ vs wavelength plot.

To compare our results, CD measurements were also conducted with a commercial spectrometer in UNAM at Bilkent University. Before examining our compounds, we wanted to test the instrument with known chiral compounds and compared the spectra of 0.02M camphor solution in ethanol. Below, the spectrum taken in UNAM and the spectrum taken by the homemade spectrometer are given. The maximum of the curve for the spectrum taken with a commercial spectrometer is at 294.0 nm and 294.5 nm for the one taken with the homemade one as seen in the figure. This shows that the homemade one is promising. However, due to the difficulties in increasing signal to noise ratio, our curve is not very smooth. That is why polynomial fitting is applied to the data and compared afterwards. Moreover, with our equipment, it was not possible to make reliable measurements at wavelengths lower than 250 nm. Therefore, we could not see the Cotton effect as it is seen in the spectrum taken in UNAM. They had the opportunity to measure the absorbance in shorter wavelengths. Accordingly, only the data for 250 nm and higher wavelengths are compared.

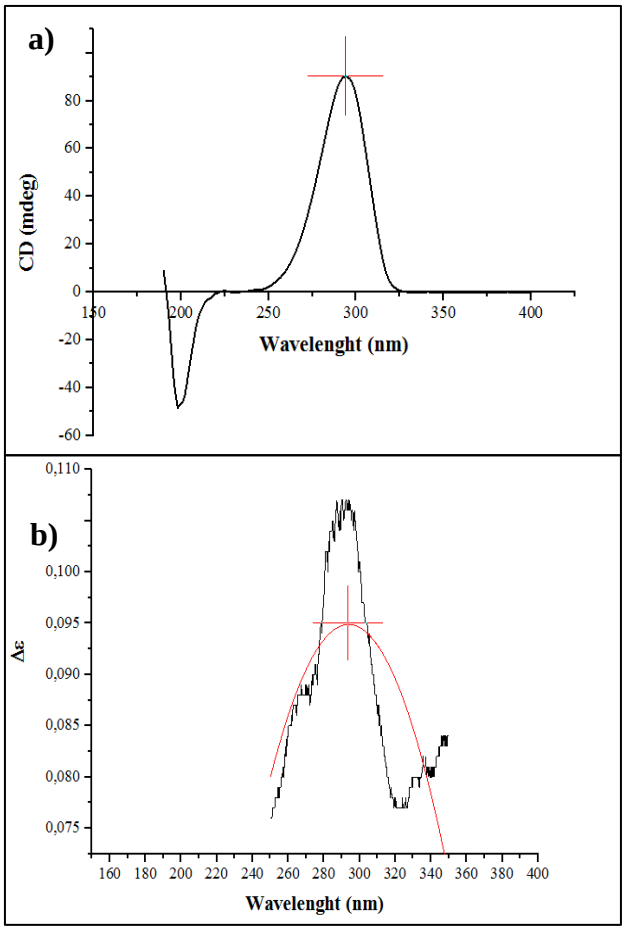

Figure 37. The CD spectrum taken in UNAM (**a**) and by the homemade spectrometer (**b**)

When it comes to our compounds, we had problems with having consistent data. Spectra tend to change for each measurement. Even for the successive measurements of the same compound did not match with each other. This problem was encountered both in data taken from the commercial instrument and the homemade one. We kept measuring the samples, however; each measurement was different from one another. Then, it was thought that this could be a clue rather than a problem. The reason for the difference in the spectra could be resulting from the fact that the systems formed by the compounds

under study in water are *dynamic*. The molecular structures could be assembling and disassembling continuously. Still, to fully understand the system's behavior, more analyses should be conducted. The selected spectra of the aqueous solutions of the sodium salts of compounds **11**, **12**, **15** and **16**, taken with the commercial instrument, are given below.

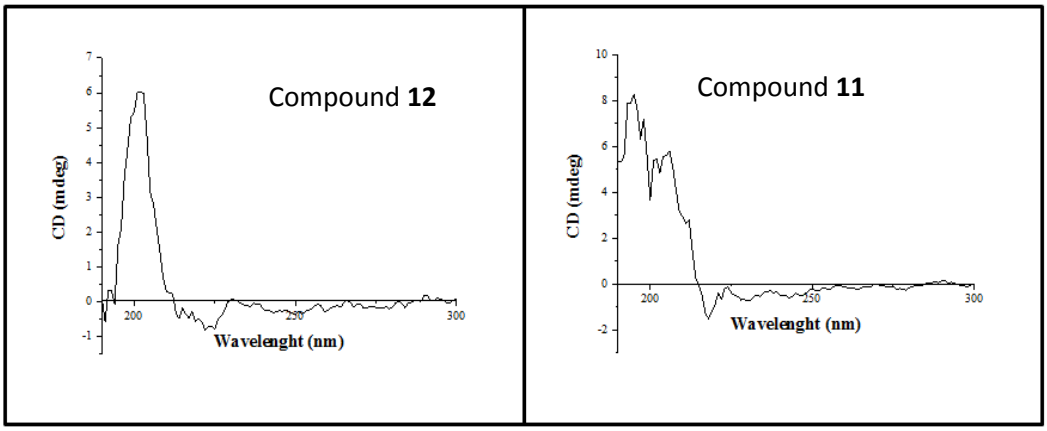

Figure 38. CD spectra of compounds **12** and **11.**

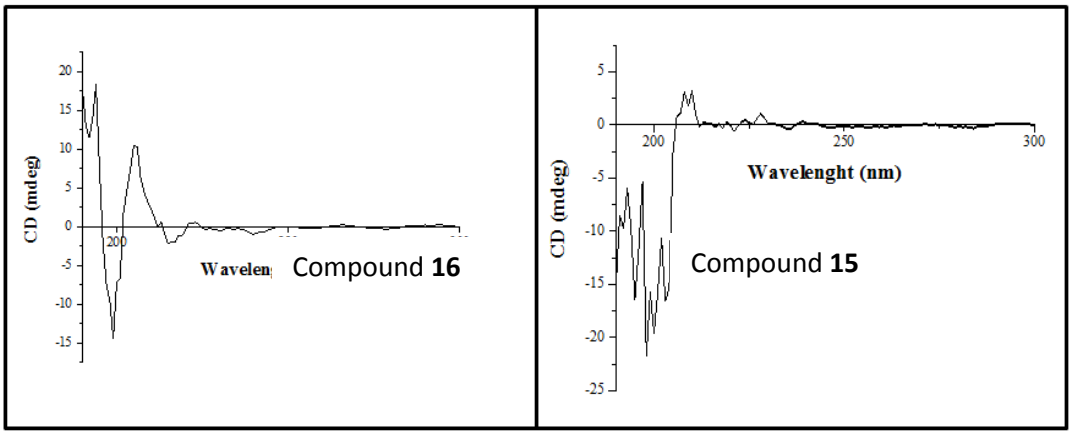

Figure 39. CD spectra of compounds **16** and **15.**

CHAPTER 4

CONCLUSION

In this thesis, differential solvation, a new concept, was introduced. Differential solvation suggests that molecular assemblies, that can be either high ordered structures or low ordered random assemblies, are formed in aqueous media by solvation derived reasons. Therefore, hydrophobic and hydrophilic interactions are the main points of this study. Whether such assemblies are formed or not due to differential solvation were analyzed by several physical methods.

To exploit this concept, we designed several molecules which theoretically show differential solvation in water. For such compounds, triethylene glycol (TEG) side chains were added. To compare the effect of differential solvation, we designed and synthesized several compounds which theoretically do not show differential solvation, and for such compounds 1,8-octanediol side chains were added. Desired compounds were synthesized and characterized successfully, and by using empirical methods, above mentioned theoretical expectations were tried to be proven.

Supporting the preliminary expectations, molecules having TEG side chain, expected to exhibit differential solvation in water, showed several different outcomes in any spectral data. They manifested red shifts in UV-Vis spectra indicating the formation of J-aggregates, by π-π stacking, more regular peak and splitting patterns in NMR, large Stock Shifts in fluorescence, and narrower size range and more uniform molecular weight distribution in DLS. Also CD analysis showed that these molecular systems are

dynamic giving different spectra in each measurement. For all spectral analyses, the data are consistent with each other. These strongly support the effect of differential solvation. However, only the compounds having *D*-alanine as chiral input showed unexpected results. For these compounds, the ones with the TEG side chain acted as not having differential solvation and accordingly formed less ordered molecular structures. On the other hand, the compounds having *L*-alanine did not give such unexpected results. It is possible to conclude that there is an anomaly for the compounds with *D*-alanine units. Unfortunately, the reasons for this behavior are not well known and need more investigation.

The chiral selectivity of the molecular assemblies is an important point. It was expected that such systems would show chiral self-sorting. In other words, the systems would not accept the molecules having opposite stereochemical configuration into the system and the ones with the same stereochemical configuration would be accepted. This part of the concept will be examined in future studies after the molecular assemblies are improved.

During this study, also a CD spectrometer was built. The major problem was the very low intensity of the resulting circularly polarized light and accordingly very low signal to noise ratio. To improve this, a more powerful light source is needed and also the optical components must be more closely located to prevent the loss of light on the path. However, the current spectrometer can measure the absorbance data, but when it is compared to a commercial spectrometer it needs more improvement. As future studies, a more compact and sensitive instrument is planned to be built with improved optical components.

To conclude, differential solvation is a very promising concept.With the current findings in this thesis and with the above mentioned future studies, it will be more sound and significant in the science of molecular assembly.

CHAPTER 5

EXPERIMENTAL SECTION

5.1. General Methods

All reagents were used as purchased from Sigma Aldrich without further purification. Proton nuclear magnetic resonance spectra (^{1}H NMR) were recorded on Bruker Avance III Ultrashield with 400 MHz and chemical shifts are reported in parts per million (ppm) downfield from TMS, using residual $CDCl_3$, DMSO-d_6 and D_2O as internal standards. The ^{13}C NMR spectra were recorded on the same instrument with 100 MHz and are reported in ppm using solvent as an internal standard ($CDCl_3$ or DMSO-d_6). Column chromatography was performed on silica gel (0.063-0.200 mm). TLC was carried out on 0.2 mm silica gel 60 F254 analytical aluminum plates. High resolution Mass spectra were recorded by Waters SYNAPT MS System.

Chemicals and all solvents were commercially available and used without further purification. Infrared (IR) spectra were recorded in the range 4000-500 cm-1 via ATR diamond. IR spectra of the synthesized compounds are given in Apendix B. Fluorescence measurements were done with PERKIN ELMER- LS 55 Luminescence Spectrometer. UV-Vis measurements were conducted by CARY 100 BIO UV-Vis spectrometer. DLS measurements were analyzed with MALVERN Zeta Sizer with the beam wavelength of 633 nm. CD analyses were done in UNAM at Bilkent University by using JASCO J-815 CD Spectrometer within 190-400 nm. Melting points were

measured on Stuart SMP11 melting point apparatus and were uncorrected. Evaporation of solvents was performed at reduced pressure, using a rotary vacuum evaporator.

5.2. Synthesis of 2-(2-(2-hydroxyethoxy)ethoxy)ethyl-4-methylbenzenesulfonate (1)[40]

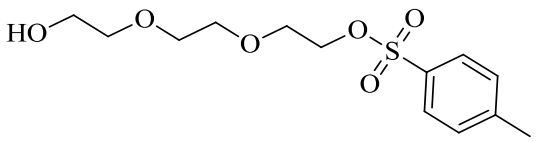

1

NaOH (0.4 g, 0.01 mol) was dissolved in 10 mL water and added to the solution of triethyleneglycol (8.9 mL, 0.07 mol) in 25 mL THF. Solution was stirred at 0 ^{o}C until complete dissolution. To this solution, tosyl chloride (1.3 g, 7.00 mmol) dissolved in THF was added dropwise over 1.5h. Solution was stirred for another 1.5 hours then, added to the ice cold water and extracted with DCM. Organics were collected and dried over $MgSO_4$ and concentrated under vacuum. The product was obtained as pale yellow oil (1.54 g, 72.28%). ^{1}H NMR ($CDCl_3$): δ 7.71 (d, *J*= 8.3, 2H), 7.27 (d, *J*= 8.0, 2H), 4.09 (t, *J*= 4.82, 2H), 3.69- 3.59 (m, 4H), 3.57-3.45 (m, 6H), 2.73 (s, 1 H), 2.37 (s, 3H)

5.3. Synthesis of 2-(2-(2-(tosyloxy)ethoxy)ethoxy)acetic acid (2) [41]

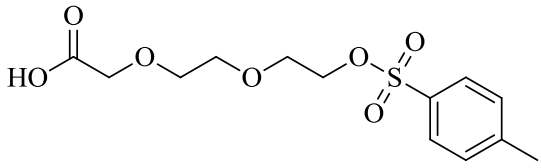

2

2-(2-(2-Hydroxyethoxy)ethoxy)ethyl 4-methylbenzenesulfonate (**1**, 0.79 g, 2.60 mmol) was dissolved in 5 mL acetone and cooled down to 0^{o}C. Jones reagent (prepared by mixing 0.5g CrO_3, 0.5 mL H_2SO_4 and 1.5 mL H_2O) was added slowly until the green

color of the solution turned into persistent orange color. To destroy the excess Jones reagent, isopropyl alcohol was added and the solution turned green again. Sodium bicarbonate was added to neutralize the solution and the solids were filtrated off. Filtrate was concentrated under vacuum and the residue was dissolved in ether and extracted with brine and then water. Organics were collected, dried on $MgSO_4$ and concentrated under vacuum. The product was obtained as brown oil (0.33 g, 39.87%). ^{1}H NMR ($CDCl_3$): δ 7.83 (d, *J*= 8.0, 2H), 7.37 (d, *J*= 7.44, 2H), 4.36- 4.00 (m, 4H), 3.79- 3.55 (m, 6H), 2.47 (s, 3H)

5.4. Synthesis of 8-hydroxyoctyl-4-methylbenzenesulfonate (3) [40]

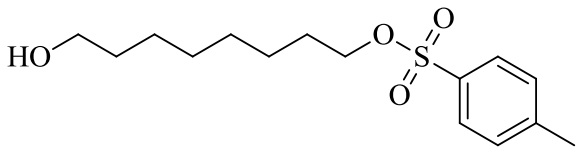

3

NaOH (0.14 g, 3.42 mmol) was dissolved in 5 mL water and added to the solution of 1,8-octanediol (0.5 g, 3.42 mmol) in 20 mL THF. Solution was stirred at 0 ^{o}C until complete dissolution. To this solution, tosyl chloride (0.65 g, 3.42 mmol) dissolved in 15 mL THF was added dropwise over 1.5h. Solution was stirred for another 2 hours then, added to the ice cold water and extracted with DCM. Organics were collected and dried over $MgSO_4$ and concentrated under vacuum. The product was obtained as as pale yellow oil (0.24 g, 23.36%). ^{1}H NMR ($CDCl_3$): δ 7.71 (d, *J*= 8.3, 2 H), 7.27 (d, J= 8.0, 2 H), 3.94 (t, *J*= 6.5, 2H), 3.54 (t, *J*= 6.6, 2H), 2.38 (s, 3H), 1.78 (s, 1H), 1.61-1.40 (m,4H), 1.28-1.12 (m, 8H).

5.5. Synthesis of 8-(tosyloxy)octanoic acid (4) [41]

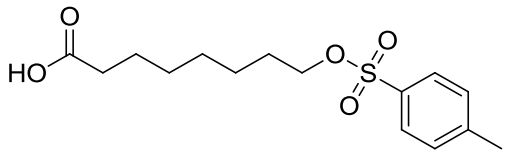

4

8-Hydroxyoctyl-4-methylbenzenesulfonate (**3**, 0.302 g, 1.01 mmol) was dissolved in 5 mL acetone and cooled down to 0^{o}C. Jones reagent (prepared by mixing 0.5g CrO_3, 0.5 mL H_2SO_4 and 1.5 mL H_2O) was added slowly until the green color of the solution turned into persistent orange color. To destroy the excess Jones reagent, isopropyl alcohol was added and the solution turned green again. Sodium bicarbonate was added to neutralize the solution and the solids were filtrated off. Filtrate was concentrated under vacuum and the residue was dissolved in ether and extracted with brine and then water. Organics were collected, dried on $MgSO_4$ and concentrated under vacuum. The product was obtained asa highly viscous yellow oil (0.26 g, 81.88%). ^{1}H NMR ($CDCl_3$): δ 7.81 (d, *J*= 7.19, 2H), 7.37 (d, *J*=7.19, 2H), 4.04 (t, *J*= 6.45, 2H), 2.48 (s, 3H), 2.40-2.26 (m, 2H), 1.71-1.28 (m, 10H).

5.6. Synthesis of 2-(2-(2-(2-hydroxyethoxy)ethoxy)ethyl)isoindoline-1,3-dione (5) [42]

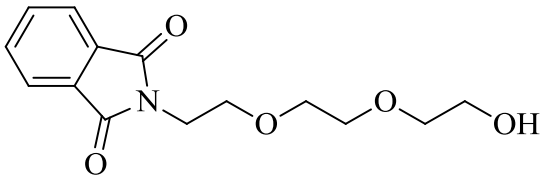

5

2-(2-(2-Hydroxyethoxy)ethoxy)ethyl 4-methylbenzenesulfonate (**1**, 1.32 g, 4.31 mmol) was dissolved in 30 mL DMF and potassium phthalimide salt (1.04 g, 5.60 mmol) was added. To accelerate the reaction, a pinch of KI was added and heated to 95^{o}C and

stirred for 2 hours. The mixture was then concentrated under vacuum to remove DMF. The residue was diluted with ethyl acetate and extracted with water and brine. Organics were collected, dried on $MgSO_4$ and concentrated under vacuum. Column chromatography with ethyl acetate:hexane (1:2) gave the desired product. The product was obtained as viscous pale yellow oil (0.67 g, 55.66%). ^{1}H NMR ($CDCl_3$): δ 7.93-7.83 (m, 2H), 7.80- 7.69 (m, 2H), 3.94 (t, *J*= 5.61, 2H), 3.78 (t, *J*= 5.63, 2H), 3.72- 3.50 (m, 8H).

5.7. Synthesis of 2-(2-(2-(1,3-dioxoisoindolin-2-yl)ethoxy)ethoxy)acetic acid (6) [43]

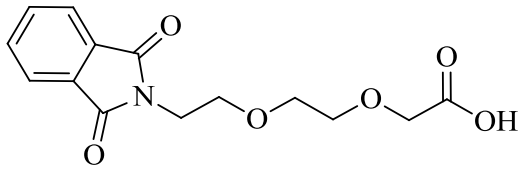

6

2-(2-(2-(2-Hydroxyethoxy)ethoxy)ethyl)isoindoline-1,3-dione (**5**, 0.25 g, 0.89 mmol) was dissolved in acetone and stirred at 0^{o}C. To this solution Jones Reagent (prepared by mixing 0.5g CrO_3, 0.5 mL H_2SO_4 and 1.5 mL H_2O) was added dropwise. After addition, the mixture was stirred for 20 minutes at 0^{o}C. Then, the mixture was put into cold water and extracted with diethyl ether. Organics were collected, dried on $MgSO_4$ and concentrated under vacuum. The product was obtained as white crystals (0.01g, 36.57%). mp 94-96^{o}C. ^{1}H NMR ($CDCl_3$): δ 7.92-7.85 (m, 2H), 7.79- 7.72 (m, 2H), 4.11 (s, 2H), 4.02- 3.62 (m, 8H)

5.8. Synthesis of 2-(8-hydroxyoctyl)isoindoline-1,3-dione (7) [42]

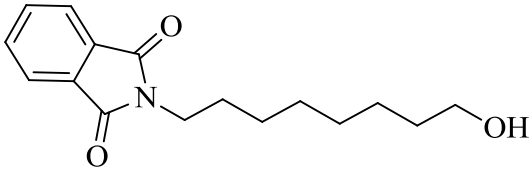

7

8-Hydroxyoctyl 4-methylbenzenesulfonate (**3**, 0.5 g, 1.67 mmol) was dissolved in 15 mL DMF and potassium phthalimide salt (0.4 g, 2.18 mmol) was added. To accelerate the reaction, a pinch of KI was added and heated to 95^{o}C and stirred for 2 hours. The mixture was then concentrated under vacuum to remove DMF. The residue was diluted with ethyl acetate and extracted with water and brine. Organics were collected, dried on $MgSO_4$ and concentrated under vacuum. Column chromatography with ethyl acetate:hexane (1:5) gave the desired product as white powder (0.24 g, 54.48%). mp 63-65^{o}C. ^{1}H NMR ($CDCl_3$): δ 7.83- 7.76 (m, 2H), 7.72- 7.63 (m, 2H), 3.73- 3.68 (t, *J*= 7.31, 2H), 3.67-3.62 (t, *J*= 6.62, 2H), 1.75- 1.36 (m, 12H)

5.9. Synthesis of 8-(1,3-dioxoisoindolin-2-yl)octanoic acid (8) [43]

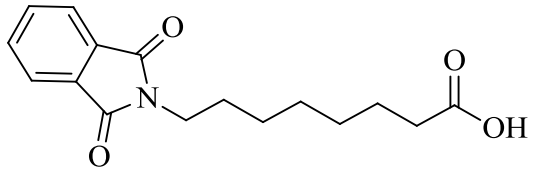

8

2-(8-Hydroxyoctyl)isoindoline-1,3-dione (**7**, 0.25 g, 0.91 mmol) was dissolved in acetone and stirred at 0^{o}C. To this solution Jones Reagent (prepared by mixing 0.5g CrO_3, 0.5 mL H_2SO_4 and 1.5 mL H_2O) was added dropwise. After addition, the mixture was stirred for 20 minutes at 0^{o}C. Then, the mixture was put into cold water and extracted with diethyl ether. Organics were collected, dried on $MgSO_4$ and concentrated under vacuum. The product was obtained as pale yellow solid (0.12 g, 45.68%). mp 69-71^{o}C. ^{1}H NMR ($CDCl_3$): δ 7.95- 7.82 (m, 2H), 7.80-7.70 (m, 2H), 3.70 (t, *J*= 7.29, 2H), 2.36 (t, J= 7.48, 2H), 1.82- 1.32 (m, 10H)

5.10. Synthesis of (S)-2-(2-(2-hydroxyethoxy)ethoxy)ethyl 2-(1,3-dioxoisoindolin-2-yl)propanoate (9) [44, 48]

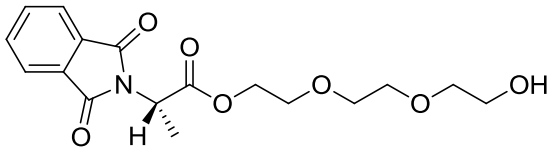

9

Triethylene glycol (0.77 mL, 5.77 mmol) was dissolved in 30 mL DCM and triethylamine (0.80 mL, 5.77 mmol) was added. N-PhthaloyL-(R)-alanyl chloride (0.98 g, 4.12 mmol) was dissolved in 15 mL DCM and added to the diol solution dropwise at 0^{o}C and stirred for 2 hours. Then the solution is stirred at room temperature overnight. It was concentrated under vacuum and column chromatography with ethyl acetate : hexane (1:2) gave the desired product as yellow oil (0.45 g, 31.09%). ^{1}H NMR ($CDCl_3$): δ 7.93-7.84 (m, 2H), 7.81-7.72 (m, 2H), 5.02 (q, *J*= 7.32, 1H), 4.33 (m, 2H), 3.80-3.48 (m, 10H), 1.72 (d, *J*= 7.33, 3H). ^{13}C NMR ($CDCl_3$): δ 169.78, 167.40, 134.16, 131.94, 123.49, 72.50, 70.57, 70.27, 68.94, 64.75, 61.53, 47.53, 15.30. ESI-MS+ m/z: exact mass calculated for $C_{17}H_{22}NO_7$ $[M + H]^+$ 352.1396, found 352.1388.

5.11. Synthesis of (S)-8-hydroxyoctyl-2-(1,3-dioxoisoindolin-2-yl)propanoate (10) [44, 48]

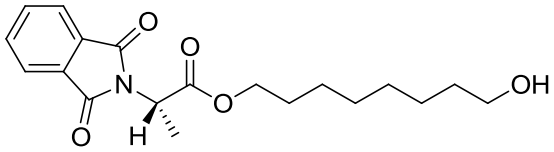

10

1,8-Octanediol (1.41 g, 6.90 mmol) was dissolved in 30 mL DCM and trimethylamine (1.35 mL, 9.66 mmol) was added. Mixture was stirred until complete dissolution. N-PhthaloyL-(R)-alanyl chloride (1.64 g, 6.90 mmol) was dissolved in 15 mL DCM and

added to the diol solution dropwise at 0^{o}C and stirred for 2 hours. Then the solution is stirred at room temperature overnight. It was concentrated under vacuum and column chromatography with ethylacetate : hexanes (1 :3) gave the desired product as viscous pale yellow oil (0.53 g, 22.11%). ^{1}H NMR ($CDCl_3$): δ 7.93-7.82 (m, 2H), 7.79-7.70 (m, 2H), 4.97 (q, *J*= 7.34, 1H), 4.19- 4.01 (m, 2H), 3.65- 3.57 (m, 2H), 1.70 (d, *J*= 7.34, 3H), 1.42- 1.15 (m, 12H). ^{13}C NMR ($CDCl_3$): δ 169.75, 167.58, 134.17, 131.94, 123.48, 66.04, 65.45, 62.92, 47.59, 32.69, 29.17, 28.98, 28.35, 25.65, 15.23. ESI-MS+ m/z: exact mass calculated for $C_{19}H_{26}NO_5$ $[M + H]^+$ 348.1811, found 348.1813.

5.12. Synthesis of (S)-2-(2-(2-((2-(1,3-dioxoisoindolin-2-yl)propanoyl)oxy)ethoxy) ethoxy) acetic acid (11) [41]

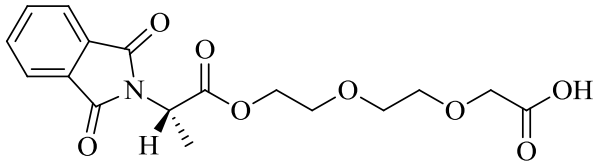

11

(S)-2-(2-(2-hydroxyethoxy)ethoxy)ethyl-2-(1,3-dioxoisoindolin-2-yl)propanoate (**9**, 0.64 g, 1.82 mmol) was dissolved in 15 mL acetone and cooled down to 0^{o}C. Jones reagent (prepared by mixing 0.5g CrO_3, 0.5 mL H_2SO_4 and 1.5 mL H_2O) was added slowly until the green color of the solution turned into persistent orange color. To destroy the excess Jones reagent, isopropyl alcohol was added and the solution turned green again. Sodium bicarbonate was added to neutralize the solution and the solids were filtrated off. Filtrate was concentrated under vacuum and the residue was dissolved in ether and extracted with brine and then water. Organics were collected, dried on $MgSO_4$ and concentrated under vacuum. The product was obtained as yellow oil (0.36, 54.10%). ^{1}H NMR (DMSO- d_6): δ 12.61 (s, 1H), 8.04-7.78 (m, 4H), 5.00 (q, *J*= 7.17, 1H), 4.36-3.86 (m, 4H), 3.65-3.37 (m, 6H), 1.55 (d, J= 7.23, H). ^{13}C NMR (DMSO- d_6): δ 171.50, 169.45, 166.94, 134.77,131.20, 123.33, 69.66, 69.62, 67.99, 67.53, 64.58, 46.86, 14.71. ESI-MS+ m/z: exact mass calculated for $C_{17}H_{20}NO_8$ $[M + H]^+$ 366.1189, found 366.1197.

5.13. Synthesis of (S)-8-((2-(1,3-dioxoisoindolin-2-yl)propanoyl)oxy)octanoic acid (12) [41]

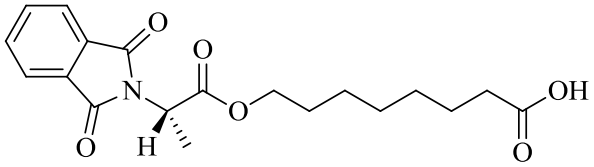

12

(S)-8-Hydroxyoctyl-2-(1,3-dioxoisoindolin-2-yl)propanoate (**10**, 0.2 g, 0.58 mmol) was dissolved in 5 mL acetone and cooled down to 0^{o}C. Jones reagent (prepared by mixing 0.5g CrO_3, 0.5 mL H_2SO_4 and 1.5 mL H_2O) was added slowly until the green color of the solution turned into persistent orange color. To destroy the excess Jones reagent, isopropyl alcohol was added and the solution turned green again. Sodium bicarbonate was added to neutralize the solution and the solids were filtrated off. Filtrate was concentrated under vacuum and the residue was dissolved in ether and extracted with brine and then water. Organics were collected, dried on $MgSO_4$ and concentrated under vacuum. The product was obtained as yellow solid (0.20 g, 96.13%). mp 65-67^{o}C. ^{1}H NMR (DMSO- d_6): δ 12.00 (s, 1H), 8.02- 7.82 (m, 4H), 4.99 (q, *J*= 7.2, 1H), 4.15- 3.90 (m, 2H), 2.13 (t, *J*= 7.36, 2H), 1.56 (d, *J*= 7.23, 3H), 1.42- 1.03 (m, 10H). ^{13}C NMR (DMSO- d_6): δ 174.25, 169.58, 166.94, 135.07, 131.17, 123.26, 65.03, 46.83, 35.55, 28.36, 28.15, 27.78, 25.06, 24.41, 14.67. ESI-MS+ m/z: exact mass calculated for $C_{19}H_{24}NO_6$ $[M + H]^+$ 362.1604, found 362.1597.

5.14. Synthesis of (R)-2-(2-(2-hydroxyethoxy)ethoxy)ethyl 2-(1,3-dioxoisoindolin-2-yl) propanoate (13) [44, 48]

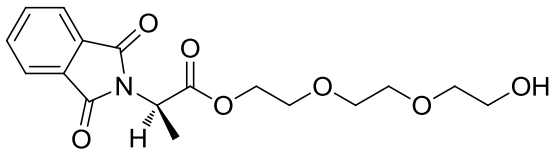

13

Triethylene glycol (0.77 mL, 5.77 mmol) was dissolved in 30 mL DCM and trimethylamine (0.80 mL, 5.77 mmol) was added. N-PhthaloyL-(R)-alanyl chloride (0.98 g, 4.12 mmol) was dissolved in 15 mL DCM and added to the diol solution dropwise at 0^{o}C and stirred for 2 hours. Then the solution is stirred at room temperature overnight. It was concentrated under vacuum and column chromatography with ethyl acetate : hexane (1:2) gave the desired product as yellow oil (0.45 g, 31.09%). ^{1}H NMR ($CDCl_3$): δ 7.90-7.84 (m, 2H), 7.79-7.72 (m, 2H), 5.02 (q, *J*= 7.32, 1H), 4.38-4.29 (m, 2H), 3.74-3.52 (m, 10H), 1.72 (d, *J*= 7.34, 3H)

5.15. Synthesis of (R)-8-hydroxyoctyl-2-(1,3-dioxoisoindolin-2-yl)propanoate (14) [44,48]

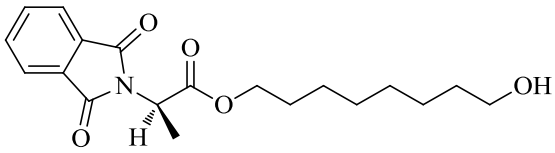

14

1,8-Octanediol (1.41 g, 6.90 mmol) was dissolved in 30 mL DCM and trimethylamine (1.35 mL, 9.66 mmol) was added. Mixture was stirred until complete dissolution. N-PhthaloyL-(R)-alanyl chloride (1.64 g, 6.90 mmol) was dissolved in 15 mL DCM and added to the diol solution dropwise at 0^{o}C and stirred for 2 hours. Then the solution is stirred at room temperature overnight. It was concentrated under vacuum and column chromatography with ethylacetate : hexanes (1 :3) gave the desired product as pale yellow oil (0.53 g, 22.11%). ^{1}H NMR ($CDCl_3$): δ 7.90-7.81 (m, 2H), 7.79-7.70 (m, 2H), 4.96 (q, *J*= 7.34, 1H), 4.23-4.07 (m, 2H), 3.61 (t, *J*= 6.62, 2H), 1.69 (d, *J*= 7.35, 3H), 1.63-1.46 (m, 4H), 1.35-1.20 (m, 8H).

5.16. Synthesis of (R)-2-(2-(2-((2-(1,3-dioxoisoindolin-2-yl)propanoyl)oxy)ethoxy) ethoxy) acetic acid (15) [41]

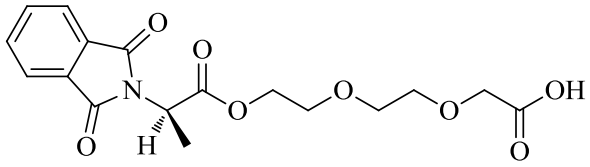

15

(R)-2-(2-(2-Hydroxyethoxy)ethoxy)ethyl-2-(1,3-dioxoisoindolin-2-yl)-propanoate (**13**, 0.18 g, 0.51 mmol) was dissolved in 15 mL acetone and cooled down to 0^{o}C. Jones reagent (prepared by mixing 0.5g CrO_3, 0.5 mL H_2SO_4 and 1.5 mL H_2O) was added slowly until the green color of the solution turned into persistent orange color. To destroy the excess Jones reagent, isopropyl alcohol was added and the solution turned green again. Sodium bicarbonate was added to neutralize the solution and the solids were filtrated off. Filtrate was concentrated under vacuum and the residue was dissolved in ether and extracted with brine and then water. Organics were collected, dried on $MgSO_4$ and concentrated under vacuum. The product was obtained as pale yellow oil (0.08g, 41.71%). ^{1}H NMR (DMSO- d_6): δ 8.05-7.58 (m, 4H), 5.01 (q, *J*= 7.19, 1H), 4.36-3.85 (m, 4H), 3.62-3.42 (m, 6H), 1.56 (d, *J*= 7.24, 3H). ^{13}C NMR (DMSO- d_6): δ 171.50, 169.45, 166.94, 134.77, 131.20, 123.33, 69.66, 69.62, 67.99, 67.56, 64.58, 46.86, 14.71.

5.17. Synthesis of (R)-8-((2-(1,3-dioxoisoindolin-2-yl)propanoyl)oxy)octanoic acid (16) [41]

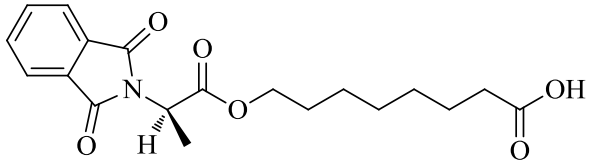

16

(R)-8-Hydroxyoctyl-2-(1,3-dioxoisoindolin-2-yl)propanoate (**14**, 0.2 g, 0.58 mmol) was dissolved in 5 mL acetone and cooled down to 0^{o}C. Jones reagent (prepared by mixing 0.5g CrO_3, 0.5 mL H_2SO_4 and 1.5 mL H_2O) was added slowly until the green color of the solution turned into persistent orange color. To destroy the excess Jones reagent, isopropyl alcohol was added and the solution turned green again. Sodium bicarbonate was added to neutralize the solution and the solids were filtrated off. Filtrate was concentrated under vacuum and the residue was dissolved in ether and extracted with brine and then water. Organics were collected, dried on $MgSO_4$ and concentrated under vacuum. The product was obtained as pale yellow solid (0.20 g, 96.13%). mp 59-61^{o}C. ^{1}H NMR (DMSO- d_6): δ 11.97 (s, 1H), 7.98-7.85 (m, 4H), 4.99 (q, *J*= 7.23, 1H), 4.04 (m, 2H), 2.13 (t, *J*=7.36, 2H), 1.54 (d, *J*= 7.23, 3H), 1.45-1.05 (m, 10H). ^{13}C NMR (DMSO- d_6): δ 170.72, 169.43, 166.99, 134.80, 131.20, 123.32, 65.06, 46.86, 33.71, 28.37, 28.14, 27.79, 25.05, 24.30, 14.71.

5.18. Synthesis of (S)-2-(2-(2-hydroxyethoxy)ethoxy)ethyl-2-(1,3-dioxo-1H-benzo[de]isoquinolin-2(3H)-yl) propanoate (17)

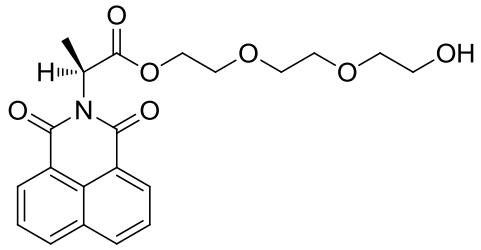

17

(S)-2-(1,3-Dioxo-1H-benzo[de]isoquinolin-2(3H)-yl)propanoic acid (**22**, 0.47 g, 1.73 mmol) and monotosylated triethylene glycol (0.5 g, 1.64 mmol) and DBU (0.26 mL, 1.73 mmol) were all disscolved in 25 mL DMF and refluxed over night. The desired product was prufied with column chromotography. (0.07 g, 10.66%). ^{1}H NMR ($CDCl_3$): δ 8.60-8.43 (m, 2H), 8.24-8.11 (m, 2H), 7.78-7.63 (m, 2H), 5.71 (q, *J*= 6.97, 1H), 4.33-4.13 (m, 2H), 3.81-3.13 (m, 10H), 1.62 (d, *J*= 6.96, 3H)

5.19. Synthesis of (S)-2-(2-(2-((2-(1,3-dioxo-1H-benzo[de]isoquinolin-2(3H)-yl)propanoyl)oxy)ethoxy)ethoxy) acetic acid (18) [41]

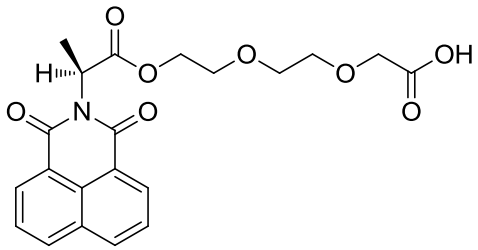

18

(S)-2-(2-(2-Hydroxyethoxy)ethoxy)ethyl-2-(1,3-dioxo-1H-benzo[de]isoquinolin-2(3H)-yl) propanoate (**17**, 0.074 g, 0.18 mmol) was dissolved in 10 mL acetone and cooled down to 0^{o}C. Jones reagent (prepared by mixing 0.5g CrO_3, 0.5 mL H_2SO_4 and 1.5 mL H_2O) was added slowly until the green color of the solution turned into persistent orange color. To destroy the excess Jones reagent, isopropyl alcohol was added and the solution turned green again. Sodium bicarbonate was added to neutralize the solution and the solids were filtrated off. Filtrate was concentrated under vacuum and the residue was dissolved in ether and extracted with brine and then water. Organics were collected, dried on $MgSO_4$ and concentrated under vacuum. However, desired product could not be isolated.

5.20. Synthesis of (S)-8-hydroxyoctyl 2-(1,3-dioxo-1H-benzo[de]isoquinolin-2(3H)-yl)propanoate (19)

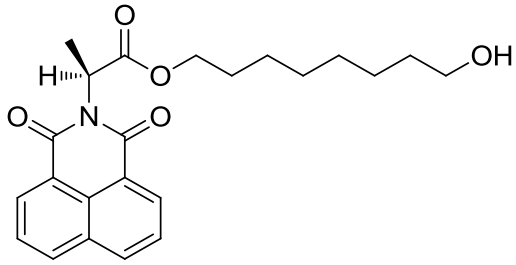

19

(S)-2-(1,3-Dioxo-1H-benzo[de]isoquinolin-2(3H)-yl)propanoic acid (**22**, 0.4 g, 1.48 mmol) and 8-chloro-1-octanol (0.236 mL, 1.40 mmol) and DBU (0.22 mL, 1.48 mmol) were all dissolved in 25 mL DMF and the solution stirred overnight. The crude product was prufied with column chromatography resulting in the desired compound. The product was obtained as orange solid (0.06 g, 9.35%). mp 53-57^{o}C. ^{1}H NMR ($CDCl_3$): δ 8.81-8.54 (m, 2H), 8.37-8.11 (m, 2H), 7.93-7.66 (m, 2H), 5.77 (q, *J*= 6.97, 1H), 4.41-3.97 (m, 2H), 3.61 (t, *J*= 6.64, 2H), 1.71 (d, *J*= 6.97, 3H), 1.63-1.23 (m, 12H). ESI-MS+ m/z: exact mass calculated for $C_{23}H_{28}NO_5$ $[M + H]^+$ 398.1967, found 398.1966.

5.21. Synthesis of (S)-8-((2-(1,3-dioxo-1H-benzo[de]isoquinolin-2(3H)-yl)propanoyl)oxy) octanoic acid (20) [41]

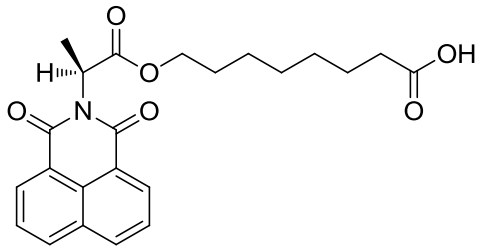

20

(S)-8-Hydroxyoctyl-2-(1,3-dioxo-1H-benzo[de]isoquinolin-2(3H)-yl)-propanoate (**19**, 0.055 g, 0.14 mmol) was dissolved in 5 mL acetone and cooled down to 0^{o}C. Jones reagent (prepared by mixing 0.5g CrO_3, 0.5 mL H_2SO_4 and 1.5 mL H_2O) was added slowly until the green color of the solution turned into persistent orange color. To destroy the excess Jones reagent, isopropyl alcohol was added and the solution turned green again. Sodium bicarbonate was added to neutralize the solution and the solids were filtrated off. Filtrate was concentrated under vacuum and the residue was dissolved in ether and extracted with brine and then water. Organics were collected, dried on $MgSO_4$ and concentrated under vacuum. The product was obtained as yellow powder (0.03 g, 52.69%). mp 81-84^{o}C. ^{1}H NMR (DMSO- d_6): δ 8.69-8.39 (m, 4H), 8.00-7.77 (m, 2H), 5.67 (q, *J*= 6.9, 1H), 4.20-3.82 (m, 2H), 2.04 (t, *J*= 7.35, 2H), 1.55 (d, *J*= 6.92,

3H), 1.47-0.86 (m, 10H). ^{13}C NMR (DMSO- d_6): δ 174.34, 169.86, 162.88, 134.82, 131.32, 131.19, 127.35, 121.62, 121.60, 64.51, 48.45, 33.55, 28.32, 28.15, 27.80, 25.19, 24.18, 14.32. ESI-MS+ m/z: exact mass calculated for $C_{23}H_{26}NO_6$ $[M + H]^+$ 412.1760, found 412.1761.

5.22. Synthesis of N-PhthaloyL-(S)-alanine (21) [45]

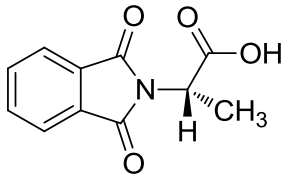

21

Phthalic anhydride (3.30 g, 0.02 mol) and *L*-alanine (2.00 g, 0.02mol) were refluxed in 70 mL glacial acetic acid overnight. Then, the acid was removed under reduced pressure. 15 mL water was added to the residue and the resulting mixture was refluxed for an additional hour. After cooling the mixture back to the room temperature, it was extracted with ether:water (1:4). Organic phase was dried on $MgSO_4$ and concentrated under vacuum. The product was obtained as white powder (4.64 g, 96.22%). mp 130-132^{o}C. ^{1}H NMR ($CDCl_3$): δ 7.93-7.84 (m, 2H), 4.86 (q, *J*=7.33, 1H), 1.55 (d, *J*=7.3, 3H). ^{13}C NMR ($CDCl_3$): δ 169.49, 167.33, 134.29, 131.97, 123.91, 47.31, 15.22.

5.23. Synthesis of (S)-2-(1,3-dioxo-1H-benzo[de]isoquinolin-2(3H)-yl)propanoic acid (22) [46]

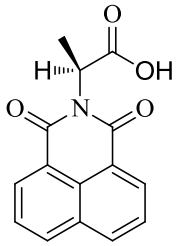

22

Lightly crushed pellets of KOH (042 g, 7.51 mmol) were added to the solution of *L*-alanine (0.75 g, 8.26 mmol) in 9 mL water and the mixture was stirred at room temperature for 20 minutes. 1,8- naphthalic anhydride (1.49 g, 7.51 mmol) in 50 mL ethanol was added to the mixture. Suspension refluxed over night and then cooled down to about 80^{o}C. 1M aq HCl was added to the mixture and stirred. Then the resulting mixture was letf to stand for a day. The precipitated solids were collected upon filtration and washed with water and dried. The product was obtained as brown powder (1.09 g, 53.90%). mp 228-231^{o}C. ^{1}H NMR ($CDCl_3$): δ 8.68-8.62 (m, 2H), 8.30-8.25 (m, 2H), 7.82- 7.77 (m, 2H), 5.85 (q, *J*= 6.95, 1H), 1.74 (d, *J*=6.96, 3H)

5.24. Synthesis of 1,8-Naphthalic Anhydride (23)[47]

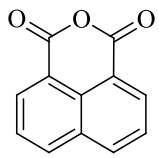

23

Acenaphthene (4g, 0.026 mol) was dissolved in 160 mL acetic acid and sodium dichromate, $Na_2Cr_2O_7$, (16.93 g, 0.06 mol) was added in small portions. The mixture then was refluxed at 70^{o}C overnight. After that, the mixture was cooled down to room temperature and cold water was added. Resulting solids were filtrated and washed with water. The product was obtained as yellow powder (4.63g, 89.86%). ^{1}H NMR ($CDCl_3$): δ 8.71-8.61 (m, 2H), 8.37-8.27 (m, 2H), 7.91-7.78 (m, 2H).

5.25. Synthesis of (2S,2'S)-ethane-1,2-diyl bis(2-(1,3-dioxoisoindolin-2-yl)propanoate) (24) [44, 48]

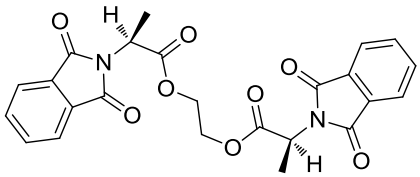

24

Ethylene glycol (0.30 mL, 5.50 mmol) was dissolved in 30 mL DCM and triethylamine (0.92 mL, 6.60 mmol) was added. N-PhthaloyL-(R)-alanyl chloride (2.65 g, 11 mmol) was dissolved in 15 mL DCM and added to the diol solution dropwise at 0^{o}C and stirred for 2 hours. Then the solution is stirred at room temperature overnight. It was concentrated under vacuum and column chromatography with ethyl acetate : hexane (1:2) gave the desired product as pale yellow powder (0.11g, 4.31%). mp 92-97^{o}C. ^{1}H NMR ($CDCl_3$): δ 7.96-7.83 (m, 2H), 7.80-7.69 (m, 2H), 4.96 (q, *J*= 7.32, 1H), 4.44-4.23 (m, 2H), 1.72-1.59 (m, 3H).

5.26. Synthesis of (2S,2'S)-oxybis(ethane-2,1-diyl) bis(2-(1,3-dioxoisoindolin-2-yl)propanoate) (25) [44, 48]

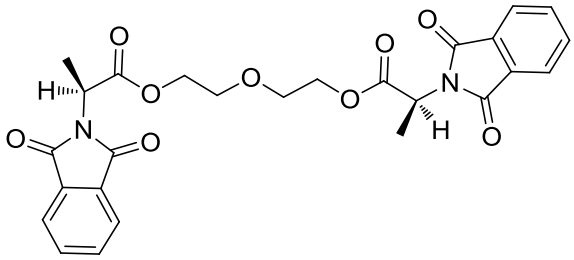

25

Diethylene glycol (0.34 mL, 3.56 mmol) was dissolved in 30 mL DCM and triethylamine (0.60 mL, 4.27 mmol) was added. N-PhthaloyL-(R)-alanyl chloride (1.69 g, 7.11 mmol) was dissolved in 15 mL DCM and added to the diol solution dropwise at 0^{o}C and stirred for 2 hours. Then the solution is stirred at room temperature overnight. It

was concentrated under vacuum and column chromatography with ethyl acetate : hexane (1:2) gave the desired product as pale yellow oil (0.56 g, 30.94%). ^{1}H NMR ($CDCl_3$): δ 7.94-7.84 (m, 2H), 7.82-7.69 (m, 2H), 5.00 (q, *J*= 7.33, 1H), 4.39 (m, 2H), 3.66-3.51 (m, 2H), 1.80-1.61 (m, 3H).

REFERENCES

(1) Oparin, A. I. 1924. Proishkhozhddenie Zhisni. Moskowski Rabocii. (In Russian, translated into English as: Oparin, A., 1938. The Origin of Life. MacMillan).

(2) Parrish, J. K.; Edelstein-keshet, L. *Science*, **1999**, *284*, 99–101.

(3) Esehenmoser, A.; Kisakurekb, M. V. *Helv. Chim. Acta*, **1996**, *79*, 1249–1259.

(4) Luisi, P. L. *The Emergence of Life: From Chemical Origins to Synthetic Biology*, 1st ed.; Cambridge: New York, 2006.

(5) Osowska, K.; Miljanić,O. Š. *Synlett.* **2011**, *12*, 1643–1648.

(6) Lesk, A. M.; Rose, G. D. *Proc. Natl. Acad. Sci. USA*, **1981**, *78*, 4304–4308.

(7) Wu, A.; Isaacs, L. *J. Am. Chem. Soc.* **2003**, *125*, 4831–4835.

(8) H.; Jolliffe, K. A.; Timmerman, P.; Reinhoudt, D. N. *Angew. Chem. Int. Ed.* **1999**, *38*, 933–937.

(9) Albrecht, M.; Schneider, M. *Angew. Chem. Int. Ed.* **1999**, *38*, 557–559.

(10) Bilgiçer, B.; Xing, X.; Kumar, K. *J. Am. Chem. Soc.* **2001**, *123*, 11815–11816.

(11) Rowan, S. J.; Hamilton, D. G.; Brady, P. A.; Sanders, J. K. M. *J. Am. Chem. Soc.* **1997**, *119*, 2578–2579.

(12) Neidle, S. *Principles of Nucleic Acid Structure*; Elsevier: New York, 2008.

(13) Chargaff, E.; Lipshitz, R.; Green, C. *J. Biol. Chem.* **1952**, *195*, 155–160.

(14) Watson, J. D.; Crick, F. H. C. *Nature.* **1953**, *171*, 737–738.

(15) Stofer, E.; Chipot, C.; Lavery, R.; Poincare, H.; Vandoeu, V.; April, R. V. *J. Am. Chem. Soc.* **1999**, 9503–9508.

(16) Kool, E. T. *Annu. Rev. Biophys. Biomol. Struct. 2001, 3,:*1–22.

(17) Guckian, K. M.; Schweitzer, B. A.; Ren, R. X.; Sheils, C. J.; Tahmassebi, D. C.; Kool, E. T. *J. Am. Chem. Soc.* **2000**, *122*, 2213–2222.

(18) Rotello, V. M.; Viani, E. A.; Deslongchamps, G.; Murray, B. A.; Rebek, J. *J. Am. Chem. Soc.* **1993**, 797–798.

(19) Calladine, C. R.; Drew, H. R.; Luisi , B. F.; Travers, A. A. *Understanding DNA: The Molecule & How It Works*, 3rd ed.; Elsevier Academic Press: Oxford, 2004.

(20) Kool, E. T. *J. Am. Chem. Soc.* **1991**, *113*, 6265–6266.

(21) Allawi, H. T.; Santalucia, J. *Nucleic Acids Res.* **1998**, *26*, 4925–4934.

(22) Elkin, L. O. Rosalind Franlin and the Double Helix. *Phys Today* **2003**, 42-48.

(23) Lewis, G. N. *Valence and the Structure of Atoms and Molecules*; The Chemical Catalog Company: New York, 1923.

(24) van der Waals, J. D. Over de Continuiteit van den Gas- en Vloeistoftoest. Ph.D. thesis, Leiden University, 1873.

(25) Mu, K.; Hobza, P. *Chem. Rev.* **2000**, *100*, 143–167.

(26) Lehn, J.-M. *Angew. Chem., Int. Ed. Engl.* **1988**, *27*, 89–112.

(27) Webber, M. J.; Appel, E. A.; Meijer, E. W.; Langer, R. *Nat. Mater.* **2016**, *15*, 13–26.

(28) Isaacs, L.; Witt, D. *Angew. Chem. Int. Ed.* **2002**, *41*, 1905–1907.

(29) Sun, H.; Prendergast, M. E.; Leowanawat, P.; Partridge, B. E.; Heiney, P. A.;

Araoka, F.; Graf, R.; Spiess, H. W.; Zeng, X.; Ungar, G.; Percec, V. *J. Am. Chem. Soc.* **2014**, *136*, 7169–7185.

(30) Roche, C.; Sun, H.; Leowanawat, P.; Araoka, F.; Partridge, B. E.; Peterca, M.; Wilson, D. A.; Prendergast, M. E.; Heiney, P. A.; Graf, R.; Spiess, H. W.; Zeng, X.; Ungar, G.; Percec, V. *Nat. Chem.* **2015**, 1–10.

(31) Urbach, A. R. *J. Chem. Educ.* **2010**, *87*, 891–893.

(32) Foss, J. G. *J. Chem. Educ.*1963, *40*, 592-597.

(33) Geiger, H. C.; Donohoe, J. S. *J. Chem. Educ.* **2012**, *89*, 1572–1574.

(34) Fenniri, H.; Deng, B.; Ribbe, A. E.; Lafayette, W. *J. Am. Chem. Soc.* **2002**, *124*, 11064–11072.

(35) *The Merck Index, An Encyclopedia of Chemicals, Drugs, and Biologicals,*14th ed; Merck Research Laboratories Division, New Jersey, USA, 2006.

(36) Ariëns, E. J. *Drug Design: Medicinal Chemistry: A Series of Monographs, Volume 3.* Academic Press: New York, 1972; p 330.

(37) Scheibe, G. *Angew. Chem.* **1937**, *50*, 212-219.

(38) Jelley, E. E. *Nature.* **1936**, *138*, 1009–1010.

(39) Würthner, F.; Kaiser, T. E.; Saha-möller, C. R. *Angew. Chem. Int. Ed.* **2011**, 50, 3376–3410.

(40) Ashton, P. R.; Huff, J.; Menzer, S.; Parsons, I. W.; Preece, J. A.; Stoddart, J. F.; Tolley, M. S.; White, A. J. P.; Williams, D. J. *Chem. Eur. J.* **1996**, *2*, 31–44.

(41) Eisenbraun, E. J. *Org. Synth.* **1965**, *45*, 28.

(42) Thomson, A.; O'Connor, S.; Knuckley, B.; Causey, C. P. *Bioorg. Med. Chem.* **2014**, *22*, 4602–4608.

(43) Dollé, F.; Hinnen, F.; Valette, H.; Fuseau, C.; Duval, R.; Péglion, J.-L.; Crouzel, C. *Bioorg. Med. Chem.* **1997**, *5*, 749–764.

(44) Iwashita, M.; Makide, K.; Nonomura, T.; Misumi, Y.; Otani, Y.; Ishida, M. *J. Med. Chem.* **2009**, *52*, 5837–5863.

(45) Mahboub, R. *Int. J. Chem. Sci.* **2009**, *7*, 28–36.

(46) Darses, B.; Jarvis, A. G.; Mafroud, A.; Dargazanli, G.; Dauban, P. *Synthesis.* **2013**, *45*, 2079–2087.

(47) Verma, M.; Luxami, V.; Paul, K. *Eur. J. Med. Chem.* **2013**, *68*, 352–360.

(48) Bian, H.; Feng, J.; Xu, W. *Med. Chem. Res.* **2013**, *22*, 175–178.

APENDICES

A. NMR SPECTRA

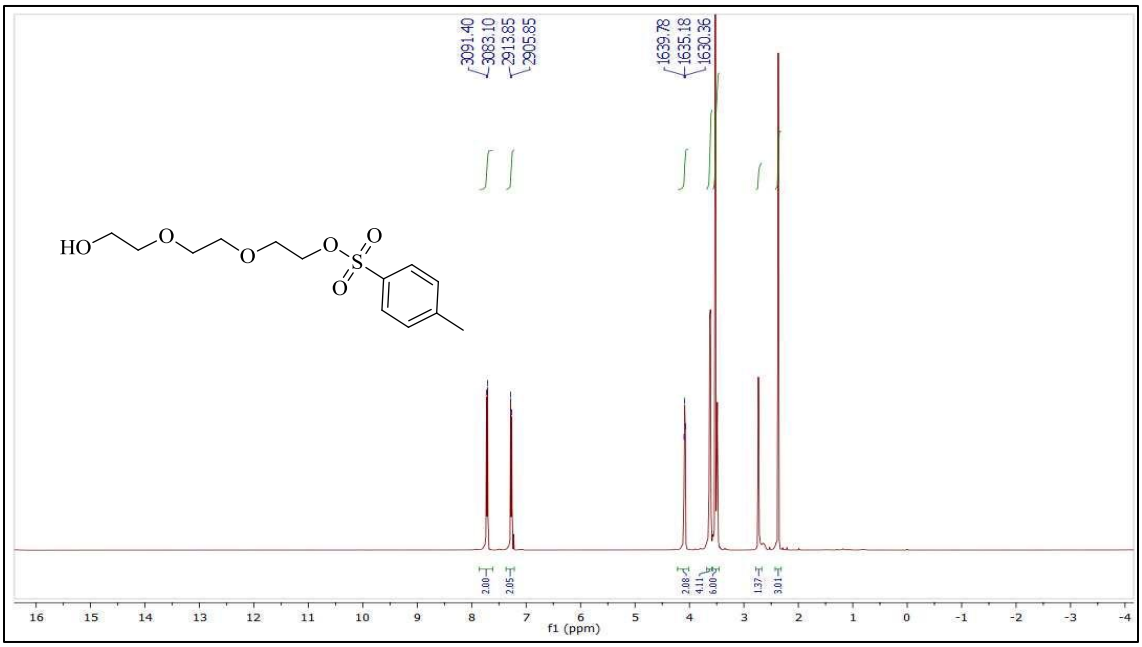

Figure 40. ^{1}H NMR Spectrum of compound **1** in $CDCl_3$

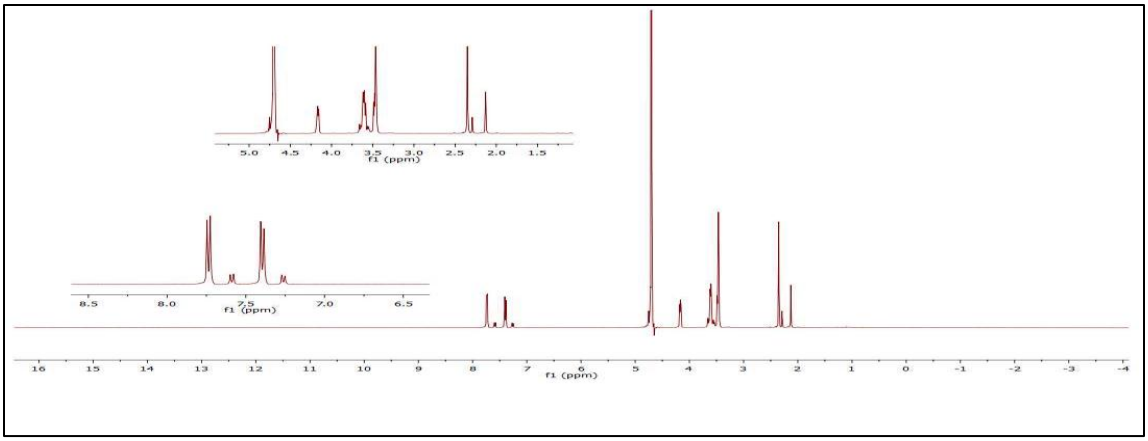

Figure 41. ^{1}H NMR Spectrum of compound **1** in D_2O

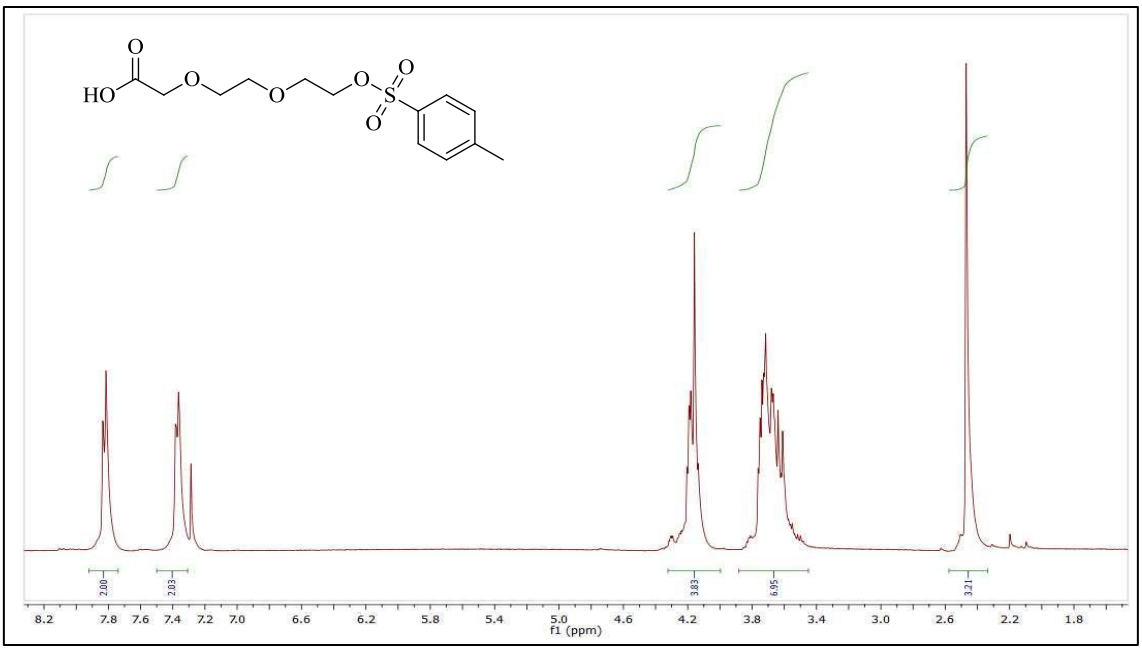

Figure 42. ^{1}H NMR Spectrum of compound **2** in $CDCl_3$

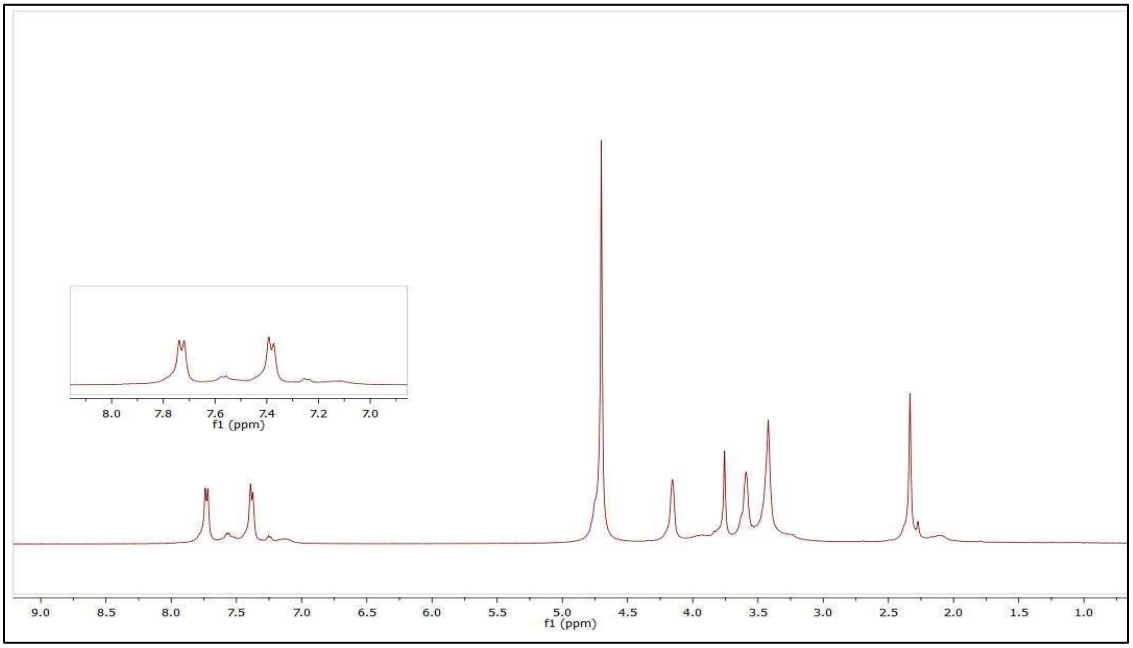

Figure 43. ^{1}H NMR Spectrum of compound **2** in D_2O

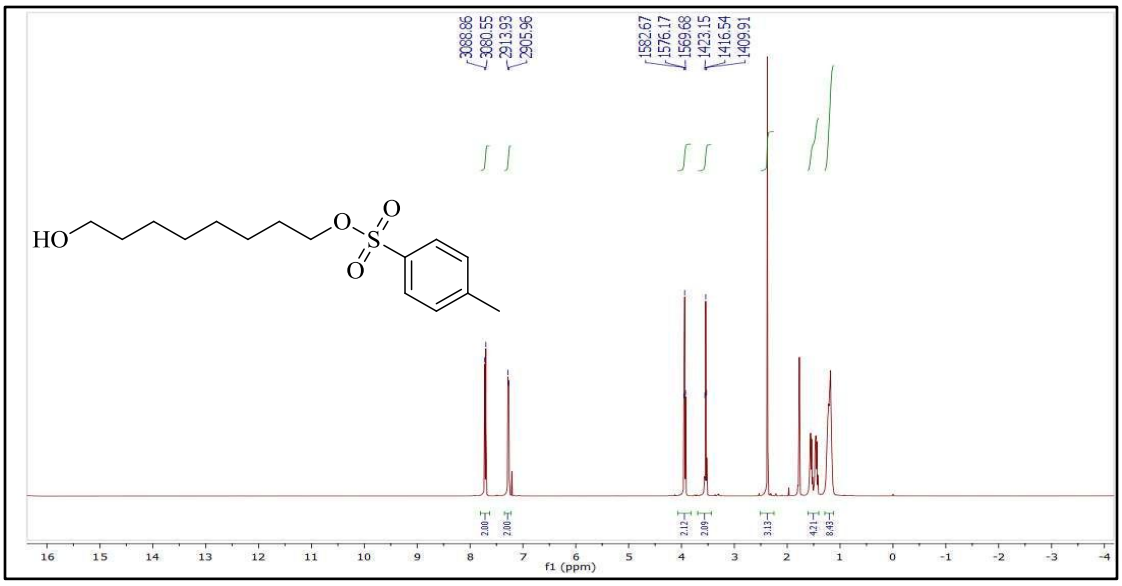

Figure 44. ^{1}H NMR Spectrum of compound **3** in $CDCl_3$

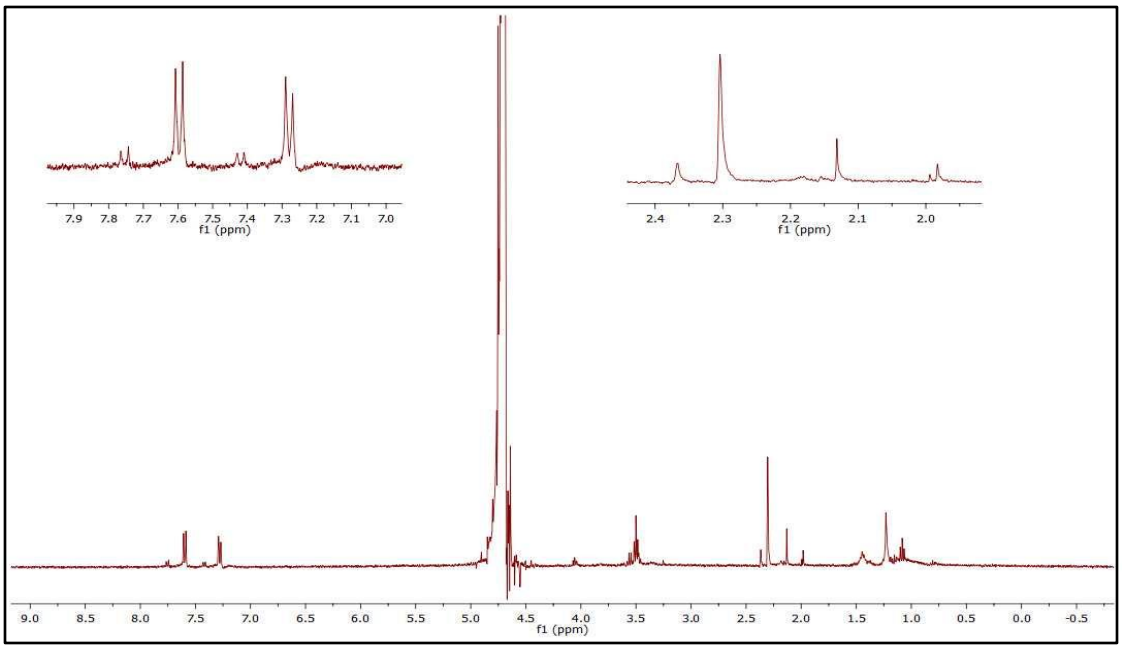

Figure 45. ^{1}H NMR Spectrum of compound **3** in D_2O

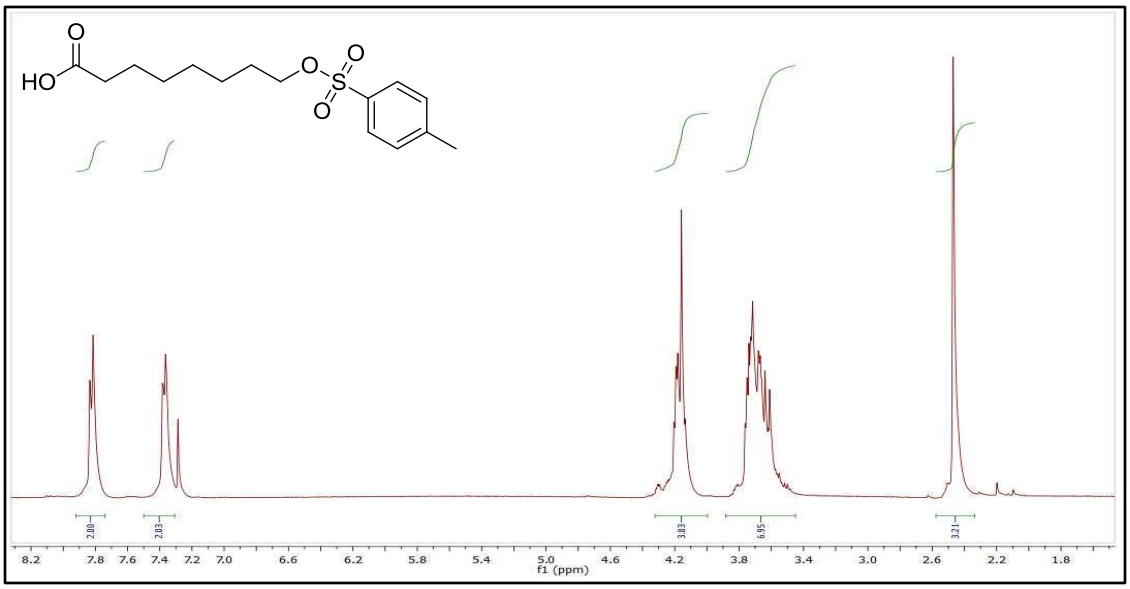

Figure 46. ^{1}H NMR Spectrum of compound **4** in $CDCl_3$

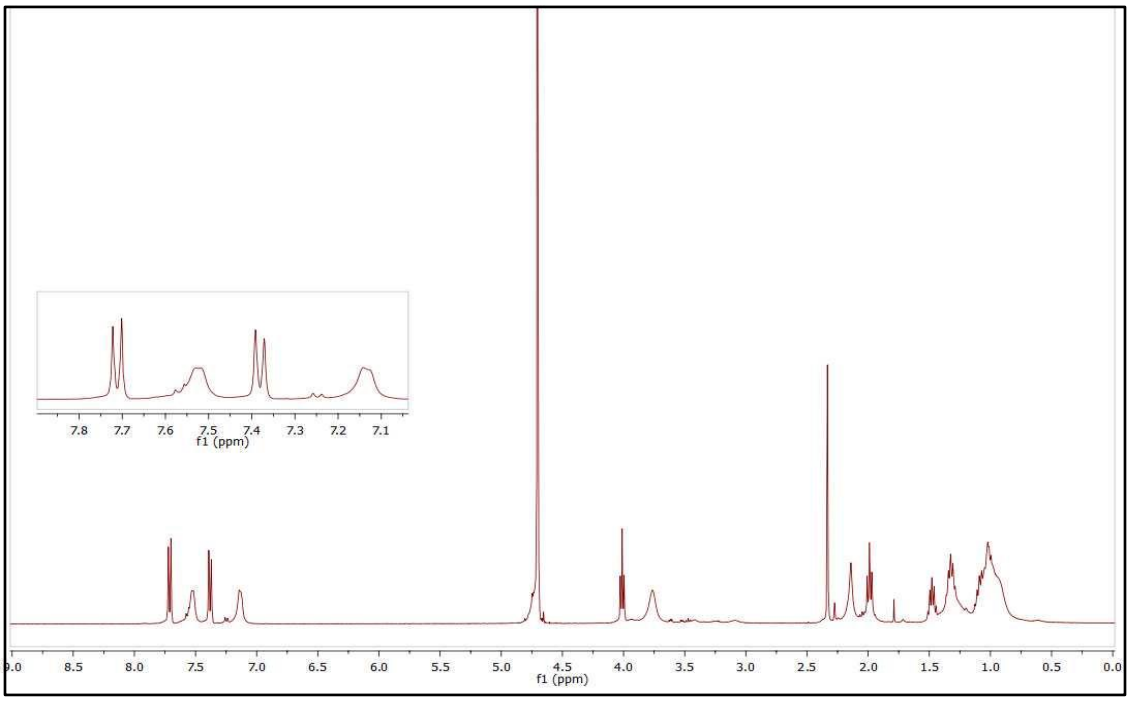

Figure 47. ^{1}H NMR Spectrum of compound **4** in D_2O

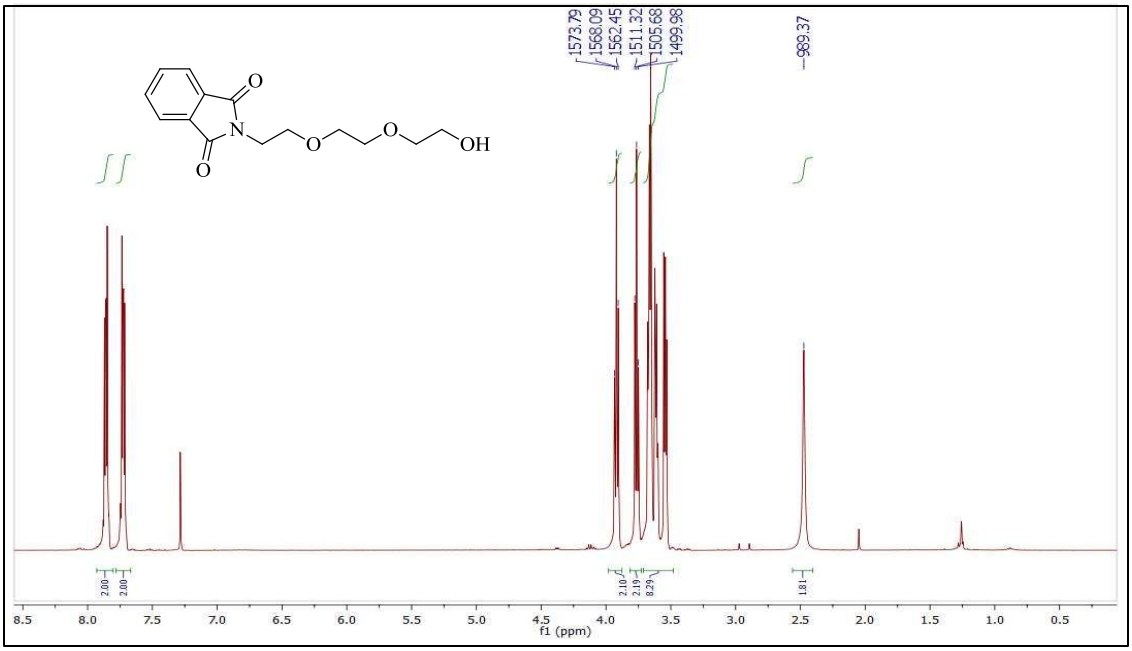

Figure 48. ^{1}H NMR Spectrum of compound **5** in $CDCl_3$

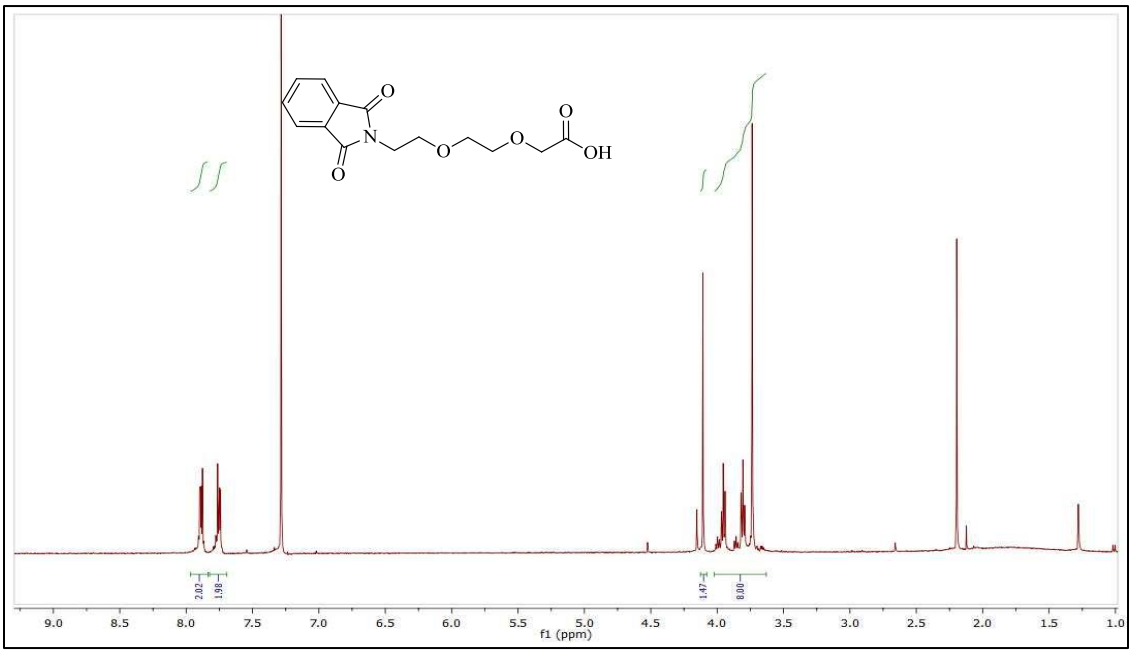

Figure 49. ^{1}H NMR Spectrum of compound **6** in $CDCl_3$

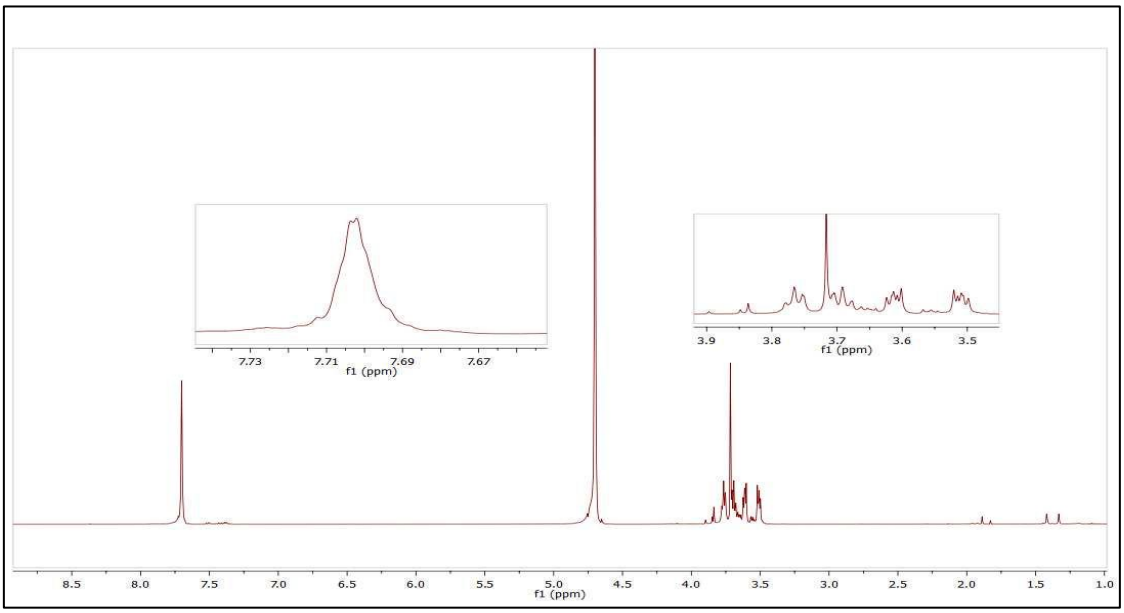

Figure 50. ^{1}H NMR Spectrum of compound **6** in D_2O

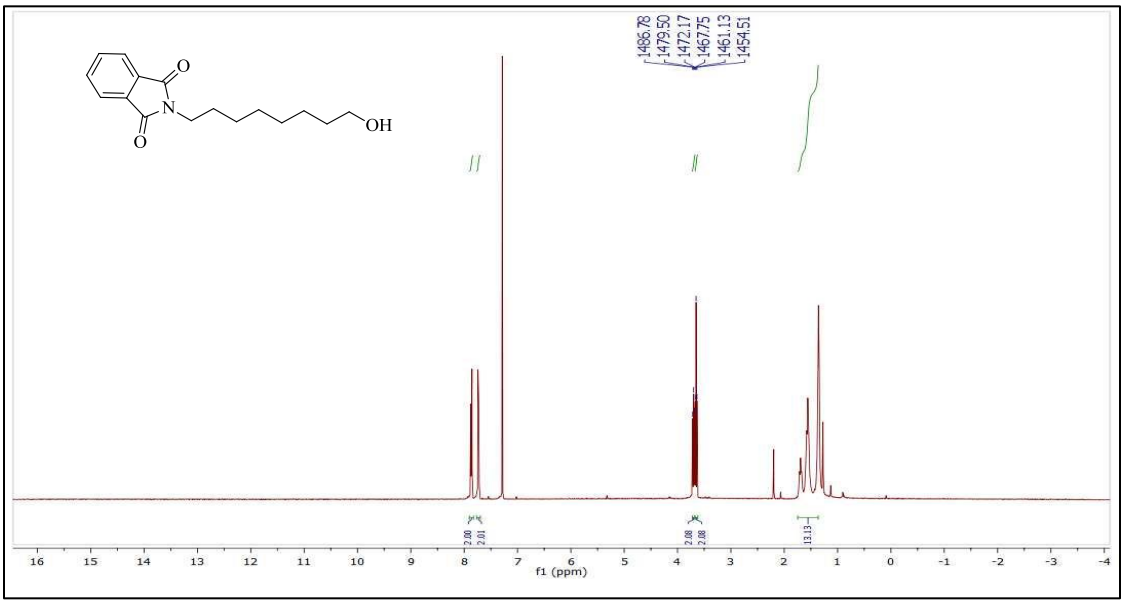

Figure 51. ^{1}H NMR Spectrum of compound **7** in $CDCl_3$

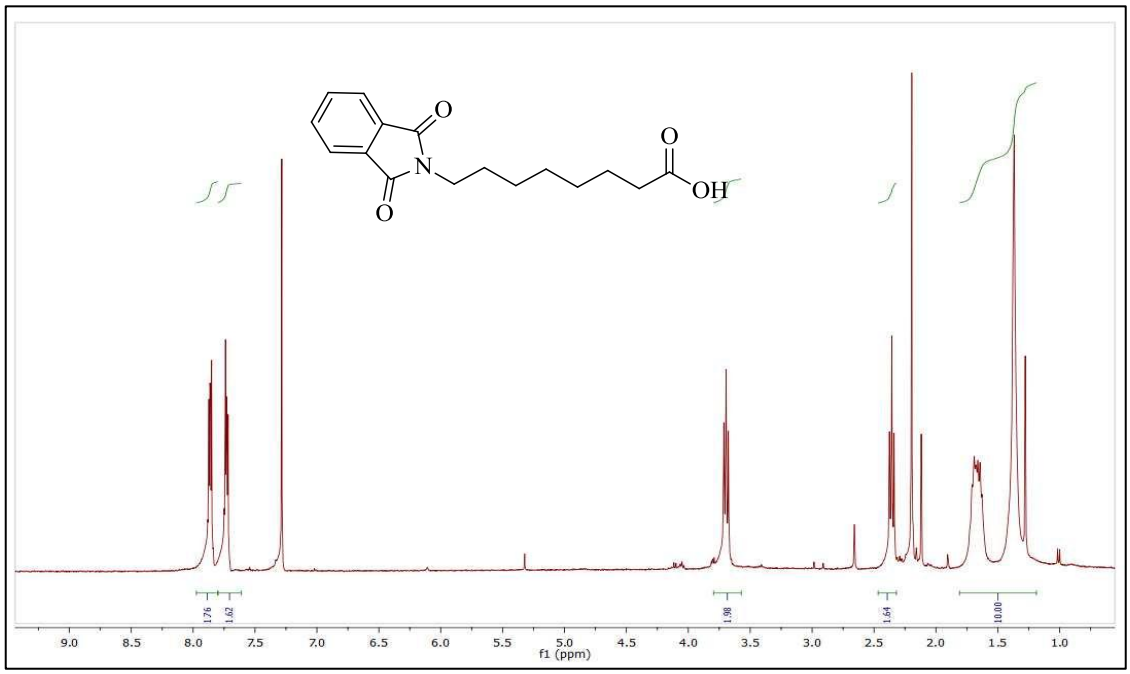

Figure 52. ^{1}H NMR Spectrum of compound **8** in $CDCl_3$

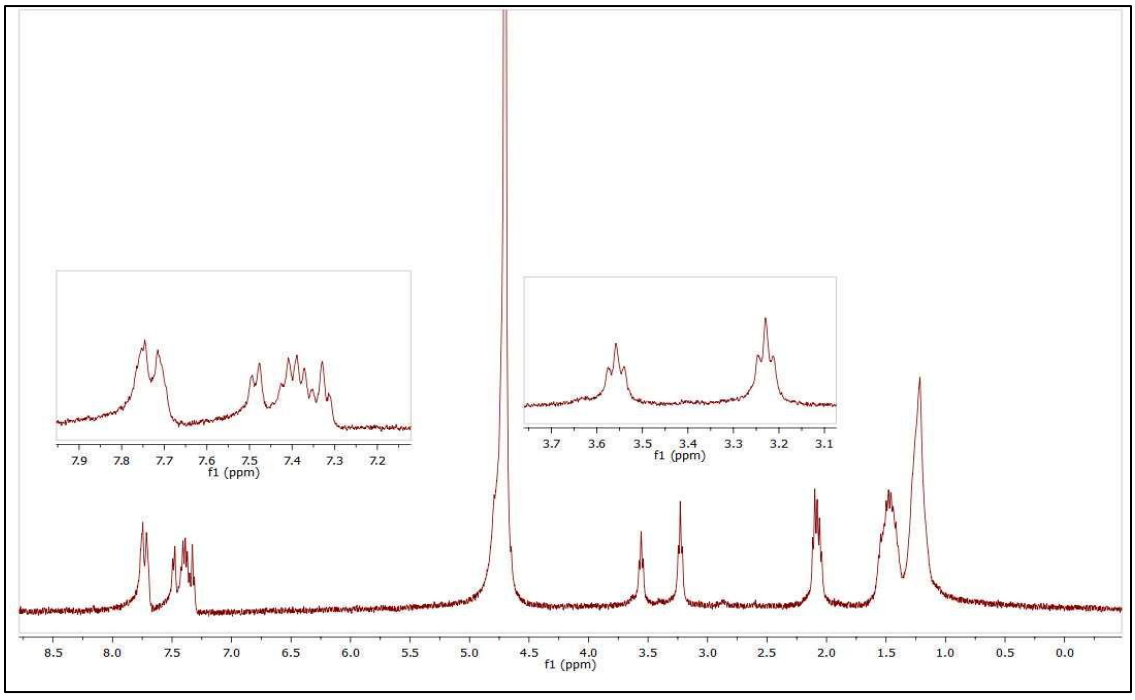

Figure 53. ^{1}H NMR Spectrum of compound **8** in D_2O

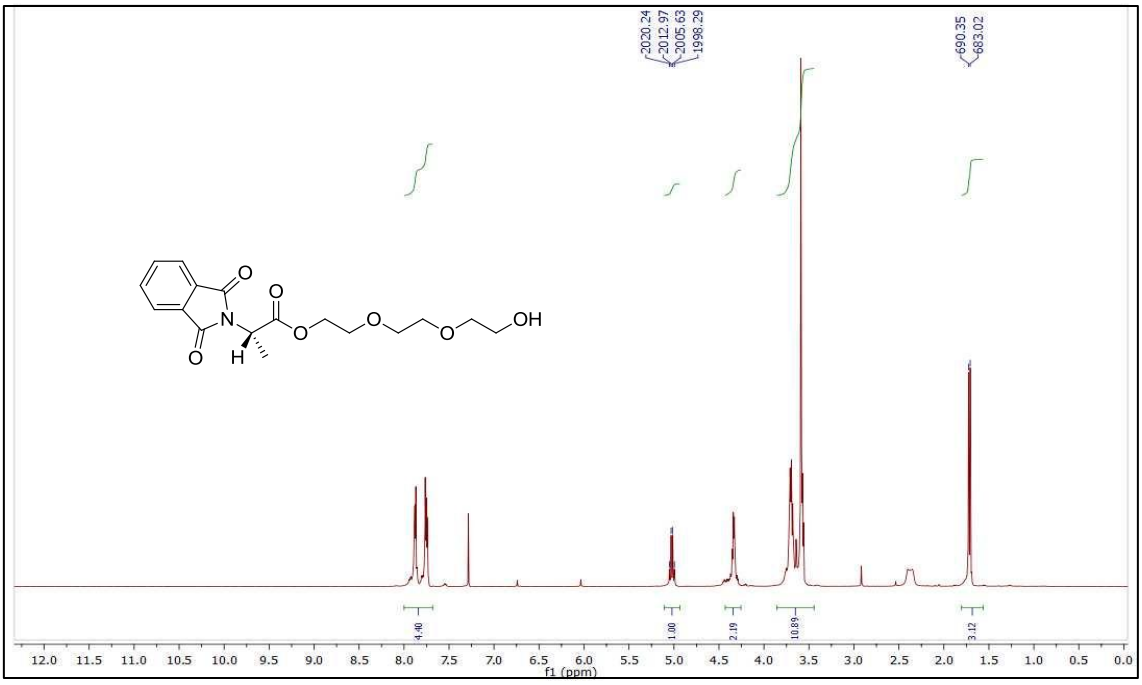

Figure 54. ^{1}H NMR Spectrum of compound **9** in $CDCl_3$

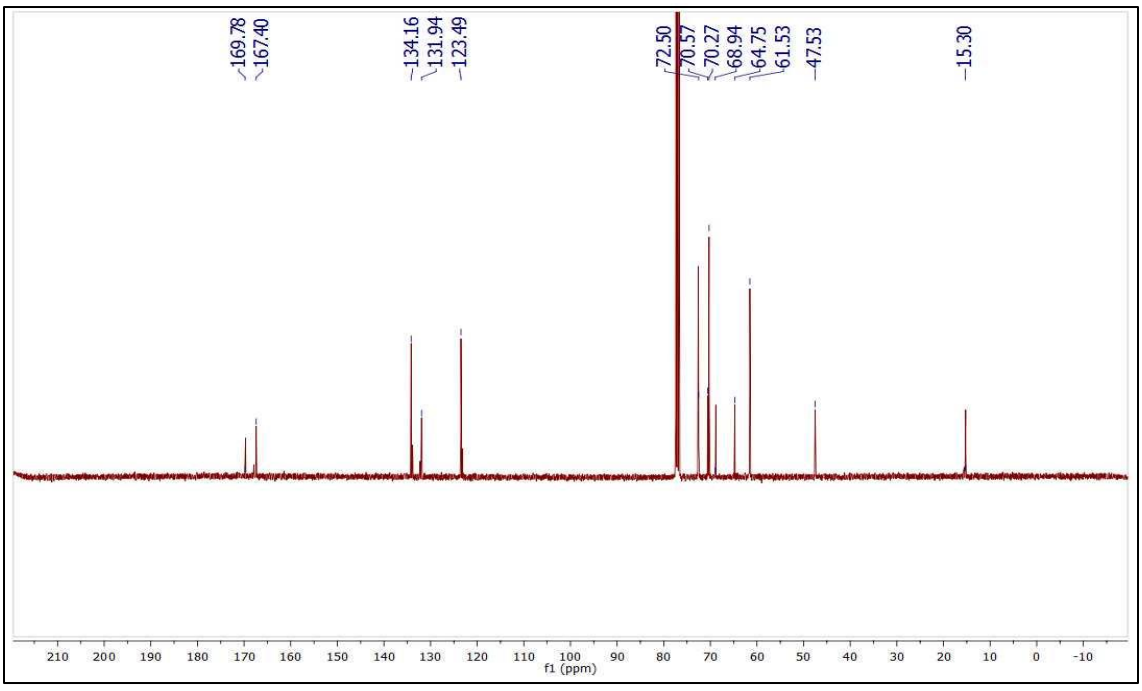

Figure 55. ^{13}C NMR Spectrum of compound **9** in $CDCl_3$

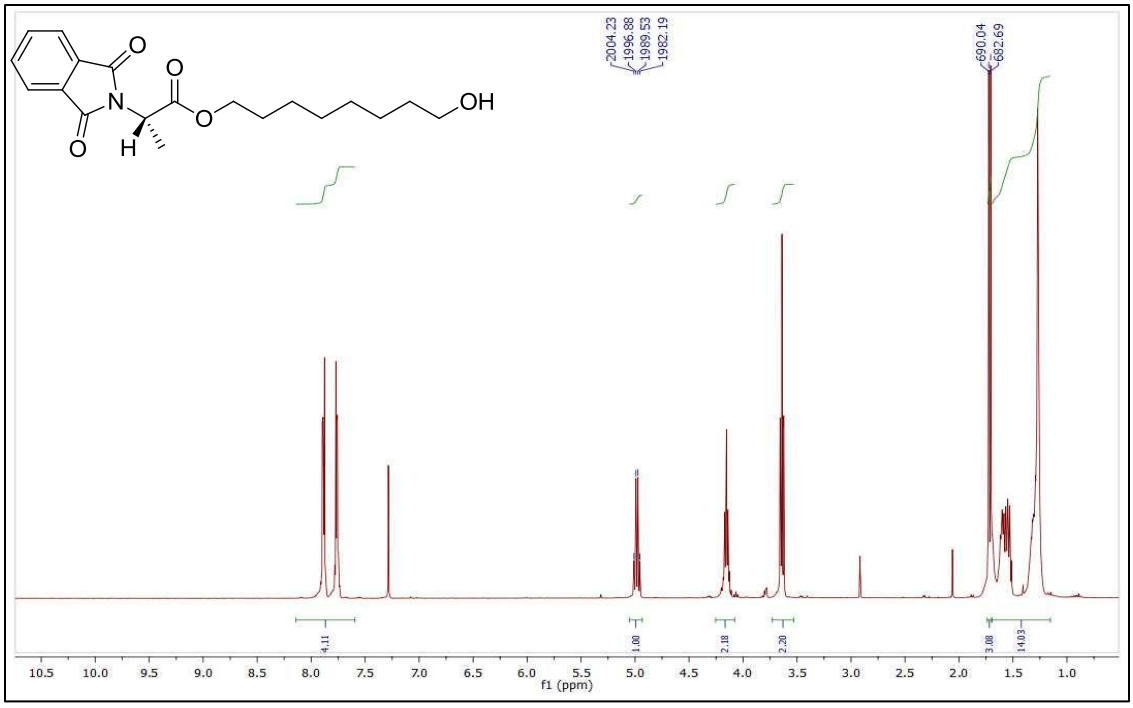

Figure 56. ^{1}H NMR Spectrum of compound **10** in $CDCl_3$

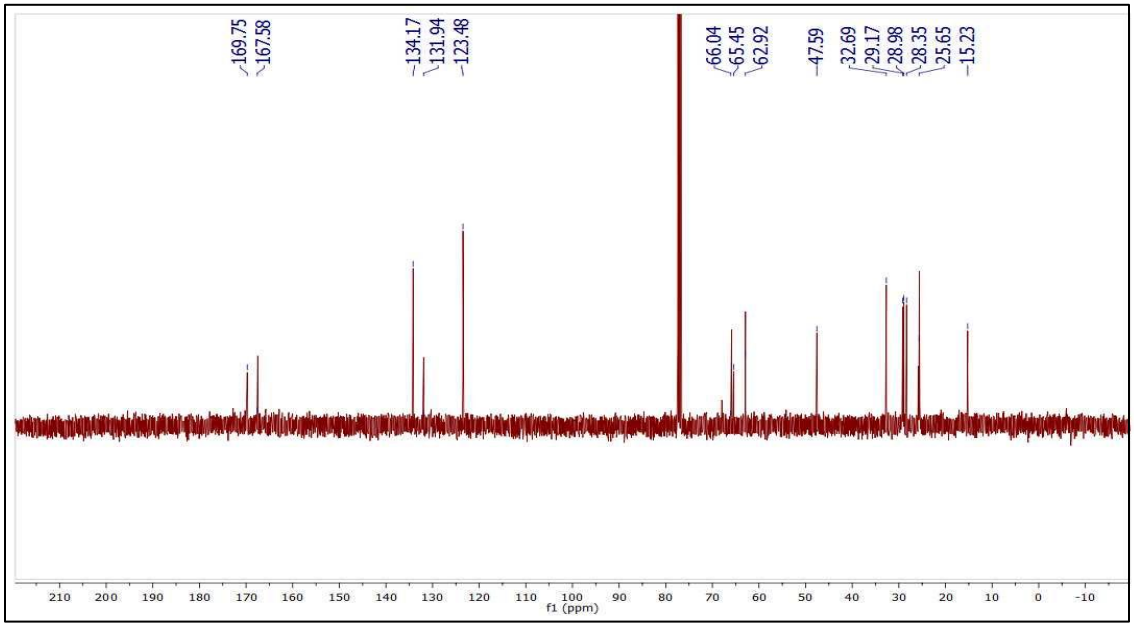

Figure 57. ^{13}C NMR Spectrum of compound **10** in $CDCl_3$

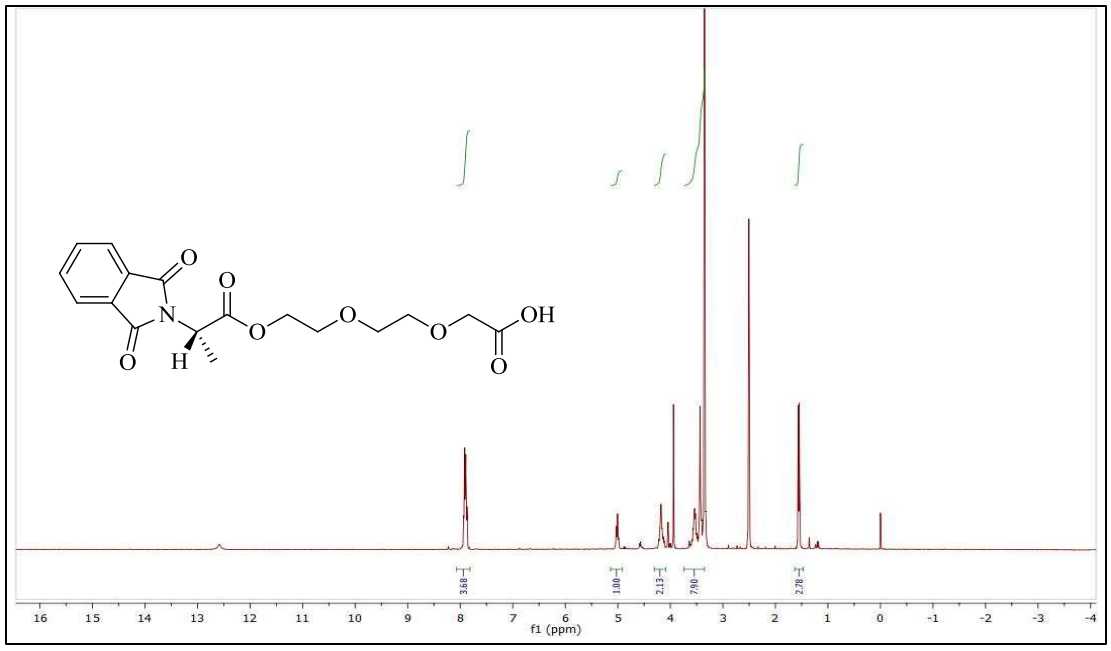

Figure 58. ^{1}H NMR Spectrum of compound **11** in DMSO-d_6

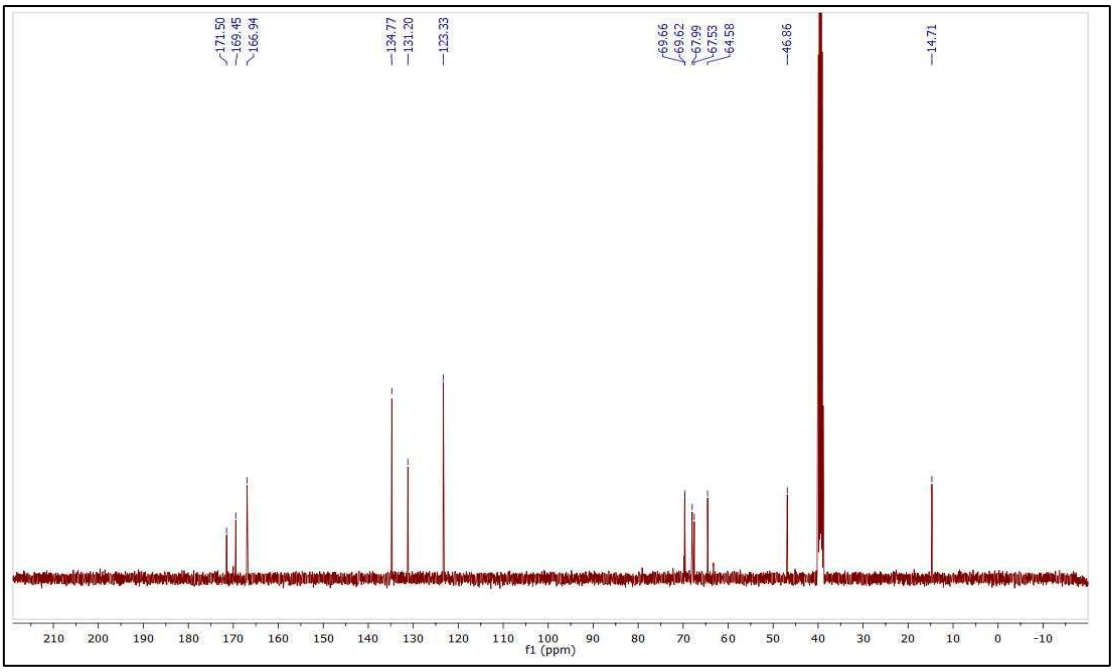

Figure 59. ^{13}C NMR Spectrum of compound **11** in DMSO-d_6

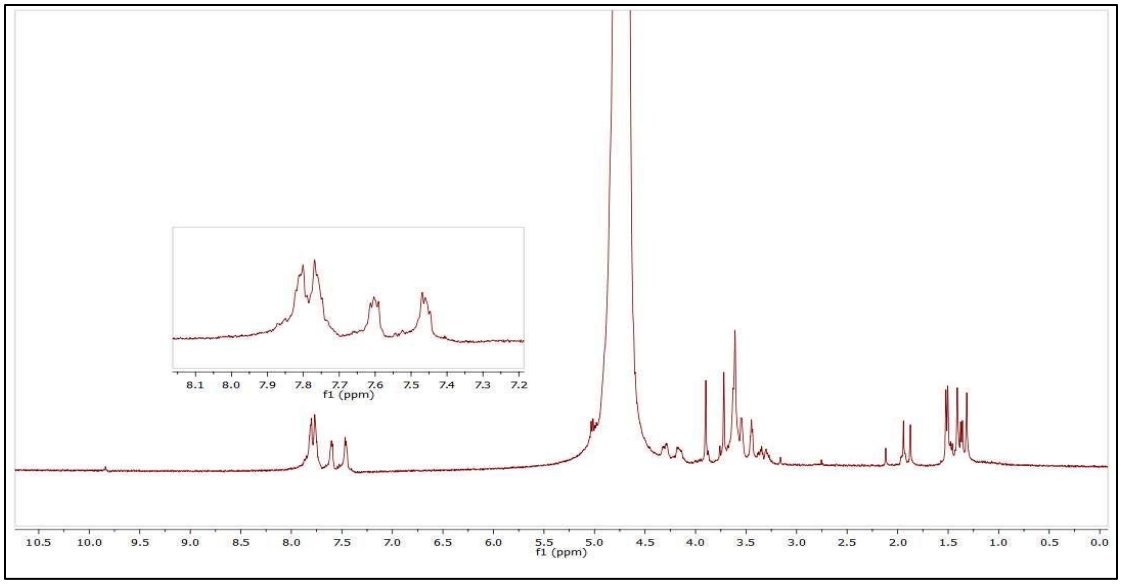

Figure 60. ^{1}H NMR Spectrum of compound **11** in D_2O

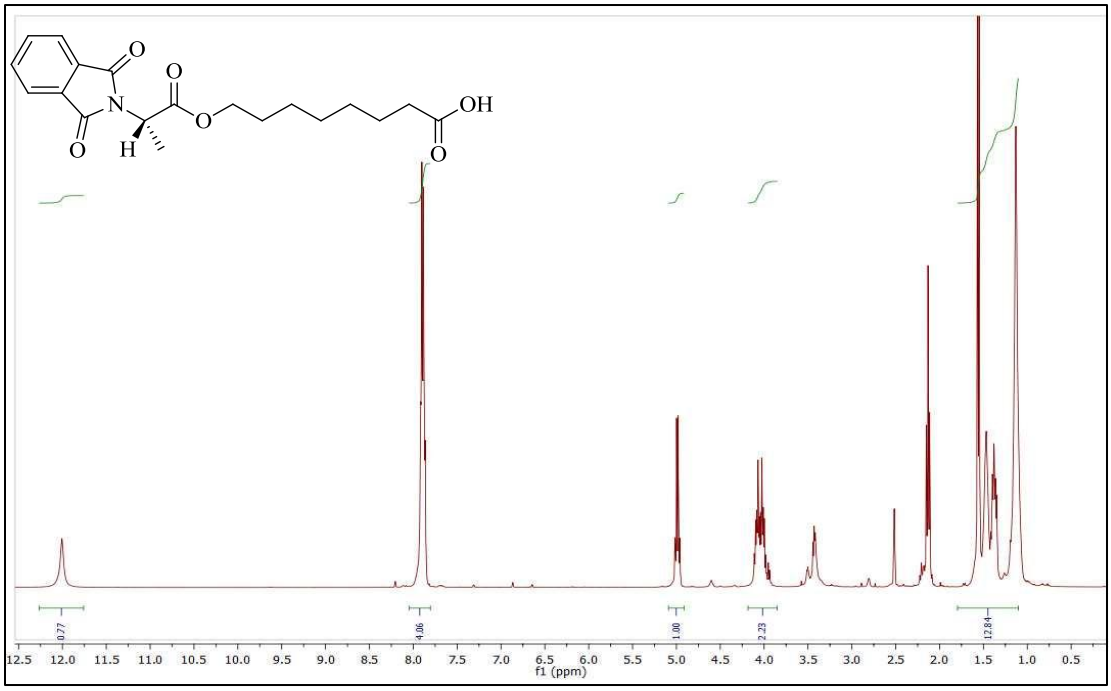

Figure 61. ^{1}H NMR Spectrum of compound **12** in DMSO-d_6

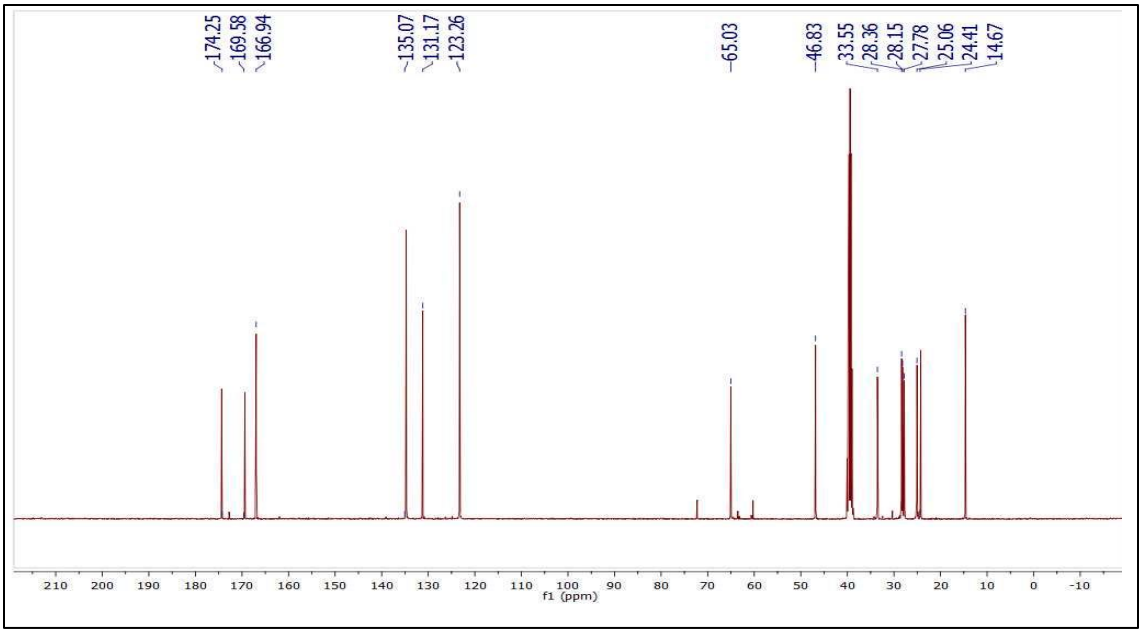

Figure 62. ^{13}C NMR Spectrum of compound **12** in DMSO-d_6

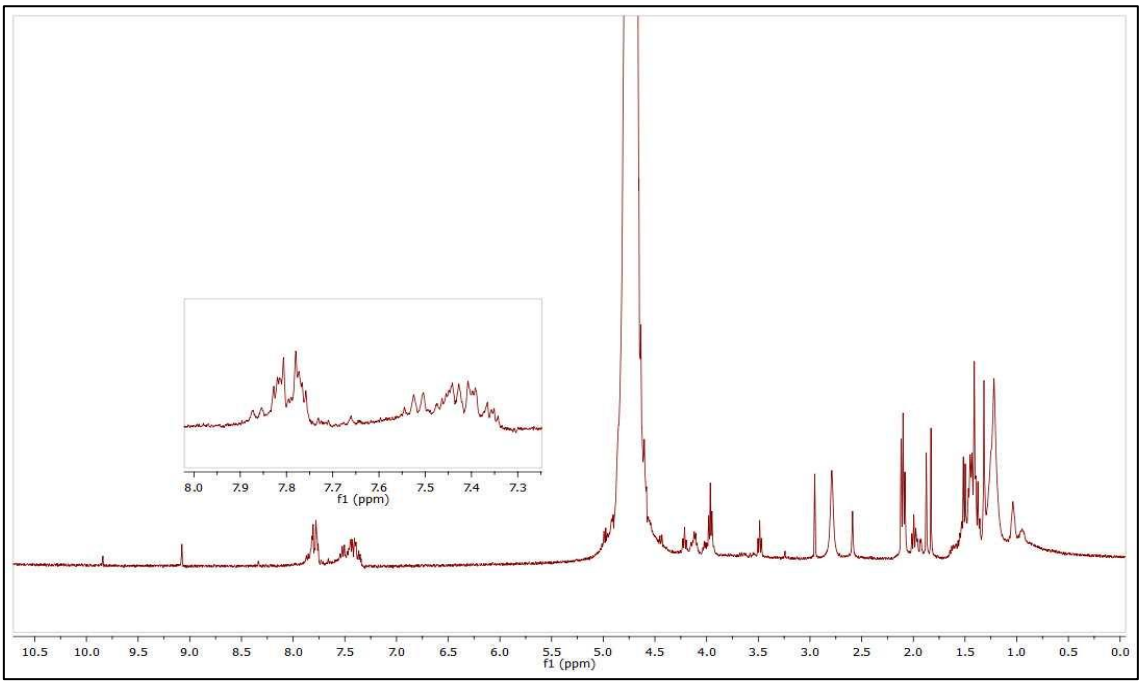

Figure 63. ^{1}H NMR Spectrum of compound **12** in D_2O

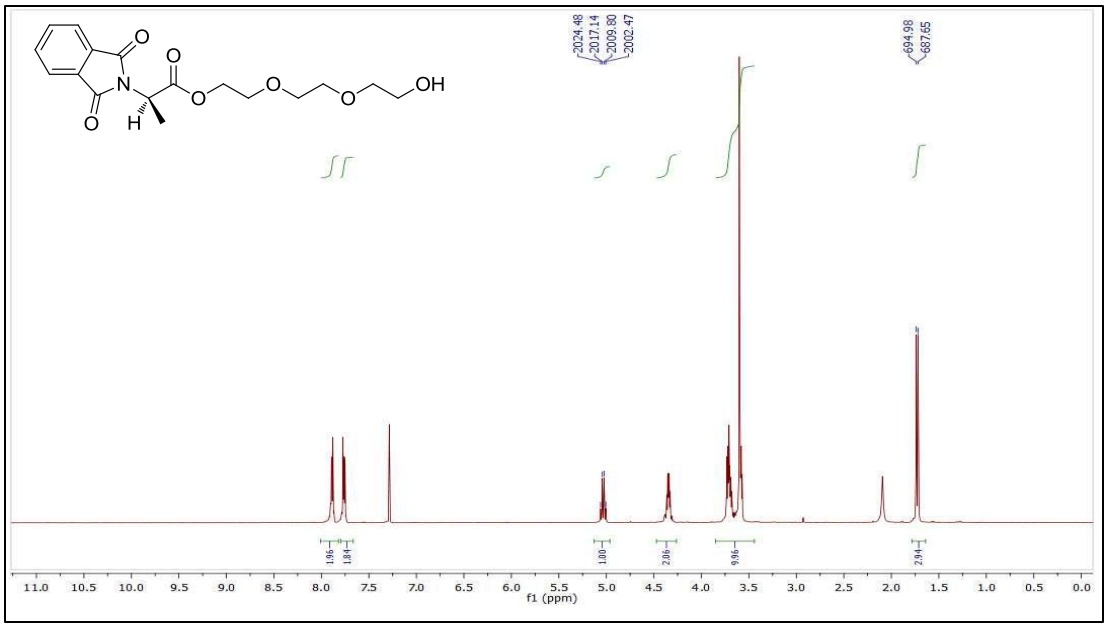

Figure 64. ^{1}H NMR Spectrum of compound **13** in $CDCl_3$

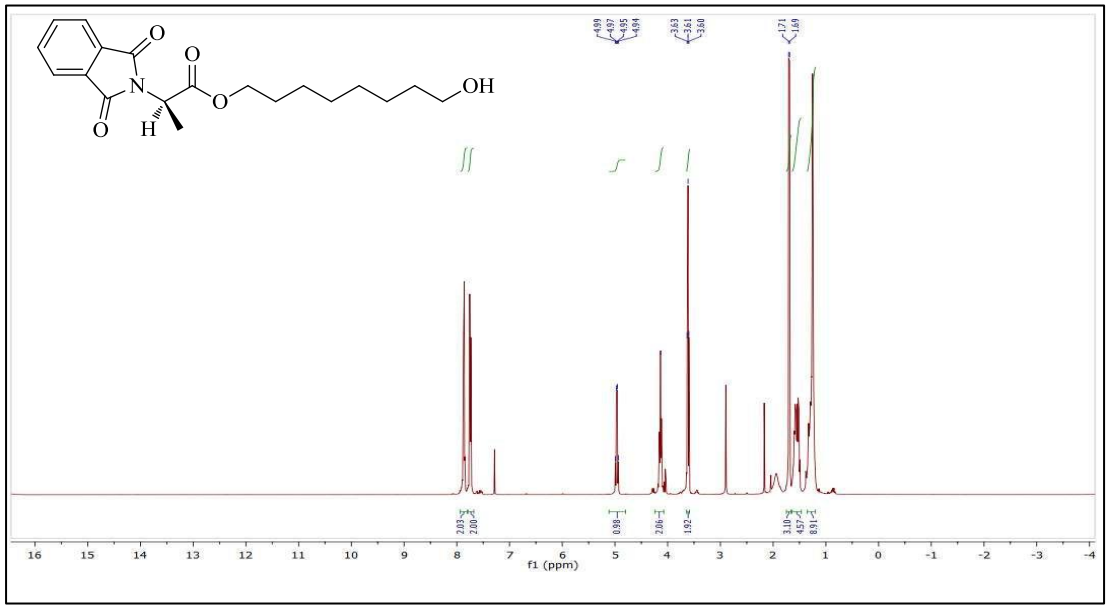

Figure 65. ^{1}H NMR Spectrum of compound **14** in $CDCl_3$

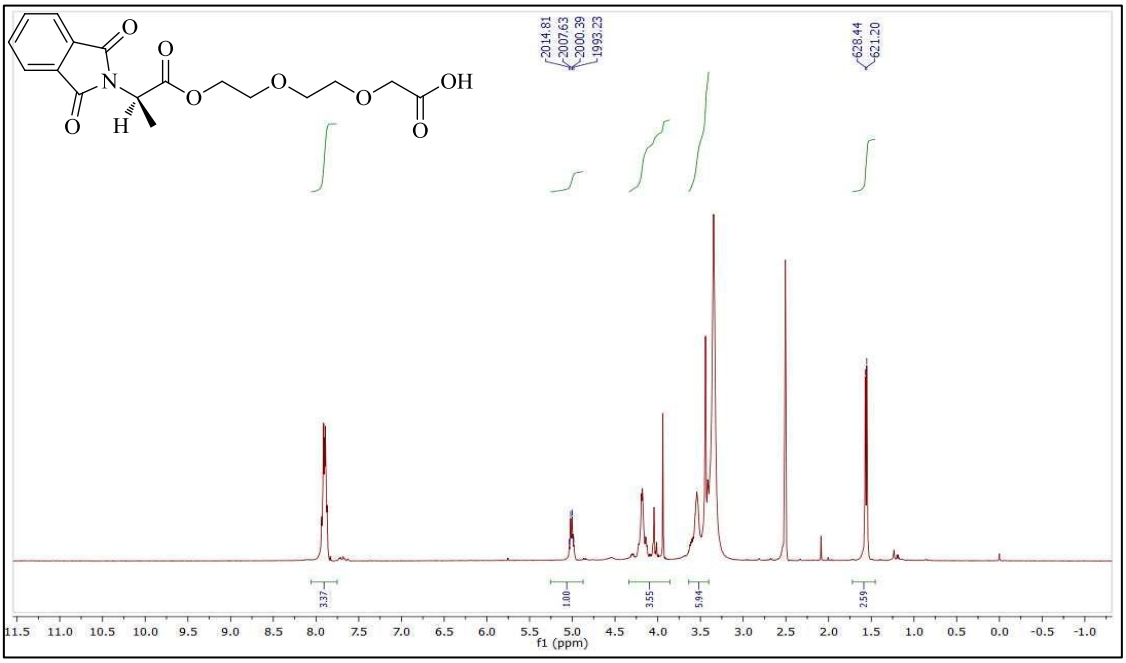

Figure 66. ^{1}H NMR Spectrum of compound **15** in DMSO-d_6

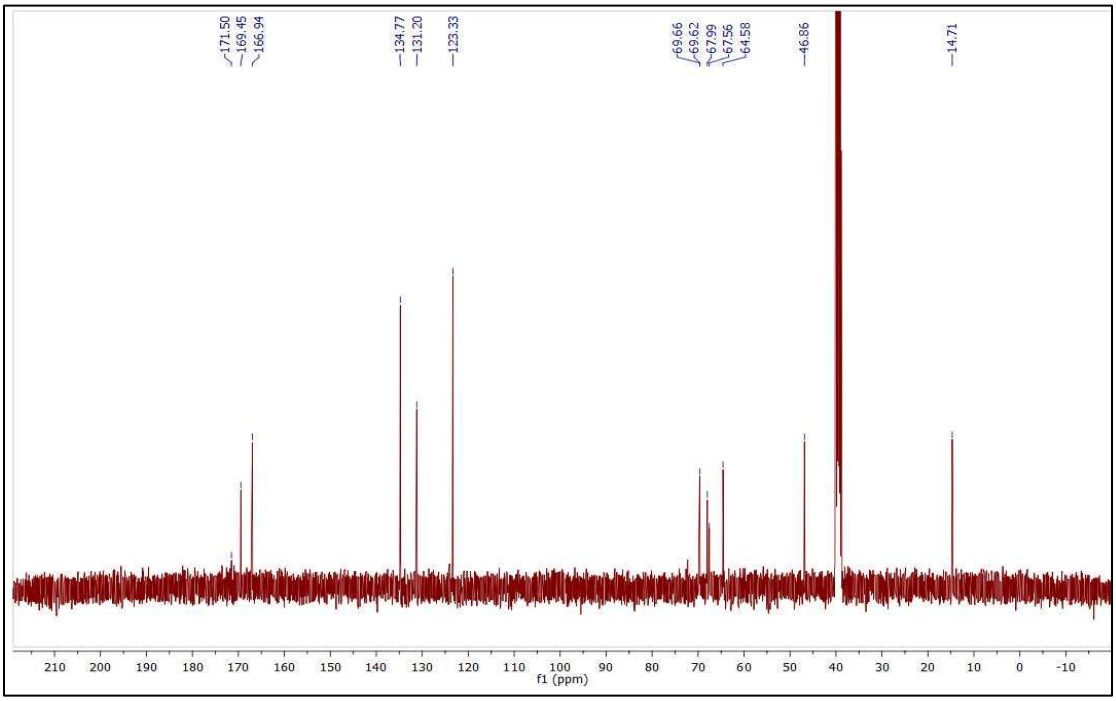

Figure 67. ^{13}C NMR Spectrum of compound **15** in DMSO-d_6

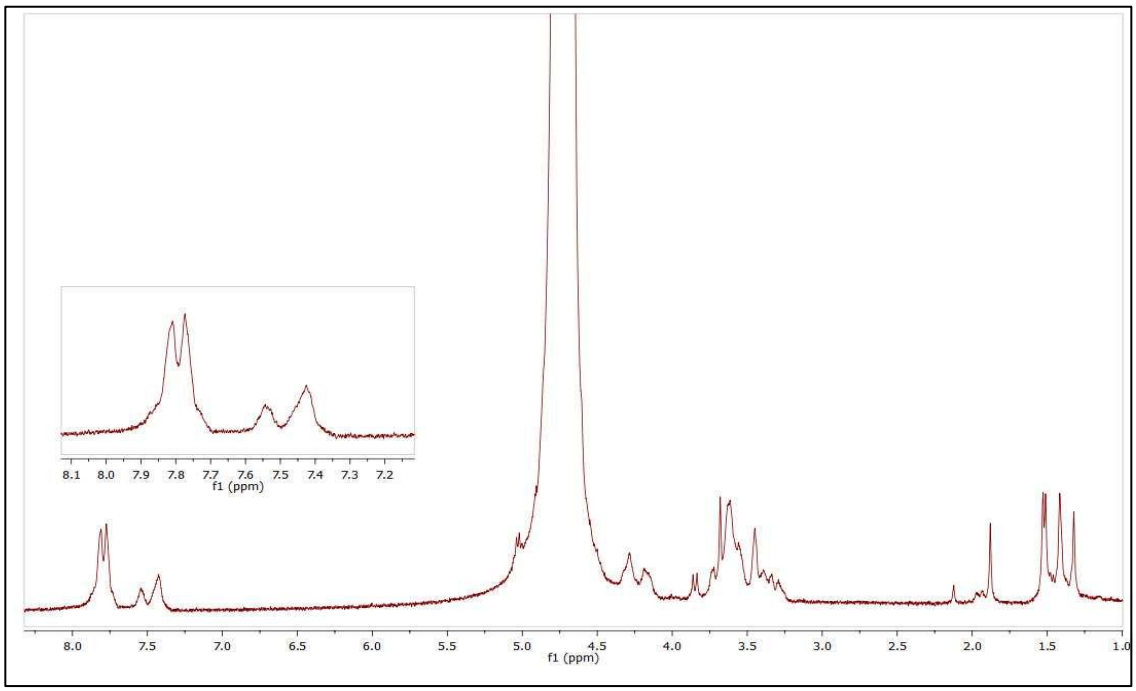

Figure 68. ^{1}H NMR Spectrum of compound **15** in D_2O

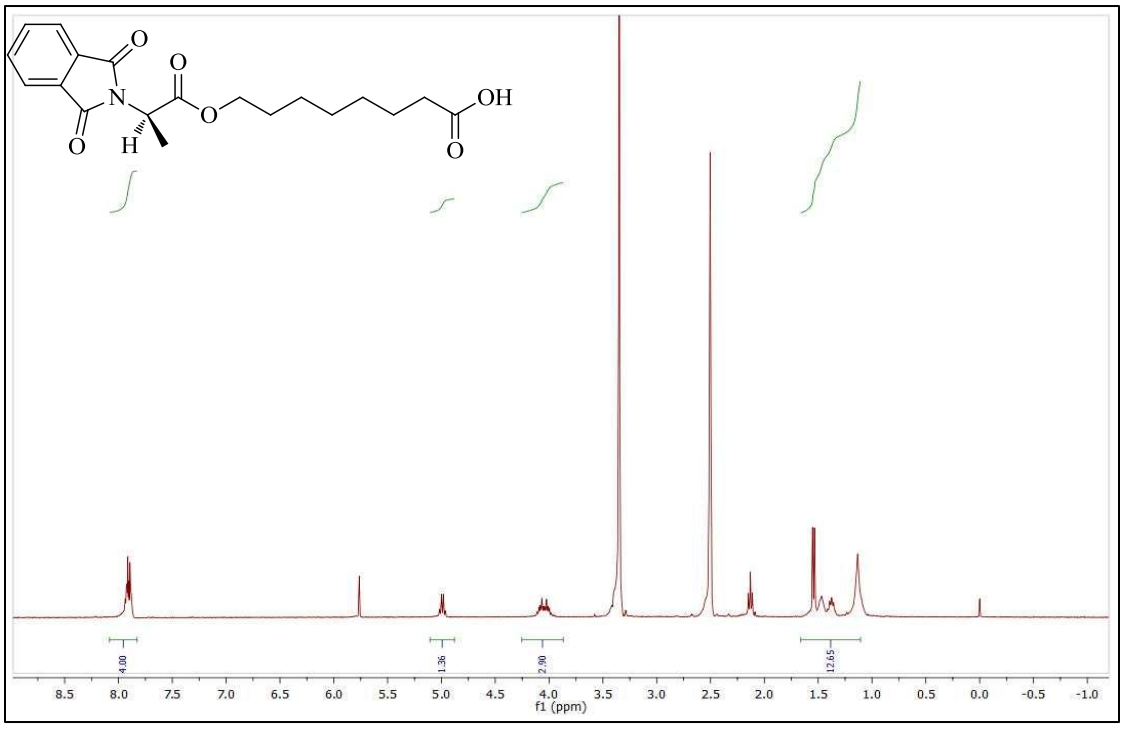

Figure 69. ^{1}H NMR Spectrum of compound **16** in DMSO-d_6

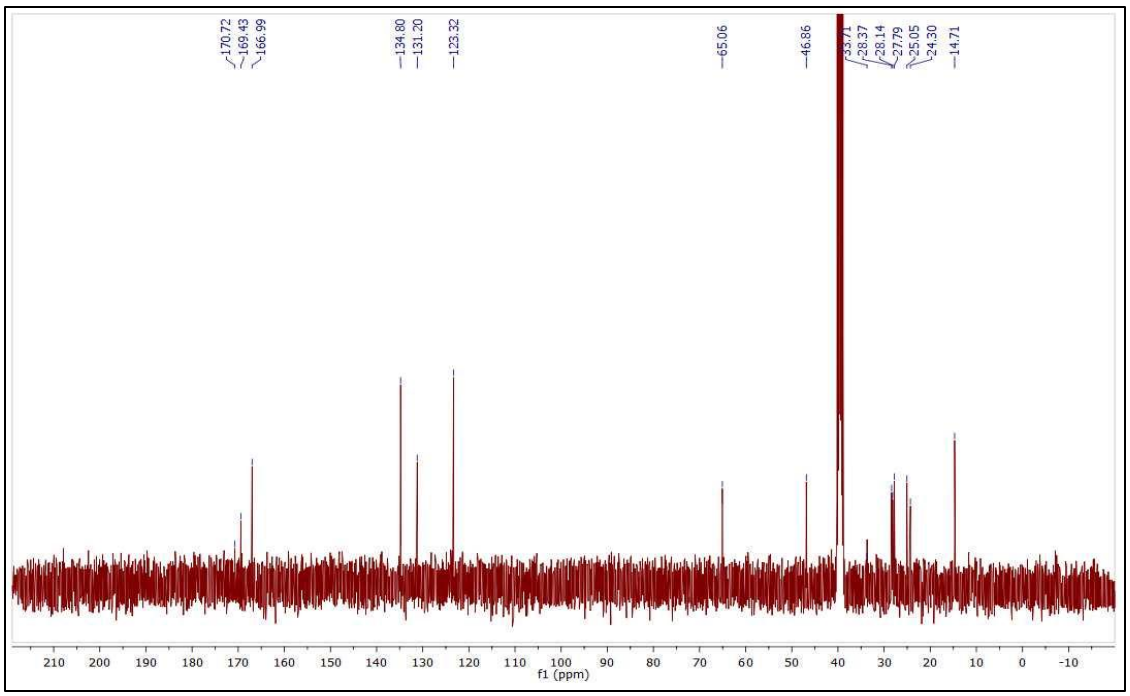

Figure 70. ^{13}C NMR Spectrum of compound **16** in DMSO-d_6

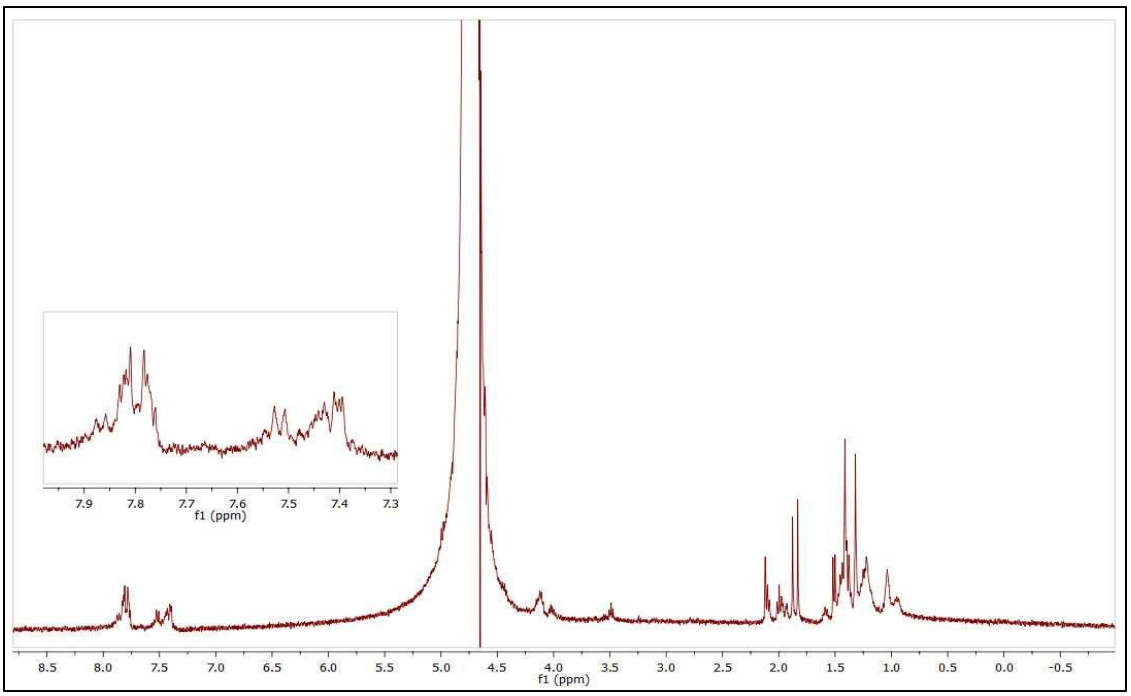

Figure 71. ^{1}H NMR Spectrum of compound **16** in D_2O

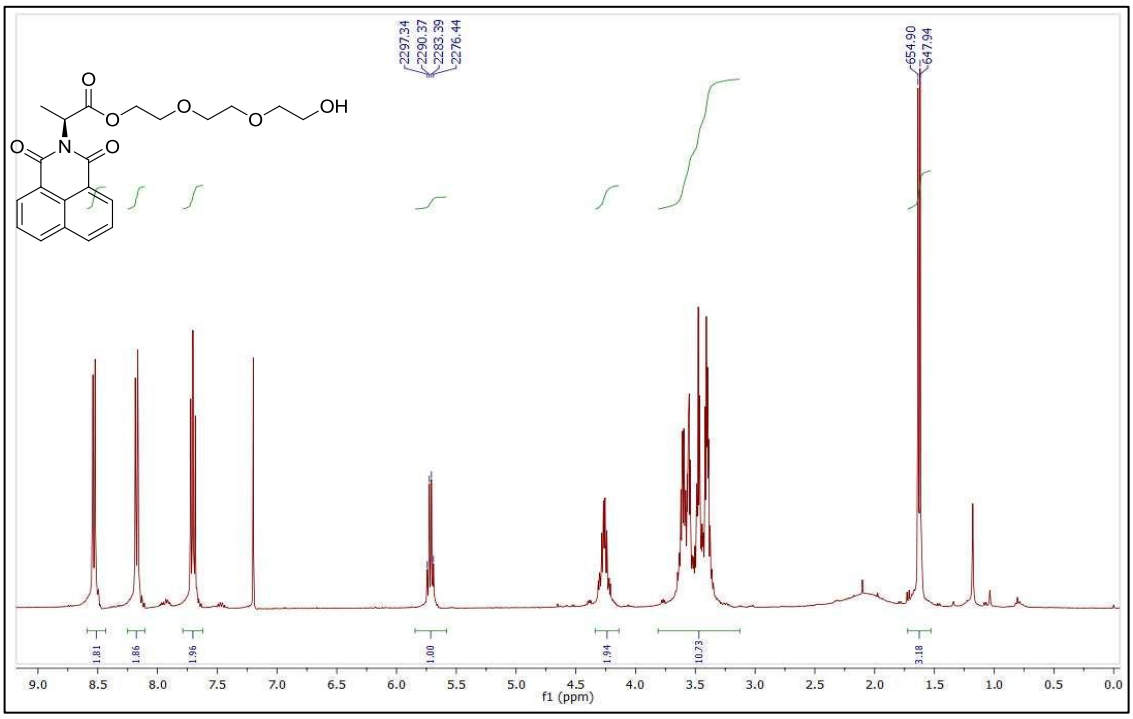

Figure 72. ^{1}H NMR Spectrum of compound **17** in $CDCl_3$

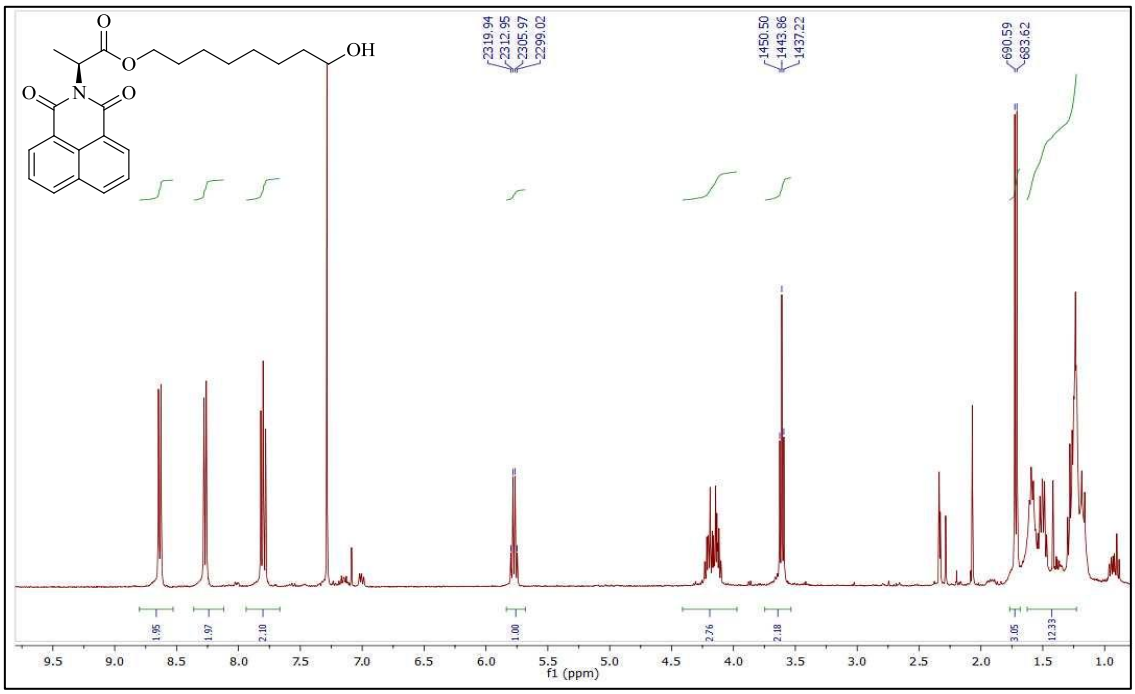

Figure 73. ^{1}H NMR Spectrum of compound **19** in $CDCl_3$

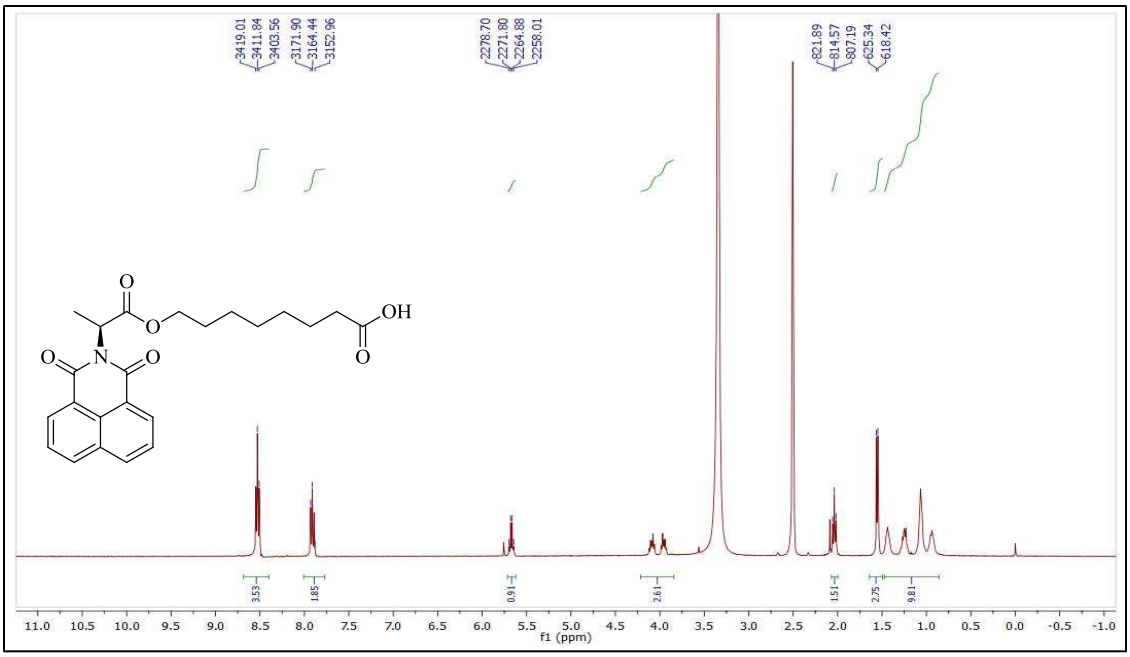

Figure 74. ^{1}H NMR Spectrum of compound **20** in DMSO-d_6

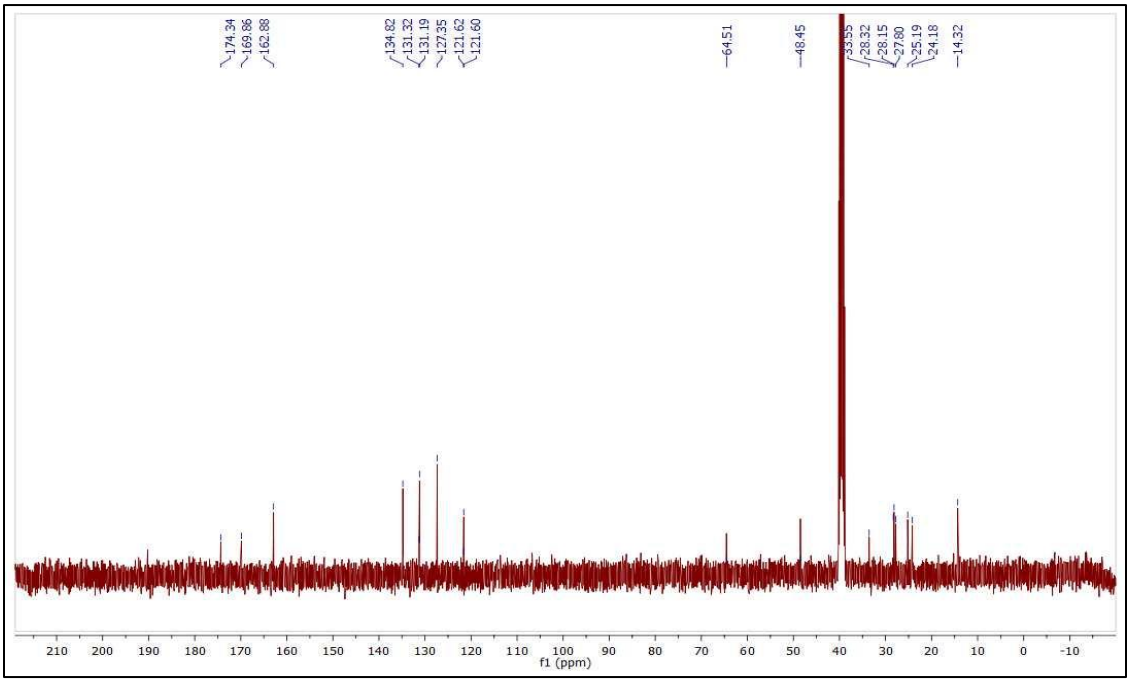

Figure 75. ^{13}C NMR Spectrum of compound **20** in DMSO-d_6

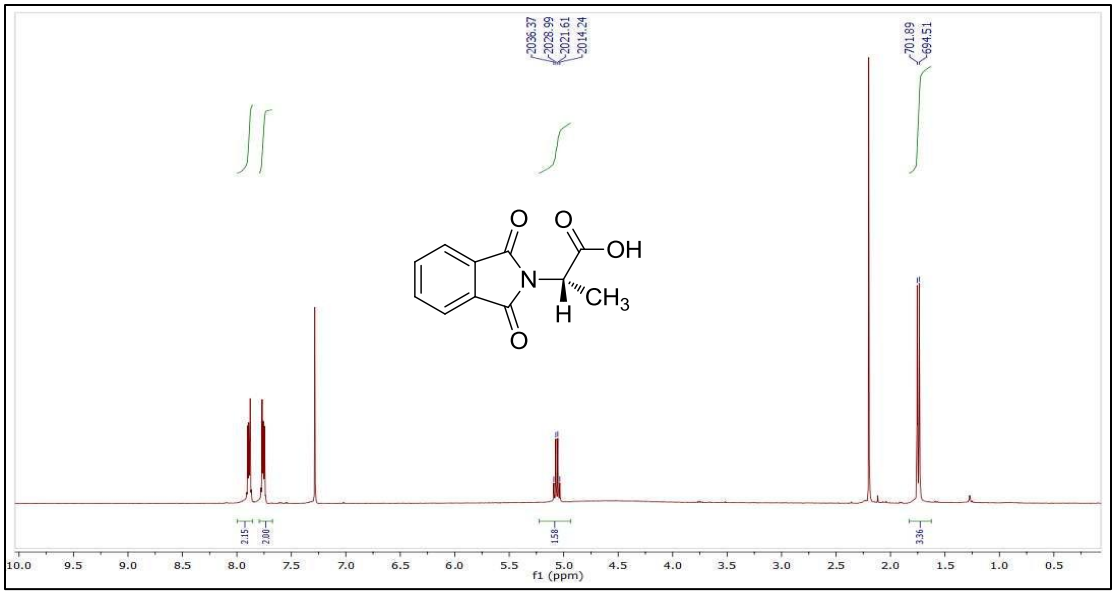

Figure 76. ^{1}H NMR Spectrum of compound **21** in $CDCl_3$

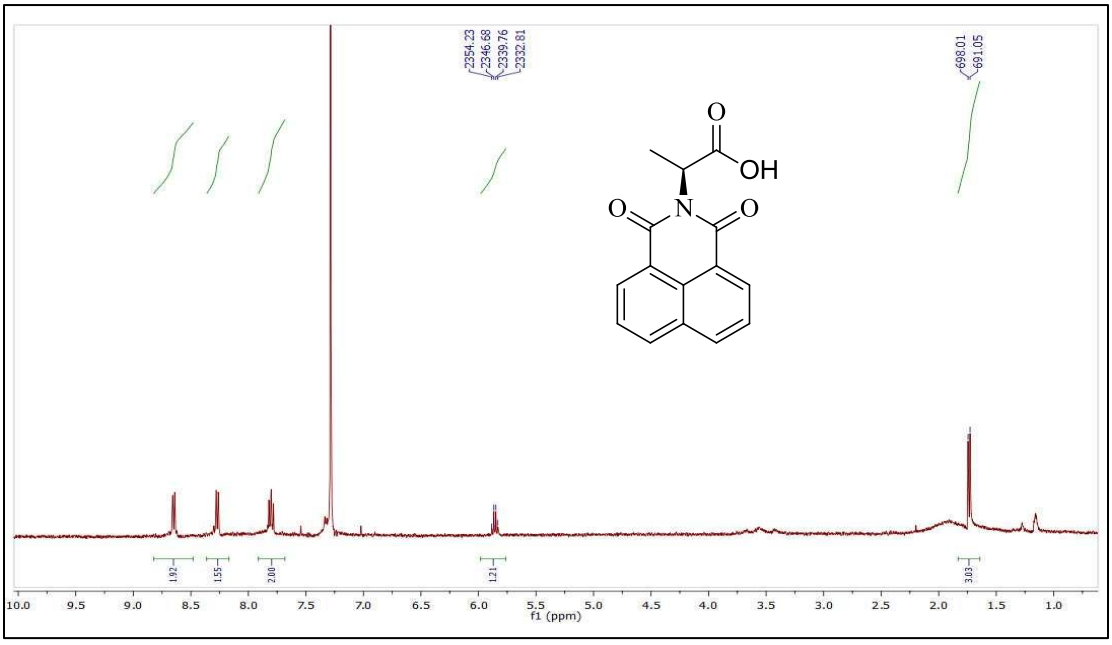

Figure 77. ^{1}H NMR Spectrum of compound **22** in $CDCl_3$

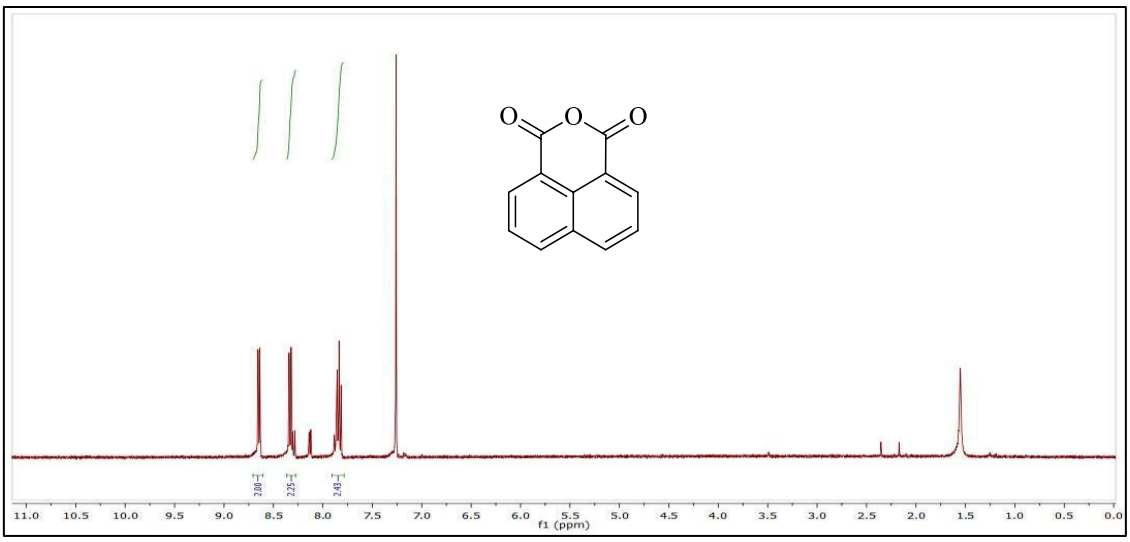

Figure 78. ^{1}H NMR Spectrum of compound **23** in $CDCl_3$

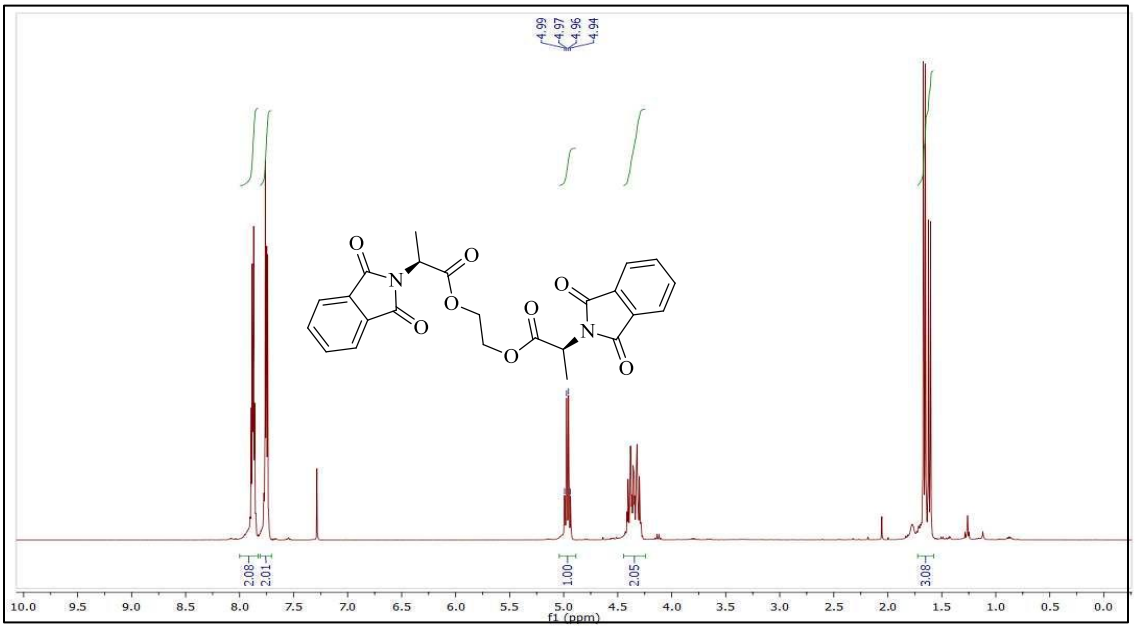

Figure 79. ^{1}H NMR Spectrum of compound **24** in $CDCl_3$

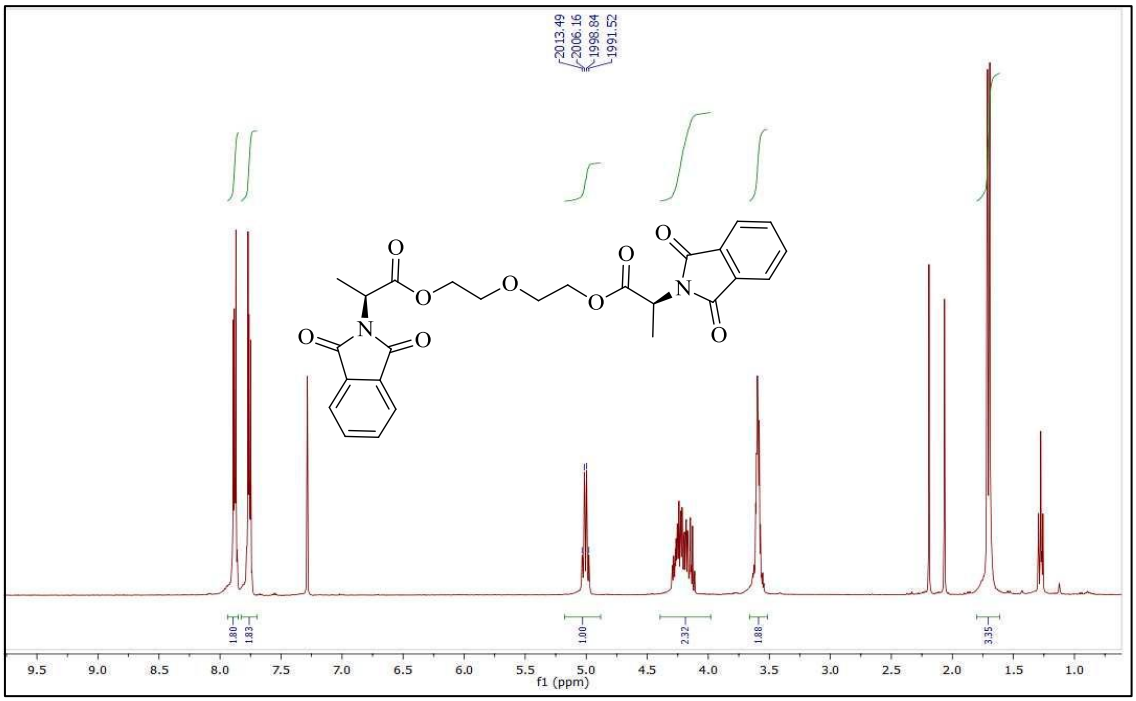

Figure 80. ^{1}H NMR Spectrum of compound **25** in $CDCl_3$

B. IR SPECTRA

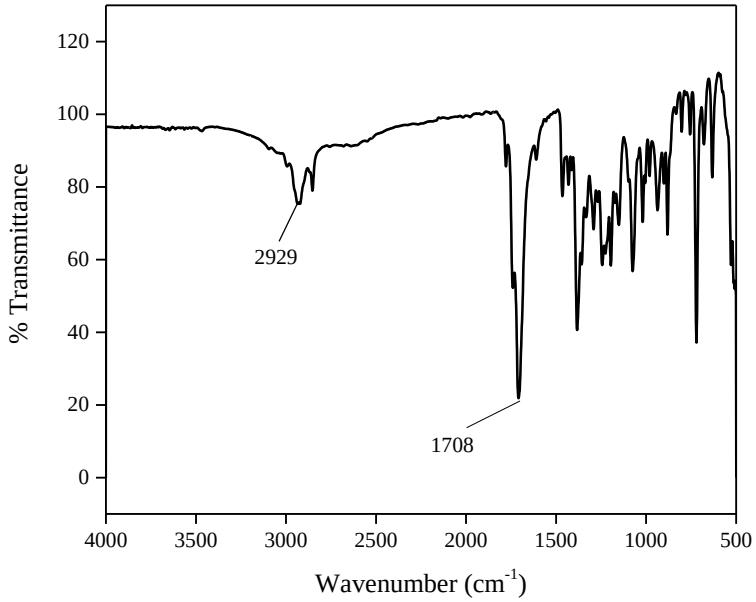

Figure 81. IR Spectrum of compound **1**

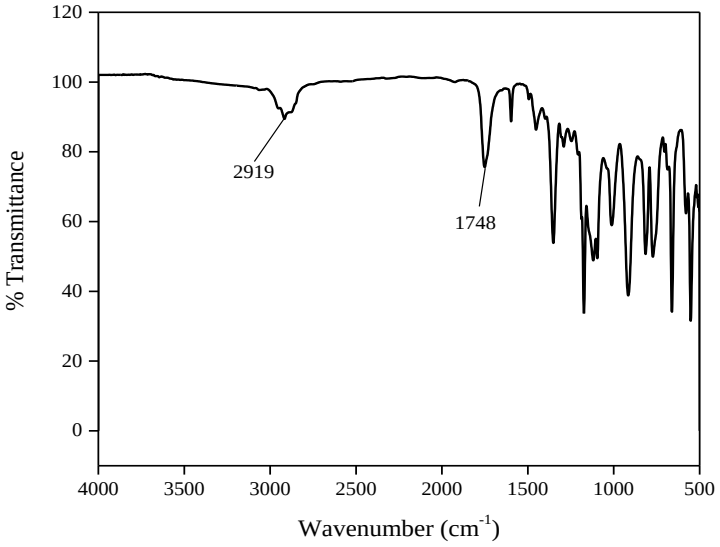

Figure 82. IR Spectrum of compound **2**

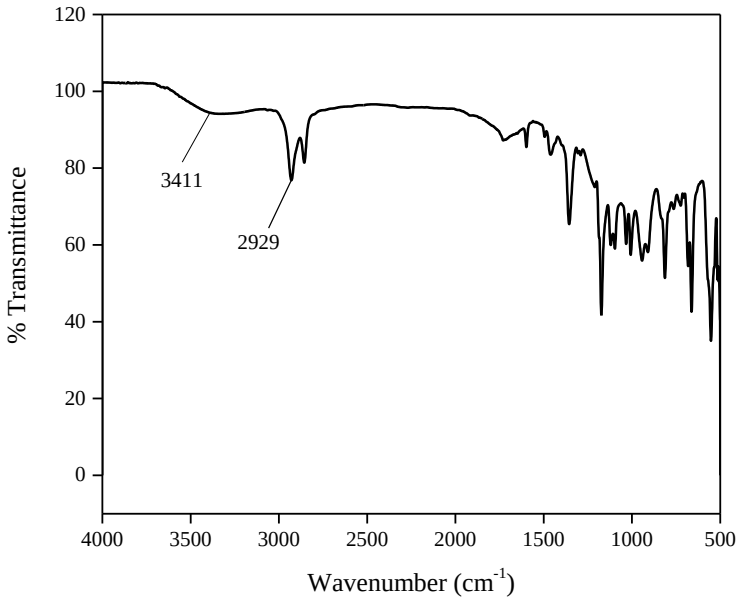

Figure 83. IR Spectrum of compound **3**

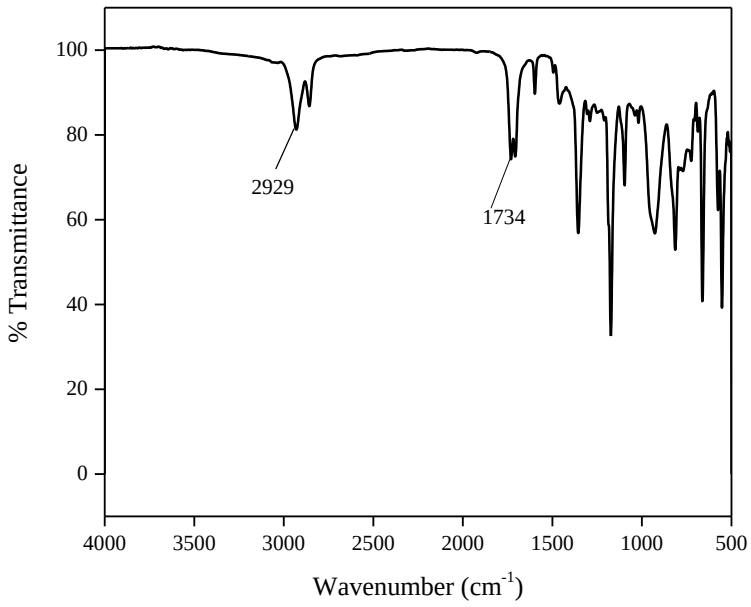

Figure 84. IR Spectrum of compound **4**

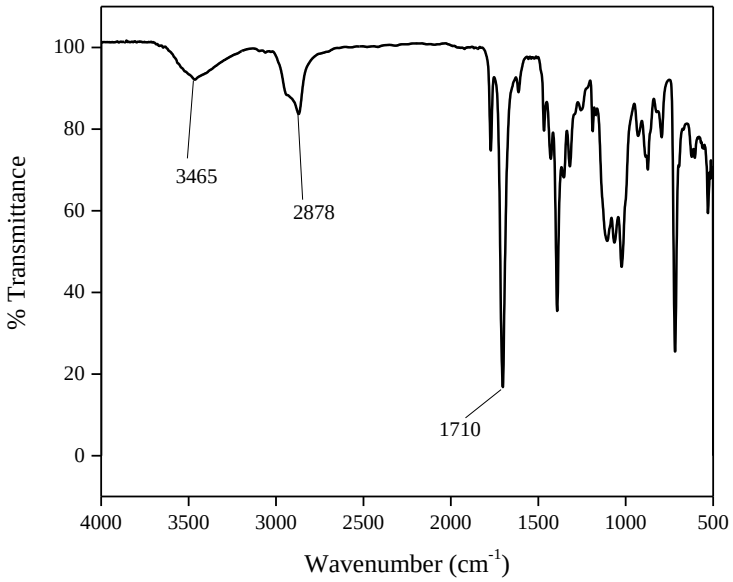

Figure 85. IR Spectrum of compound **5**

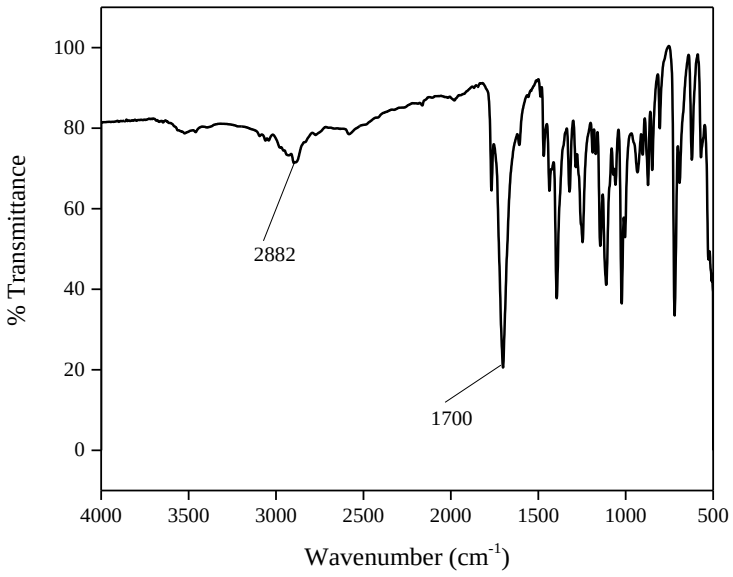

Figure 86. IR Spectrum of compound **6**

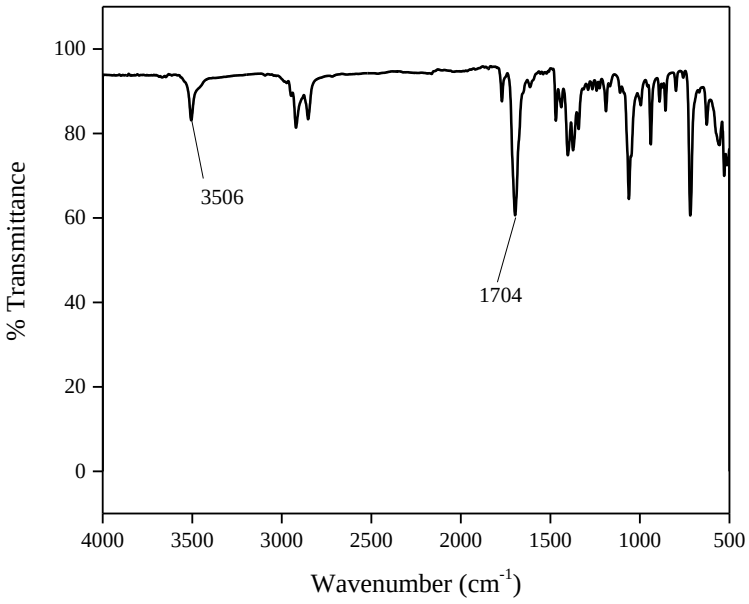

Figure 87. IR Spectrum of compound **7**

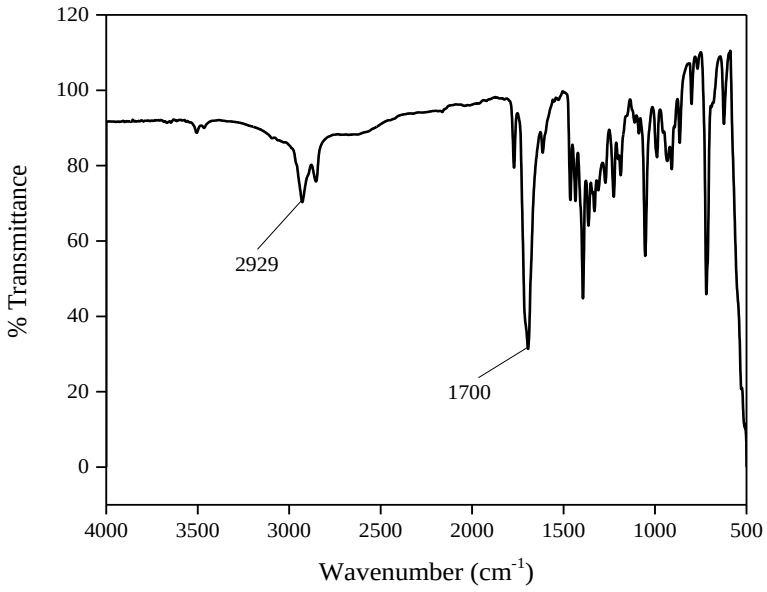

Figure 88. IR Spectrum of compound **8**

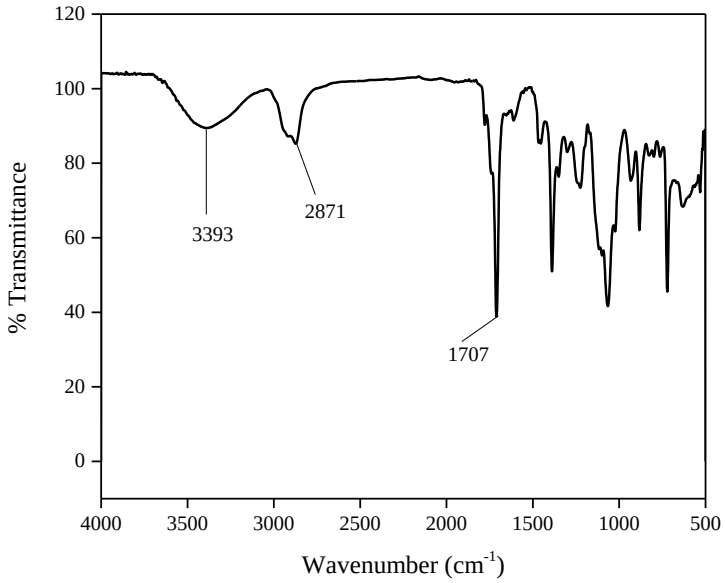

Figure 89. IR Spectrum of compound **9**

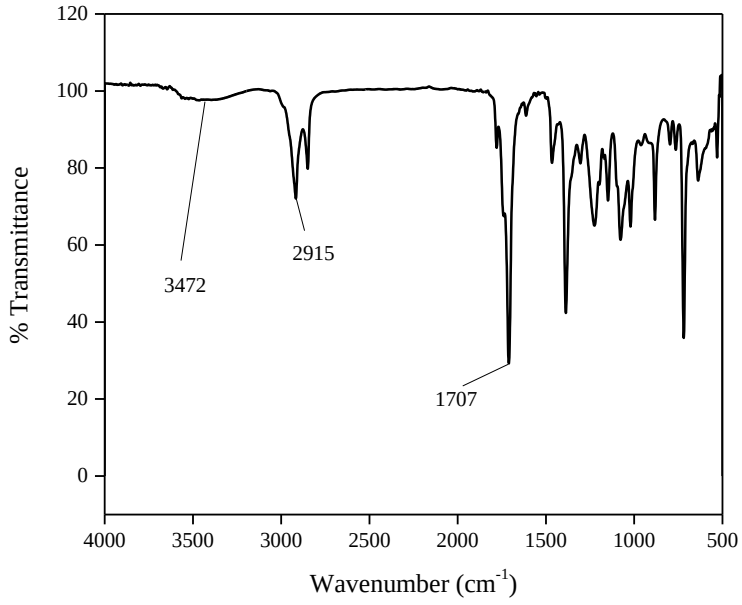

Figure 90. IR Spectrum of compound **10**

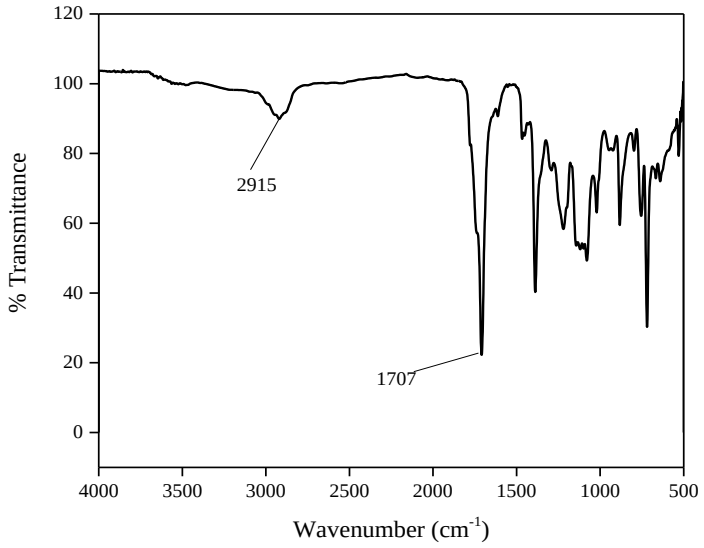

Figure 91. IR Spectrum of compound **11**

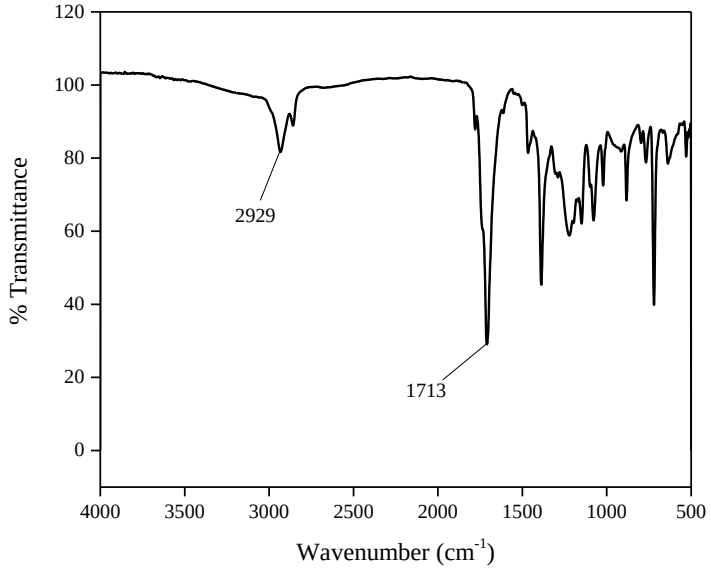

Figure 92. IR Spectrum of compound **12**

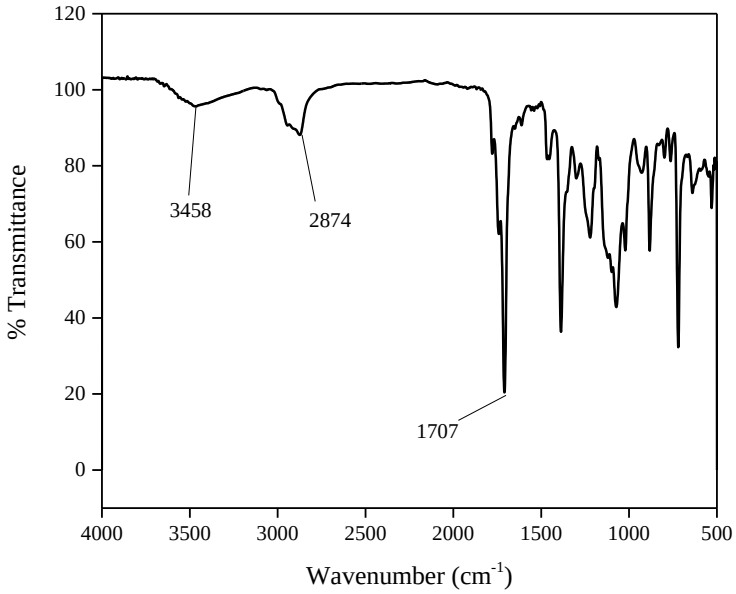

Figure 93. IR Spectrum of compound **13**

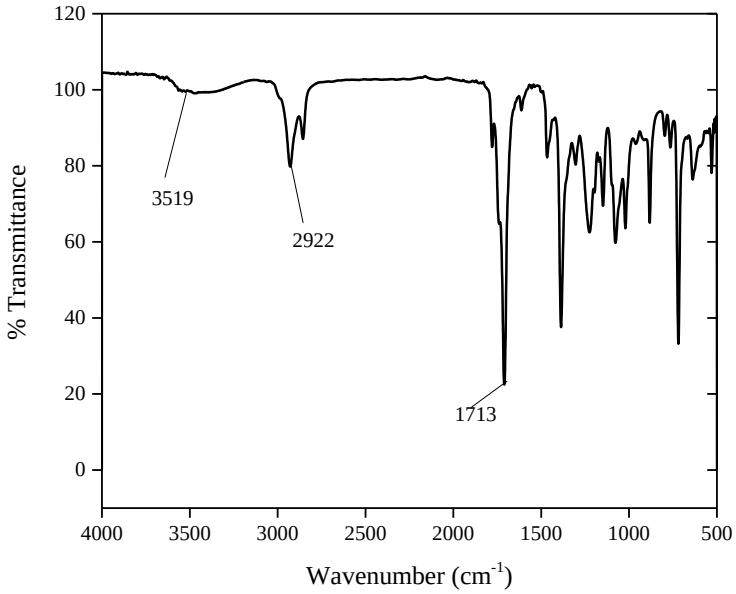

Figure 94. IR Spectrum of compound **14**

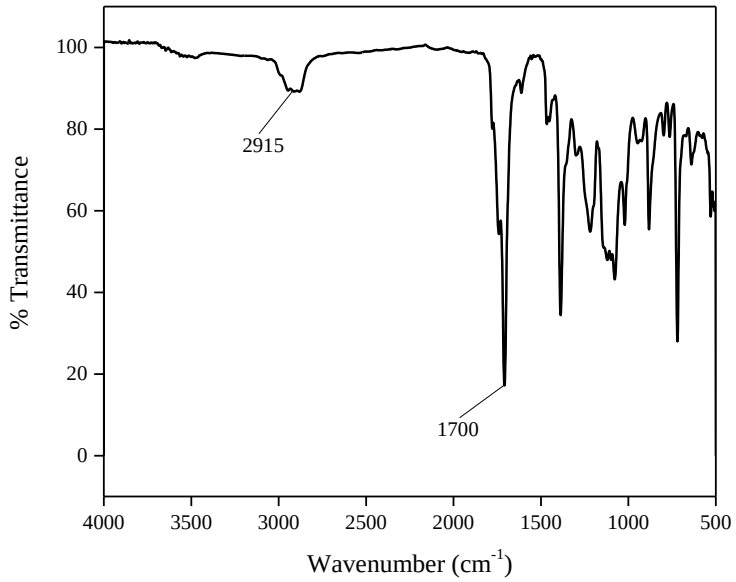

Figure 95. IR Spectrum of compound **15**

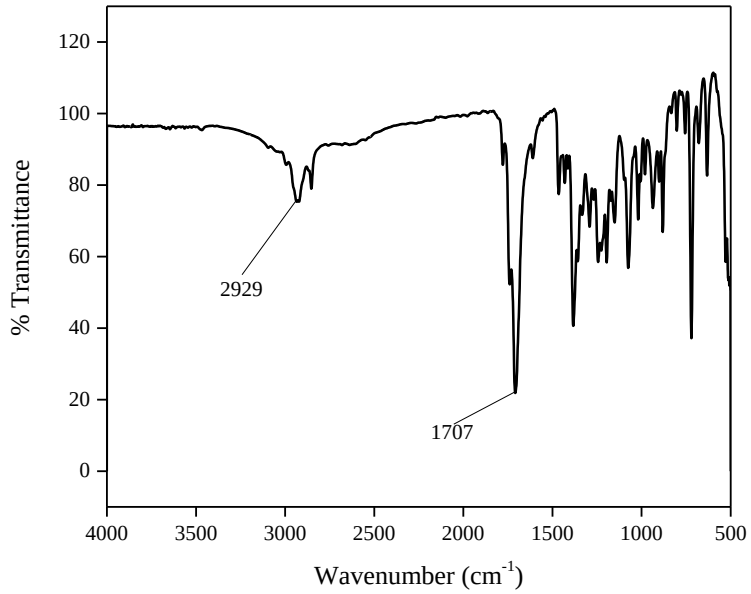

Figure 96. IR Spectrum of compound **16**

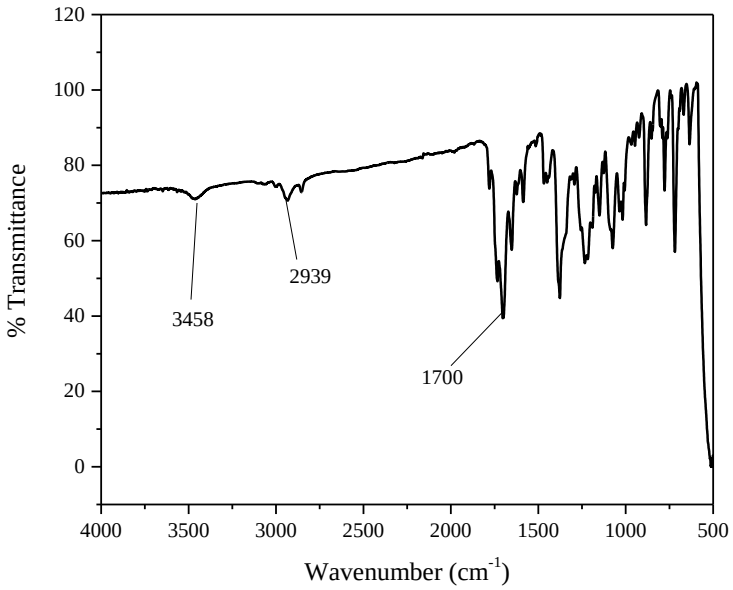

Figure 97. IR Spectrum of compound **19**

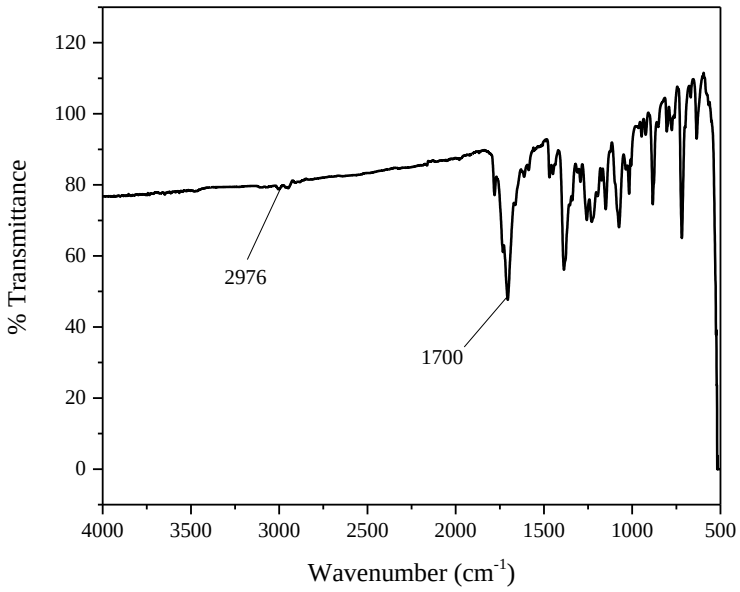

Figure 98. IR Spectrum of compound **20**

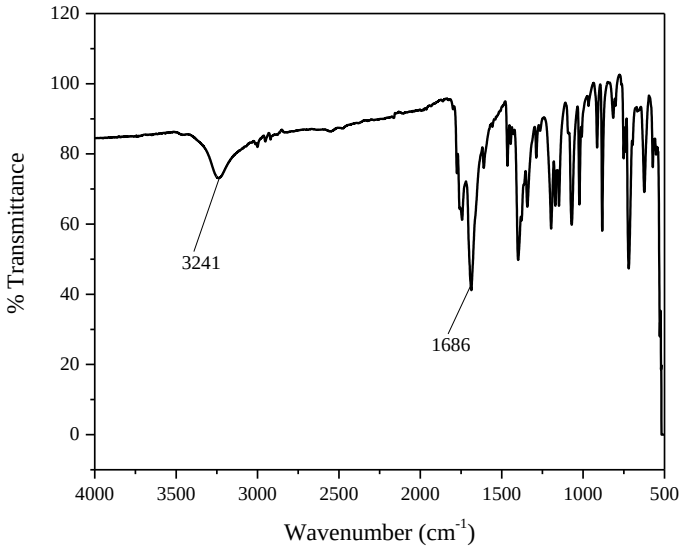

Figure 99. IR Spectrum of compound **21**

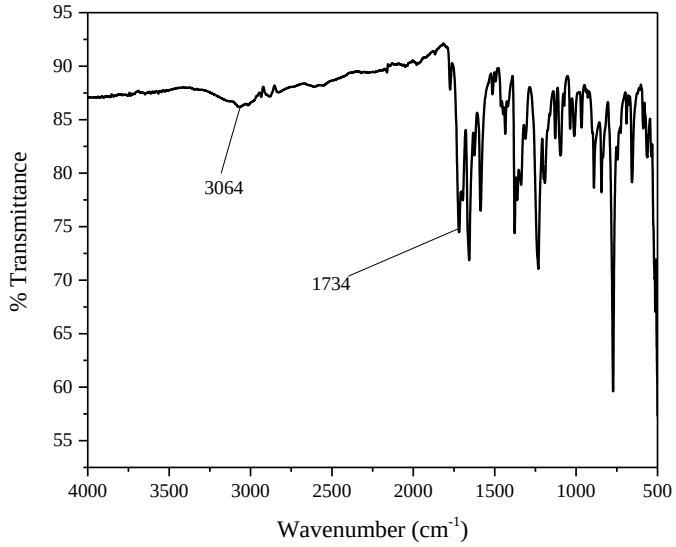

Figure 100. IR Spectrum of compound **22**

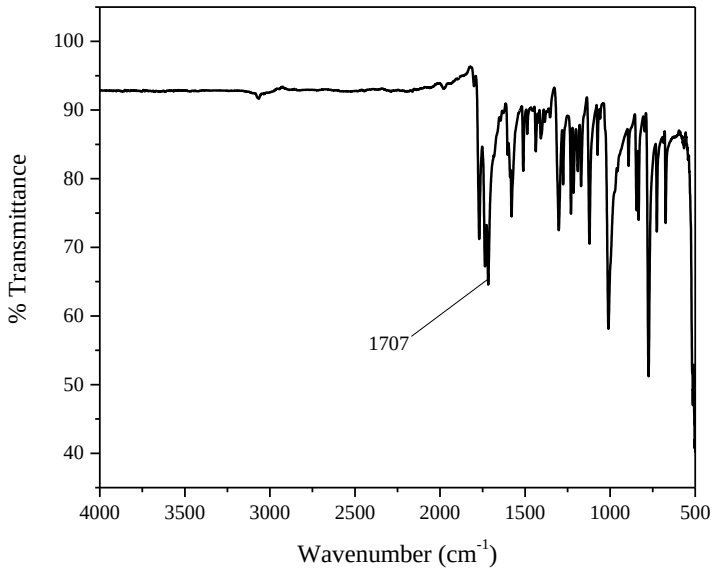

Figure 101. IR Spectrum of compound **23**

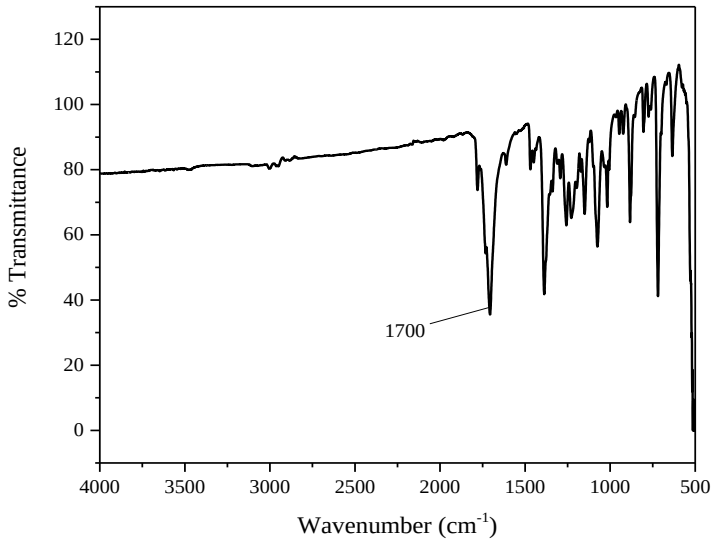

Figure 102. IR Spectrum of compound **24**

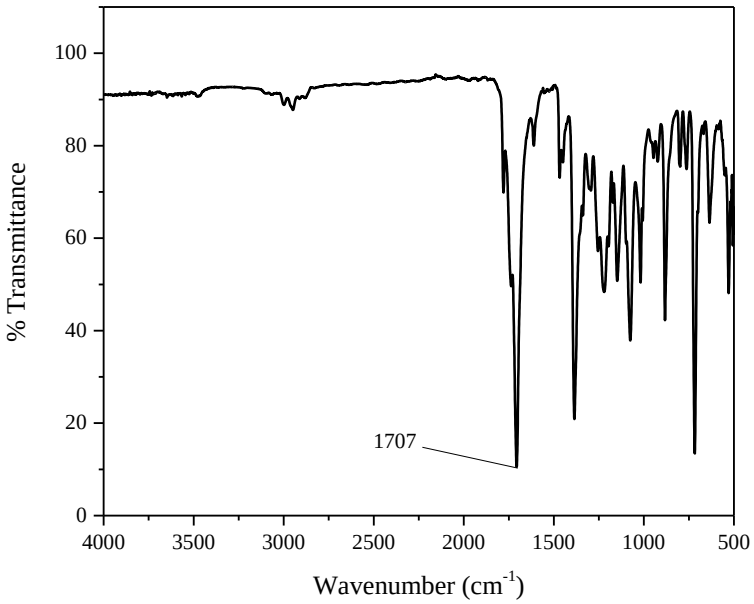

Figure 103. IR Spectrum of compound **25**

C. UV-Vis SPECTRA OF THE HEATED AND COOLED SOLUTIONS

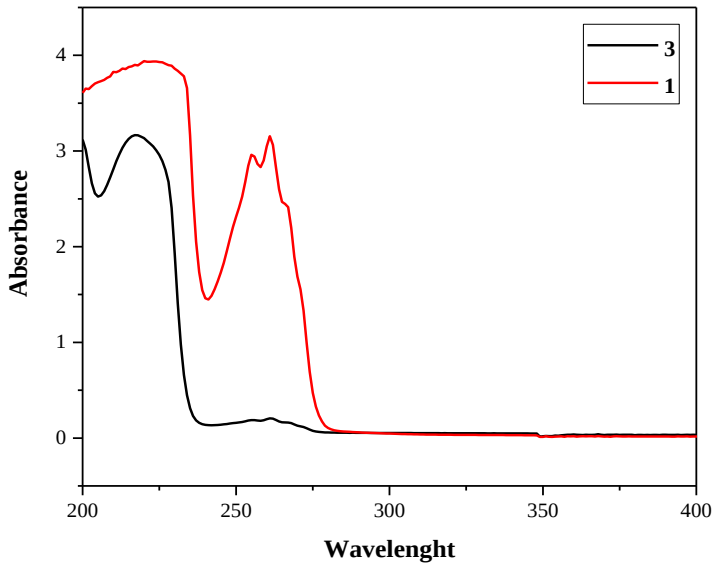

Figure 104. UV-Vis Spectra of **1** and **3** (0.01 M in water)

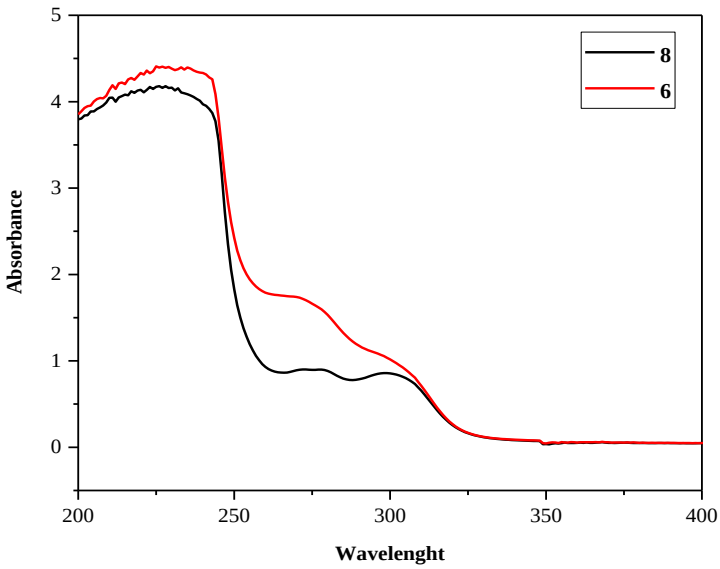

Figure 105. UV-Vis Spectra of **6** and **8** (0.001 M in water)

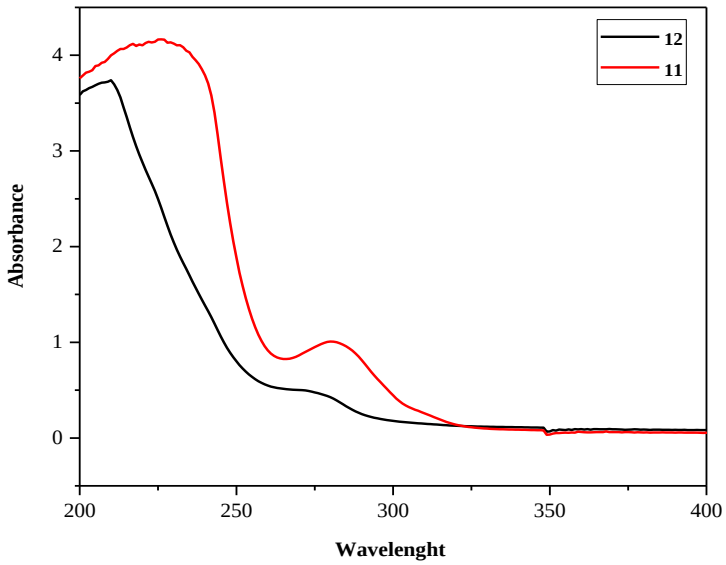

Figure 106. UV-Vis Spectra of **11** and **12** (0.001 M in water)

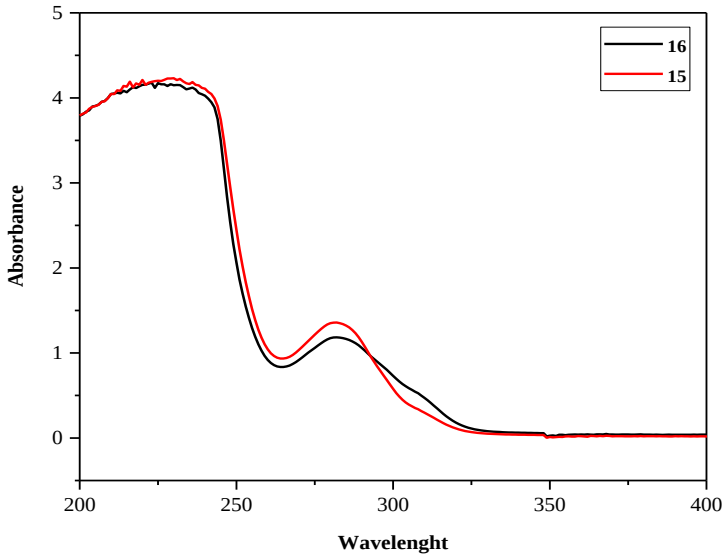

Figure 107. UV-Vis Spectra of **15** and **16** (0.001 M in water)